SLAC/AP-99
March 1995
(AP)

Impedance Study for the PEP-II B-factory*

S. Heifets, K. Ko, C. Ng, X. Lin, A. Chao, G. Stupakov, M. Zolotorev, J. Seeman,
U. Wienands, C. Perkins, M. Nordby, E. Daly, N. Kurita, D. Wright
Stanford Linear Accelerator Center, Stanford University, Stanford, CA 94309

E. Henestroza, G. Lambertson, J. Corlett, J. Byrd, M. Zisman
Lawrence Berkeley Laboratory, Berkeley, CA 94720

T. Weiland
University of Technology, FB18, Schlongortenstr. 8, D64289, Darmstadt, Germany

W. Stoeffl, C. Belser
Lawrence Livermore Laboratory, Livermore, CA 94550

Abstract

The paper summarizes results on the impedance study of the components of the PEP-II B-factory[1].

* Work supported by Department of Energy contract DE-AC03-76SF00515

Table 1. Parameters of the PEP-II B-factory

parameter		HER/LER	
energy	E	9.0/3.1	GeV
average radius	R	350.03	m
rf frequency	f_{rf}	476.0	MHz
harmonic number	h	3492	
revolution frequency	f_0	136.3	kHz
dc beam current	I_B	0.986/2.14	A
number of bunches	n_b	1658	
particles per bunch	N_B	$(2.72/5.91)\,10^{10}$	
gap	$n_g; l_g$	88; $0.05{*}2\pi R$	
bunch spacing	s_B	1.26	m
momentum comp.	α	$(2.41/1.31)\,10^{-3}$	
energy spread	δ	$(6.1/8.1)\,10^{-4}$	
bunch length	σ_B	1	cm
damping time	τ_x	(36.8/40.4)	ms
z-Partition number	J_E	1.9969/2.0116	
number of cavities	n_{cav}	24/8	
loss/turn	U_0	3.57/0.87	MeV
synchrotron tune	Q_s	0.0516/0.033	
voltage/cavity	V_{rf}	0.77/0.64	MV
cavity shunt imped.	R_s	3.5	MΩ
average beta-x	β_x	(14.5/10.84)	m
average beta-y	β_y	(13.84/9.95)	m

Introduction

There is no need to emphasize how important is to minimize the beam impedance for a lepton machine with the beam current of several amperes and large number of bunches. The paper summarizes results of the impedance studies of the components of the B-factory[1]. The prime goal of this activity was to support the design of the vacuum chamber and, at the same time, to get reasonable model of the machine impedance, which can be used later for detail studies of the collective effects. The work was carried out combining analytic approach with extensive simulations with available numerical codes such as MAFIA and ABCI.

The main parameters of the B-factory relevant to the paper are given in Table 1.

The paper is organized in the following way. First, we discuss limitations on the impedance given by the beam dynamics. After that, we list the impedance generating elements in the electron high energy ring (HER) and mention the difference with the positron low energy ring (LER). The analysis of the impedance of each element follows. At the end, we summarize results giving the parameters of the impedance of the HER.

In the Appendix 1 we summarize for completeness the definitions of the impedances and wakes together with some useful relations. In Appendix 2 we discuss the mode trapping. Appendix 3 describes the power loss of a train of bunches.

Constraints on the impedance

Impedances should be minimized to reduce the wake fields excited by the beam which, interacting with the beam, may make the beam unstable. Coherent effects impose certain limitations on the magnitude of the impedance.

The longitudinal wake field modifies the RF potential well and, as a result, changes the bunch shape $\rho(s)$. For a purely inductive impedance L, a single bunch self-consistent potential is

$$U = \frac{s^2}{2\sigma_B^2} + \Lambda L \rho(s) \qquad (1)$$

where $\int \rho(s)ds = 1$, and dimensionless

$$\Lambda = \frac{N_B r_e}{2\pi\gamma\alpha\delta^2 R}, \quad r_e = \frac{e^2}{mc^2}, \quad \gamma = \frac{E}{mc^2}. \tag{2}$$

For small s,

$$U = [1 - \frac{\Lambda L}{\sigma_B\sqrt{2\pi}}]\frac{s^2}{2\sigma_B^2}. \tag{3}$$

For the HER at the nominal $I_B = 1\,A$, $\Lambda/\sqrt{2\pi} = 0.88510^{-3}$ and 10% bunch lengthening may be expected for

$$L = 225\ nH, \quad \text{or} \quad Z/n = 0.2\ \Omega. \tag{4}$$

The microwave longitudinal instability sets the limit on the effective impedance $(Z/n)_{eff}$ defined as Z/n averaged with the bunch spectrum

$$(\frac{Z}{n})_{eff} < \frac{2\pi\alpha(E/e)\delta^2}{I_{peak}} \tag{5}$$

where, for a Gaussian bunch, the peak bunch current is $I_{peak} = I^{av}_{bunch}\sqrt{2\pi}R/\sigma_B$. For the nominal CDR[1], Table 1, the limit is $(\frac{Z}{n})_{eff} < 0.97$ Ohms for the HER and $(\frac{Z}{n})_{eff} < 0.14$ Ohms for the LER. Sometimes the SPEAR scaling $(\frac{Z}{n})_{eff} = (\frac{Z}{n})(\sigma_B/b)^{1.68}$ is used to relate effective and machine impedances. For the average $< b >= 3.3$ cm the machine impedance is 7.4 times larger than the effective impedance giving $(Z/n) = 7.2$ Ohms for the HER, and $(Z/n) = 1.03$ Ohms for the LER. However, SPEAR scaling may not necessarily be valid for PEP-II. Note, that a purely inductive impedance does not lead to the microwave instability.

The transverse microwave (transverse fast blow-up) instability limits the effective broad-band impedance for a given average bunch current;

$$|Z_\perp| < \frac{4Q_s(E/e)b}{I^{av}_{bunch} < \beta_\perp > R} \tag{6}$$

where Q_s is the synchrotron tune, and $< \beta >$ is the average transverse beta function. At the nominal CDR currents, an average $< \beta_\perp >= 10$ m, and a beam aperture

$b = 2.5$ cm, the criterion limits impedance to $|Z_\perp| = 21$ MΩ/m for the HER, and $|Z_\perp| = 2.3$ MΩ/m for the LER.

The transverse mode-coupling instability limits the imaginary part of the effective transverse impedance

$$ImZ_\perp < \frac{4Q_s(E/e)b}{I^{av}_{bunch} < \beta_\perp > R} \frac{4\sqrt{\pi}}{3} \frac{\sigma_B}{b} \tag{7}$$

and gives for PEP-II essentially the same constraints as the fast blow-up instability.

The slow head-tail instability sets some loose limit on the chromaticity of the ring and is not important for this note.

The transverse impedance also causes closed orbit distortion and changes the betatron tune. However, these effects are small. They may be enhanced by a factor $Q_L c/(\pi f_m s_B)$ proportional to the loaded Q_L factor of a higher-order mode (HOM) exited by a train of bunches if the frequency of a mode f_m of the narrow band impedance is in resonance with the bunch spacing $f_m s_B/c = integer + 1/4$, or with the frequency of a coherent coupled-bunch mode of the train.

The maximum kick from a single mode to a bunch centroid with the offset r is

$$\theta = \frac{\Delta p_\perp}{p} = \frac{4\pi N_B r_e}{Z_0 \gamma} (\frac{2r}{s_B}) \frac{R}{Q} Q_L, \qquad r_e = \frac{e^2}{mc^2} \tag{8}$$

provided that the mode frequency is in resonance with the bunch spacing.

For example, one of the strongest Rf cavity dipole HOM with parameters $f = 1674.2\ MHz$, $R/Q = 0.31\ k\Omega/m$, and loaded $Q_L = 2134$, gives the maximum transverse impedance $Z_\perp = (R/Q)Q_L = 0.66\ M\Omega/m$. Take $N_B = 6 \times 10^{10}$, offset $r = 1$ cm, $\gamma = E/mc^2 = 6 \times 10^3$, $r_e = e^2/mc^2 = 2.8 \times 10^{-13} cm$. Then $\theta = 1.0 \times 10^{-5}$ is much smaller than the divergence angle within a beam. The HOM of a cavity with length l is equivalent to a quad with the focusing length $F = l/\theta$. The betatron tune shift given by the mode is $\Delta Q_\perp = -\beta_\perp/(4\pi F)$ and, for $l = 10$ cm, $\beta_\perp = 11$ m, $\Delta Q_\perp = 4. \times 10^{-4}$. Hence, under the resonance condition the maximum tune shift due to the strongest HOM of the 8 RF cavities $\Delta Q_\perp = 0.6 \times 10^{-3}$ in the LER is still much smaller than the beam-beam tune shift ($\xi = 0.03$).

More limitations come from coupled bunch instabilities.

In the longitudinal case, the growth rate for n_b equally spaced bunches

$$\frac{1}{\tau_n} = \frac{I_B \alpha}{4\pi (E/e) Q_s} \sum_{p=-\infty}^{\infty} \omega_{pn} e^{-(\omega_{pn}\sigma_B)^2} Re Z_l(\omega_{pn})$$

where $\omega_{pn} = \omega_{rev}[pn_b + n + Q_s]$, should be compared to the damping time $\tau_l = 20$ msec. (This conservative approach ignores additional possible Landau damping and head-tail effect). That limits the impedance at any resonance frequency $f = \omega_{pn}/2\pi$. For the CDR parameters of the rings:

$$(\frac{f}{GHz})(\frac{ReZ}{k\Omega}) e^{-(2\pi f \sigma_B/c)^2} < 19.5 \ (HER); \quad < 4.1 \ (LER). \tag{9}$$

Similarly, comparison of the growth rate of the transverse coupled-bunch instability

$$\frac{1}{\tau_{\perp,n}} = \frac{I_B f_{rev} \beta_\perp}{(E/e)} \sum_{p=-\infty}^{\infty} e^{-(\omega_{pn}\sigma_B)^2} Re Z_\perp(\omega_{pn}) \tag{10}$$

where $\omega_{pn} = \omega_{rev}[pn_b + n + Q_\perp]$, with the damping time $\tau_\perp = 40$ msec limits the transverse impedance at any resonance frequency f_{pn}

$$\frac{ReZ_\perp}{K\Omega/m} e^{-(\omega\sigma_B/c)^2} < 119.8 \ (HER); \qquad < 26.6 \ (LER). \tag{11}$$

The longitudinal loss factor gives the energy loss of a beam and defines the power deposited in the beam pipe by an uncorrelated train of bunches

$$P = \Delta E f_0 = \frac{Z_0 I_B^2 \kappa_l s_B}{4\pi} \tag{12}$$

where $Z_0 = 120\pi \ \Omega$ is the impedance of the vacuum. For a 1 A current and $s_B = 1.26$ m, a loss factor of $\kappa_l = 1$ V/pC corresponds to $P = 4.16$ kW of microwave power.

In summary, the main limitations on impedance come from the bunch lengthening, power deposition, and multibunch stability. Single bunch stability does not seem to be a strong limiting factor.

Table 2. Impedance generating elements, HER PEP-II B-factory

RF Cavities	RF cavities	24
	RF cavities tapers	48
Arcs	Copper chamber(m)	1440
	Dipole screens	192
	BPM	198
	Arc bellows module	198
	Collimators	2
	Dipole offsets	384
	Quad pump slots	198
	Arc flex jonts	198
	Flange/gap rings	398
	Early x-ray mask	6
Straights	SS 304L pipe (m)	760
	BPM	92
	Collimators	6
	Pump ports	92
	Sliding joints	92
	Flex joints	92
	Flange/gap rings	184
	Gate valves	16
	Tapers octag./round	12

IR	IR Be chamber	1
	IR masks	
	Q2 septum	2
	Collimators	4
	IR pump ports	2
	Special BPMs	2
	High power dumps	2
Feedback	Feedback pickups	4
	Longitud. kicker	1
	Transverse kicker	1
Inject/Abort	Injection port	1
	Kicker ceramic	3
	Abort dump port	1
Arcs Diagnos.	Synch. light monitor	2
	SSRL xray port	2
Str. Diagnos.	BB curent monitors	1
	DC current transf.	1
	Tune monitor	1
	Profile monitor	1
IR Diagnos.	Luminosity monitor	1
Other	Pulsed separator	4
	PPS stopper	1

Impedances of the components

The list of impedance generating elements in the HER (including interaction region (IR)) is given in Table 2. The LER is different only in a few aspects. First, the LER has an Al vacuum chamber in the arcs and, because LER dipoles are short, an ante-chamber with discrete pumps is used instead of HER distributed ion pumps (DIPs). In the LER, the impedance of the antechamber "replaces" the impedance of the dipole screens of the HER. Secondly, wigglers give an additional contribution to the LER impedance budget.

RF cavities

The dominant contribution to the impedance comes, of course, from the damped RF cavities, see Fig. 1.

The loaded Q_L factor of the HOMs for a damped cavity is relatively low and the width-of a HOM is large compared to the revolution frequency. For this reason, the variation of the HOM frequency in the non-identical cavities (HOM detuning) is not important and the total impedance of the cavities is proportional to the number of cavities.

Table 3 summarizes the main longitudinal monopole and transverse dipole modes found numerically with the code URMEL and those measured on a prototype cavity[1].

The total narrow-band loss, Eq. (A1-15), of a cavity is $\kappa_l = 0.26$ V/pC. This is the sum of the loss-factors of the monopole HOM-s below the 2.5 GHz cut-off frequency of the beam pipe with $b = 4.76$ cm radius. The loss factor of the fundamental mode adds 0.167 V/pC. The total loss factor of a cavity calculated by ABCI from the wake field excited by a bunch going through the cavity, is $k_l = 0.55$ V/pC, Hence, the broad-band loss from the modes above the cut-off frequency is 0.12 V/pC.

The longitudinal wake field of a RF cavity is depicted in Fig. 2. The real and imaginary parts of a RF cavity broad-band impedances are depicted in Figs. 3a, and 3b for monopole HOMs, and Figs. 4a, 4b for dipole HOMs. The beam pipe radius is $b = 4.49$ cm.

Table 3. Single RF Cavity Monopole HOMs

	freq (MHz)	R/Q	$R_s(M\Omega)$	Q_L(num/mes)	$(R/Q)Q_L(k\Omega)$
1	489.6	108.8	5.036	/31926	3472.28
2	769.8	44.97	1.782	26/28	1.26
3	1015.4	0.006	0.0002	169/246	0.001
4	1291.0	7.68	0.692	66/	not visible
5	1295.6	6.57	0.265	/907	5.96
6	1585.5	5.06	0.216	/178	0.90
7	1711.6	4.75	0.404	not visible	
8	1821.9	0.06	0.006	/295	/0.018
9	1891.0	1.68	0.075	not visible	
10	2103.4	3.52	0.235	/233	0.82
11	2161.9	0.02	0.002	/201	0.004
12	2252.2	1.21	0.068	/500	0.61

Table 4. Main RF cavity Dipole HOMs, $r_0 = 4.7625$ cm

	f (MHz)	R/Q (Ω)	Q_L(calc/meas)	$(R/Q)(Q_L/kr_0^2\,(k\Omega/m)$
1	679.6	0.001	35/-	not visible
2	795.5	9.876	121/122	31.86
3	1064.8	31.990	38/-	not visible
4	1133.2	0.320	76/112	0.65
5	1208.2	0.385	2266/1588	10.3
6	1313.2	10.336	/498	80.1
7	1429.0	5.999	/3955	342.0
8	1541.0	2.065	/59	1.62
9	1586.2	5.262	/178	12.1
10	1674.2	14.732	/2134	385.0
11	1704.4	0.285	/444	1.52
12	1761.9	0.330	/7129	27.3

Eight cavities in the LER with the nominal beam current would generate, see Eq. (12), 16.6 kW of power propagating downstream from the cavities and absorbed in the walls. For the TM modes in the round pipe with the radius $r = b$, the power absorbed in the wall within the distance $l = 1/\alpha_P$ is $P(z) \propto e^{-\alpha_P z}$, where

$$\alpha_P = \frac{k}{k_z}\frac{\delta}{b}.$$

Here $k = \omega/c$, $k_z = \sqrt{k^2 - k_m^2}$, k_m is the cut-off frequency of the m-th propagating mode. The bunch spectrum starts to roll-off above frequencies $k\sigma \simeq 1$. For a $\sigma_B = 1$ cm bunch, the roll-off starts at the frequency $f \simeq 4.77$ GHz. For such a frequency, the skin depth is $\delta \simeq 1\mu m$, and the absorbtion length in the beam pipe with radius $b = 4.76$ cm is of the order of $l \simeq 500$ m. Hence, the wall power deposition from the cavities is $29.0\, W/m$.

The broad-band transverse kick-factor of a RF cavity $k_\perp = 5.266$ V/pC/m at $b = 4.49$ cm.

The maximum narrow-band (NB) impedance of a single cavity $(R/Q)Q_L = 5.96\,\mathrm{k}\Omega$ at $f = 1.296$ GHz, see Table 3, is larger than the $3.4\mathrm{k}\Omega$ limit set by Eq. (9) for the LER. The coherent stability of PEP-II therefore requires a feedback system. Optimization of the vacuum chamber should be considered, in this context, as an attempt to minimize the requirements on the feedback system.

The same is true for the dipole modes. The dipole modes $f = 1.429$ GHz and $f = 1.674$ GHz, see Table 4, have maximum impedances much higher than allowed by Eq. (11). Transverse stability depends again on the bunch-by-bunch transverse feedback system.

Resistive wall

The longitudinal resistive wall impedance is given by[2]

$$\frac{Z_l}{n} = Z_0 \frac{(1-i)}{2}\frac{\delta}{b}\frac{L}{2\pi R}F(a/b) \qquad (13)$$

where

$$\delta = \sqrt{\frac{2c}{Z_0 \sigma \omega}}$$

is the skin depth, $F = 1$ for a circular pipe with radius b and $F(a/b) = 0.97$ for a rectangular beam pipe with a ratio of height to width of $b/a = 2.4/4.6 = 0.52$.

The transverse resistive wall impedance for a circular pipe is

$$Z_\perp = \frac{2R}{b^2}\frac{Z_l}{n}. \tag{14}$$

The transverse impedance of a rectangular pipe can be estimated from the impedance of two parallel planes separated by a distance $2b$[3]:

$$Z_\perp = BZ_0\frac{(1-i)}{2}\frac{2R}{b^2}\frac{\delta}{b}\frac{L}{2\pi R}, \tag{15}$$

$B = \pi^2/24$ or $B = \pi^2/12$ for motion parallel or perpendicular to the planes, respectively.

For the 1300 m copper beam pipe of the HER arcs with a conductivity $1/\sigma = 17.7\ \mathrm{n}\Omega - m$, the longitudinal and transverse impedances are $Z_l = 0.823(1-i)\sqrt{n}\Omega$, $Z_x = 0.435/\sqrt{n}\ \mathrm{M}\Omega/m$,$Z_y = 0.87/\sqrt{n}\ \mathrm{M}\Omega/m$. The 900 m straight circular stainless-steel pumps with $b = 4.6$ cm and $1/\sigma = 900\ \mathrm{n}\Omega - m$ give $Z_l = 2.16(1-i)\sqrt{n}\ \Omega$ and $Z_\perp = 0.74/\sqrt{n}\ \mathrm{M}\Omega/m$.

Combining the two contributions, the total resistive wall impedances are

$Z_l = 2.98(1-i)\sqrt{n}\ \Omega$, $Z_x = 1.175/\sqrt{n}\ \mathrm{M}\Omega/m$, $Z_y = 1.61/\sqrt{n}\ \mathrm{M}\Omega/m$.

The longitudinal impedance at the roll-off frequency of the bunch $k\sigma_B = 1$, or $n = 3.5\times10^4$, is 0.56 kΩ, still within the limit of Eq. (9). Transverse impedance gives the dominant contribution to the total impedance at low frequencies and is higher than the limit Eq. (11). Again, stability of the beam relies on a transverse feedback system.

The loss factor and the power deposition per unit length due to the resistive wall (RW) impedance in a circular beam pipe are

$$\frac{dk_l}{ds} = \frac{1}{2\pi b}\sqrt{\frac{2}{Z_0\sigma}}\frac{\Gamma(\frac{3}{4})}{\sigma_B^{3/2}}, \qquad \frac{dP}{ds} = \frac{e^2}{2\pi b}\frac{n_b N_B^2 f_0}{\sigma_B^{3/2}}\sqrt{\frac{2}{Z_0\sigma}}\Gamma(\frac{3}{4}) \tag{16}$$

where n_b is number of bunches per ring, N_B is the number of particles per bunch, and f_0 is revolution frequency.

The copper coating on the stainless steel (SS) beam pipe may be used to reduce impedance and heating due to synchrotron radiation from upstream dipoles. The impedance depends on the thickness t of the coating: it decreases exponentially from the value for the SS pipe for $t = 0$ to the value of the copper pipe for $t \simeq \delta_{Cu}$ [4]

$$\frac{Z_l}{n} = Z_0 \frac{(1-i)}{2} \frac{\delta}{b} \frac{L}{2\pi R} \zeta(t/\delta) \tag{17}$$

where

$$\zeta(x) = \frac{1+\lambda+(1-\lambda)F(x)}{1+\lambda-(1-\lambda)F(x)}, \quad \lambda = \sqrt{\frac{\sigma_{SS}}{\sigma_{Cu}}}, \quad F(x) = e^{-2(1-i)x}. \tag{18}$$

The factor ζ goes to 1 for a thickness of the order of the skin depth of the coating.

The wall conductance at the transitions between arcs and straight sections has a jump. The impedance generated by such a jump in the conductivity may be estimated as the impedance of a step with a width equal to the difference of the skin depths and is negligible small.

HER DIP-screen

The screen separates the beam pipe and DIP-s in the HER dipole vacuum chamber. We considered several possible designs of the screen. The issues here were the screen vacuum conductance, beam impedance, crosstalk between the plasma in the DIP and the beam, screening the beam from dust particles, which may be produced in the DIP chamber, and screening the DIPs from the scattered synchrotron radiation and from penetration of TE modes, which may be generated by an offset beam or by TM/TE mode conversion in the beam pipe. The impedance issue includes the broad band impedance as well as the narrow-band impedance produced by the interference of waves generated by openings in the screen or by trapped modes.

The final design of the screen is based on the old T. Weiland idea of using continuous narrow longitudinal grooves cut halfway through the screen with small holes cut through another half of the screen thickness, see Figs. 5a,b. Grooves with the height w and depth d attenuate the beam field at the slot opening by a factor $e^{-\pi d/w}$ for frequencies $\omega/c < \pi/w$. For $w = 3$ mm chosen for the grooves, this condition is true

for all frequencies within the $\sigma_B = 1$ cm bunch spectrum. For $w = d$, the attenuation factor is $e^{-\pi} = 0.043$, and the broad-band impedance is reduced by the square of this factor, i.e. by a factor 500.

Narrow grooves also preclude the DIP plasma discharge affecting the beam. Continuous grooves reduce the broad-band impedance and eliminate complications of the narrow band impedance. Tilted grooves make efficient screening of the beam from dust particles and screening of the DIPs from the scattered synchrotron radiation.

Small 3 mm diameter holes give large enough vacuum conductance while simultaneously preventing penetration of the TE modes through the screen. A hole acts as an antenna for an incoming TE mode with a dipole moment proportional to r^3. The ratio of the radiated power to incoming power of a TE wave generated in the beam pipe with radius b by a bunch with rms length σ_B may be estimated as (see Eq. A1-37)

$$\frac{\Delta U_{rad}}{\Delta U_{in}} \simeq 0.3(\frac{r^3}{b\sigma_B^2})^2. \tag{19}$$

Hence, the penetration length of a TE mode scales with the hole radius as $(1/r)^6$ and, for 3 mm holes, is larger then the absorbtion length of such modes in the beam pipe walls. The hole separation is chosen large enough to make the gap impedance small. This prevents a significant crosstalk between holes, which could result in the adding-up of their dipole moments. The mesh reduces the total vacuum conductance by less than 4%.

There will be 192 of 5.6 m long screens, 6 grooves and 8400 holes per screen.

Each hole has an inductance (see Eqs. A1-24, A1-25) $L = 3.5 \times 10^{-5}$ nH, giving $L = 56.5$ nH for all holes of the 192 screens. The attenuation in the grooves reduce the total inductance of the holes to $L = 0.1$ nH.

The holes make the tolerance on the tilt of the grooves in respect with the beam direction very loose.

The total transverse impedance of the HER DIP screens is (Eq. A1-29) $Z_\perp = -i\,0.06\ k\Omega/m$.

The resistive part of the impedance and the loss factor (Eq. A1-32) for frequencies within the bunch spectrum are negligible small: $k_l = 5.5 \times 10^{-5}$ V/pC.

LER Antechamber

The LER antechamber, see Figs. 6a,b, replaces the DIP vacuum chamber of the HER and is similar to the antechamber of the ALS. The impedance of the ALS antechamber was measured and modeled with MAFIA[5]. The broad-band impedance is generated mostly by the discontinuity of the antechamber slot at the ends. The narrow-band impedance would correspond to modes trapped in the antechamber. Simulations and theory show that the dependence of the impedance on the length of the slot saturates when it becomes several times the rms bunch length at several σ_B (several cm). Excitation of the modes of the antechamber by the beam may be attenuated significantly if the slot of the ante-chamber is narrow and long: it works exactly in the same way as the grooves in the DIP screen. Fig. 7 shows the field pattern at the slot opening which confirms this statement. The attenuation factor found with MAFIA agrees with the simple formula $e^{-\pi d/w}$. However, the opening of the slot has to be large to accommodate the vertical size and the position jitter of the beam. Calculations were carried out with slot heights of 1.8, 1.4,and 1.0 cm. In all cases, the wake field is inductive and small, with the maximum values 0.04, 0.12, and 0.31 mV/pC, respectively, for a slot 40 cm long and 1 cm deep (see Fig. 8). Dependence on the depth c of the antechamber slot was compared for $c = 1$, 12, and 26 cm: the difference is negligible small. The calculated inductive $Z/n = 0.5$ $\mu\Omega$ or $L = 5.7 \times 10^{-4}$ nH is quite small and agrees with measurements. No trapped modes were found.

Abort system

Beam abort system requires a long 3 cm wide and 12 cm deep (from the beam to the bottom) vacuum chamber under the beam terminated with the dump[6]as shown in Figs. 9a, 9b. To minimize the impedance, the chamber is screened with 2 shallow RF tapers (down and back up to the beam pipe). The taper going down may be very long and gives negligible small impedance. The aborted beam goes through the taper going up. The angle α of this taper is limited by the energy deposition, which

depends on the radiation length X_0, and the thickness t of the screen: $\alpha > t/X_0$. MAFIA calculations for a 3 m long structure with two (up- and down-) tapers 8.5 cm high and angle $\alpha = 0.048$ give an inductive wake field with $L = 0.23$ nH. The loss factor is $k_l = 4.5 \times 10^{-3}$ V/pC. No narrow-band trapped modes were found.

Interaction Region

The interaction region is a complicated 3-D set of masks and tapers as shown in Fig. 10a, and 10b. It was modeled with MAFIA as a whole structure. The broad-band wake field is approximately inductive with $L = 5$ nH (see Fig. 11). The loss factor of the total structure is $k_l = 0.12$ V/pC. Most of the power lost due to the broad-band impedance propagates downstream and is absorbed outside the IR.

The main issue for the IR is heating. The heating in the IR comes mostly from the modes trapped in the central Be pipe ± 20 cm around the IP, 3 watts of ohmic losses in the Be pipe, and, to a much smaller extent, from the losses in upstream components of the beam pipe, mainly from the IR septum. The broad-band impedance has maximum $ReZ = 0.46\,\mathrm{k}\Omega$ at 6 GHz as result of averaging of the trapped modes.

The $l = 40$ cm Be pipe with radius $b = 2.5$ cm and adjacent masks with circular openings on both sides was modeled separately. The loss factor of this section is $k_l = 0.012$ V/pC. A number of the trapped modes are confined in the 40 cm Be pipe due to the adjacent masks, see Fig. 12. The frequencies of the modes range from 4.6 GHz to 5.92 GHz. The frequency interval at the low frequency end is about 50 MHz. The spacing increases to 150 MHz at the upper frequency end. The trapped modes are, basically, TM_{01} modes of the pill-box cavity with frequencies

$$\frac{\omega}{c} = \sqrt{(\frac{\nu}{b})^2 + (\frac{n\pi}{l})^2}. \tag{20}$$

The lowest radial number $\nu = 2.4$ and the number of the half waves n along the structure in the range from $n = 1$ to $n = 12$.

Both beams excite the modes simultaneously. For a symmetric structure, the amplitude A of the even modes ($n = 2m$) excited by a bunch is proportional to $(N_+ + N_-)\sin(kl/2)$, and for odd modes ($n = 2m + 1$), $A \propto (N_+ - N_-)\cos(kl/2)$

where $N_\pm$ is the number of particles per bunch in each beam. Therefore, the power deposited in even modes scales as $P \propto (N_+ + N_-)^2$. For an IP placed asymmetrically at a distance l_1 from one end of the pipe, the amplitude of the even and odd modes is

$$A_\pm \propto (N_+ + N_-)[\sin(kl_1) \pm \sin(kl_2)] + (N_+ - N_-)[\cos(kl_1) \mp \cos(kl_2)] \qquad (21)$$

and odd modes can be excited even for equal number of particles in both beams.

The power deposition within the Be pipe depends on the Q-factor of the modes.

The resistive $Q \simeq 1.25\,10^4$ in our case is very large. The loaded Q_L depends on the coupling of the trapped modes to the propagating modes in the beam pipe on the other side of the masks, where the beam pipe radius is much larger than that for the Be pipe. We estimate for round openings in the masks that

$$Q_{ext} \simeq (\frac{\pi f_m l}{c})(\frac{b}{a_0})^2 \frac{1}{W_t} \qquad (22)$$

where a_0 is the radius at the neck of the masks, and W_t is the probability of tunneling through the mask for a mode with frequency f_m:

$$W_t = |e^{-\int dz|q(z)|}|^2, \qquad |q(z)| = \sqrt{(\frac{\nu}{a(z)})^2 - (\frac{2\pi f_m}{c})^2} \qquad (23)$$

The integral may be estimated as

$$\int dz|q(z)| \simeq \frac{2\sqrt{2}}{3}\Delta^{3/2}\frac{\nu}{a'} \qquad \Delta = \frac{\nu c}{\omega_m a_0} - 1, \qquad (23)$$

where $a' = |da/dz|$ is the slope of the mask.

For our case, this approach gives $Q_{ext} = 1200$ for a typical $f_m = 5.7$ GHz, and $a_0 = 1.5$ cm. In this case, only 10% of the power loss goes to the Be pipe wall.

In principal, detuning from a resonance can be done by heating of the Be pipe. The temperature dependence of the mode frequency

$$\frac{\Delta f}{f} \simeq \frac{(\Delta l/l)}{1+(\frac{\nu l}{\pi n b})^2} \tag{25}$$

is different for different n: the coefficient is equal to $1/50$ for $n = 1$, and $1/2$ for $n = 12$. For $(\Delta l/l) \simeq 10^{-5}\Delta T$, and $\Delta T \simeq 100^o$ the frequency shift for the mode $n = 12$ is small but comparable with the width of the resonance.

The power loss to an even mode with the loss factor κ_m and loaded Q_m^L is (see Eq. (A3-5))

$$P = P_0 D, \qquad P_0 = I_\Sigma^2 \kappa_m \frac{s_B}{c} \tag{26}$$

where $P_0 = 480\,\mathrm{W}$ is the power loss of uncorrelated bunches, and $I_\Sigma = I_+ + I_-$. The enhancement factor D for a train of bunches with bunch spacing s_B (see Eq. (A3-6))

$$D = (\frac{c}{\omega_m s_B})\frac{1/Q_m^L}{(\Delta\omega_m/\omega_m)^2 + (1/2Q_m^L)^2} \tag{27}$$

depends on the detuning of the mode frequency from the resonance frequency ω_r, $\omega_r s_B/(2\pi c) = integer$. Far away from the resonance $\Delta\omega_m/\omega_m >> 1/2Q_m$ and we get the factor $D << 1$. At the resonance

$$D_{max} = \frac{4Q_m^L c}{\omega_m s_B} \tag{28}$$

and, for $s_B = 120$ cm and $f_m \simeq 6$ GHz, $D_{max} >> 1$ provided that $Q >> 70$. For $Q_m = 1200$, the enhancement $D_{max} = 16$, and $D_{min} = 4.4 \times 10^{-3}$. If only 3 out of 12 trapped modes are resonant, the power loss is $P = 3 \times (1/12) \times 480W \times D_{max} = 1.92$ kW. Power dissipated in to the wall itself in this case is $P_{wall} = 192$ W.

The frequency spectrum of a train of bunches also has frequencies at the multiples of the revolution frequency ω_0. The number of independent coherent modes is equal

to the number of bunches n_B. If the amplitude of the coherent mode is A_l, the power loss of a particle due to this mode is (Eq. A3-17)

$$P \simeq 2I_{av}^2(\frac{A_l\omega_l}{2c})^2(R/Q)_l Q_L^l. \tag{29}$$

The rms amplitude of the coherent modes is of the order of $A_l \simeq 2\sigma_B/\sqrt{n_B}$, and the power loss due to single coherent mode is $2I_{av}^2(\sigma_B\omega_l/c)^2(Q_L/n_B)(R/Q)_l$. The number of such modes within the resonance width $\omega_l/(Q_L)$ is $\omega_l/(2Q_L\omega_0)$. The total loss of the coherent modes

$$(2/\pi)(\sigma_B\omega_l/c)^2 P_0$$

is independent of Q_L and is smaller than the uncorrelated power loss P_0.

Hence, the wall power loss is acceptable provided there is a careful design of the pipe and adjacent masks to avoid resonances with the bunch spacing.

Injection port, kicker ceramic

The injection port generates impedance due to a 2×12 cm slot in the tapered beam pipe wall with the average pipe radius $b = 3.8$ cm (see Fig. 13 a,b). Both broad-band impedances, of the slot and the taper, calculated with MAFIA, are mostly inductive. The slot gives an inductance $L = 0.025$ nH and a loss factor $k_l = 1.5 \times 10^{-3}$ V/pC. The contribution of the taper is larger: $L = 0.15$ nH and $k_l = 5.4 \times 10^{-3}$. Including both contributions, the injection port gives $L = 0.17$ nH and $k_l = 6.9 \times 10^{-3}$ V/pC. No indication of the trapped modes was found.

Kicker ceramic section ($\epsilon = 9 >> 1$, thickness $\Delta b = 4$ mm, tube radius $b = 2.75$ cm) for the injection kicker (length $l = 1.25$ m) have a thin titanium coating (resistivity $\rho_{coat} = 43\ \mu\Omega - \text{cm}$). The wake field generated by the ceramic section depends[7] on the parameter

$$V = \frac{\sigma_B \rho_{coat}}{Z_0(\Delta b)t}. \tag{30}$$

where $t = 0.75\mu m$ is the thickness of the coating. For this coating thickness, $V << 1$

and the wake

$$W(s) = \frac{2l}{tb}\frac{\rho_{coat}}{Z_0}\rho(s) \tag{31}$$

is mostly resistive, Eq. Appendix 1-22,

$$R_\Omega = \frac{l\rho_{coat}}{2\pi bt}. \tag{32}$$

For $l = 1.25$ m, resistive part of the impedance $R_\Omega = 5.7\ \Omega$; the loss factor $k_l = 0.04$ V/pC.

The inductive impedance corresponds to $L = 0.5\,10^{-3}$ nH.

BPM

There are 290 sets of 4-button BPMs, see Fig. 14, in the HER. A BPM should have high sensitivity within the bandwidth 1 GHz, but, at the same time, must have low power going to the cables, low beam impedance, and low heating inside of the the BPM structure. We compared several designs of a BPM.

A 2 cm diameter round button has reasonable sensitivity but the impedance has resonance at 6 GHz with relatively high shunt impedance. The problem may be avoided making the button asymmetric. In particular, a narrow bridge across the gap eliminates the resonance but makes power to the cable too high.

Measurements confirmed the results of MAFIA simulations quite well, see Figs. 15a,b.

The final version of the BPM uses a round button with $a = 1.5$ cm diameter. Such a design (see Fig. 16) satisfies requirements for sensitivity, heating, and power output to the cables.

For a 4-button BPM and $N_B = 3 \times 10^{10}$, the sensitivity[9]is defined by the impedance 0.5Ω at 1 GHz.

The impedance of a single button is generated by a $w = 2$ mm round slot. Impedance of a slot can be esimated as difference of the impedances of two round

holes with radii a and $a+w$. That gives polarizability $\alpha_e + \alpha_m = 2wa^2$ and

$$L = \frac{2wa^2}{\pi b^2}$$

or $L = 5.7 \times 10^{-3}$ nH per button, $L = 6.8$ nH for 300 4-button BPMs. Kurennoy[8] estimate is smaller: $\alpha_e + \alpha_m = wa^2/8$. MAFIA[9] gives $L = 3.7 \times 10^{-2}11$ nH and the loss factor $k_l = 2.7 \times 10^{-3}$ V/pC for a 4-button BPM; $L = 11$ nH, and $k_l = 1$ V/pC for 300 BPMs.

Hence, the power loss by the beam is $P = 126$ W per BPM at the current 3A. Power output to a cable is found by direct calculations of the fields at the port and is 9 W per cable. The 1 cm beam offset in the direction to a button can increase the power to the cable by a factor of 2 because the frequency harmonic of the field depends on the distance as $1/r$.

Transverse broad-band impedance of 300 BPMs found in simulations[9] is $Z_x = 6.7\,k\Omega/m$, and $Z_y = 5.5\,k\Omega/m$. There is a mode of the narrow-band longitudinal impedance with the total shunt impedance 6.5 $k\Omega$ at $f = 6.8$ GHz for 300 BPMs. The field pattern of the mode indicates that this mode is a TE_{11} mode (in respect with the button axis). Transverse narrow-band impedance Z_x has a mode with the total $R_s = 90\,k\Omega/m$ at $f = 6.8$ GHz, and $Z_y = 120\,k\Omega/m$ at $f = 6.2$ GHz.

The impedance is only slightly more than required by the conservative estimate of Eq. (9) and may increase the power of the feedback amplifier not more than by 5%.

Ceramic in the BPM has $\epsilon = 10$ and the loss tangent of the ceramic $\delta_c = 0.0007$. The power absorbed in the ceramic with thickness $h = 3$ mm by a propagating wave

$$\frac{P}{P_{in}} = (\frac{\omega}{c})\frac{h}{2}\epsilon\delta_c \qquad (33)$$

is $P = 12$ mW per button for $P_{in} = 126$ W loss per BPM and $f = 7.5$ GHz.

The power absorbed in the thin Ni layer at the edge of the ceramic in a coax with characteristic impedance $Z_W = (Z_0/2\pi)\ln(b/a)$ and radii a, b is

$$\frac{P}{P_{in}} = (\frac{\omega}{c})\frac{\mu\delta h}{d_{eff}} \tag{34}$$

where for TEM wave

$$1/d_{eff} = \frac{(a+b)}{2ab\ln(b/a)}, \tag{35}$$

and δ is the skin depth of Ni. Note, that $\mu\delta$ scales as $\sqrt{\mu}$. The permeability μ of Ni rolls off at high frequencies very rapidly and at 7 GHz is of the order $\mu = 3$, see Fig. 17, reducing the power loss to Ni to $P = 46.8mW$ per button for the loss $P_{in} = 126$ W per BPM.

The fraction of power absorbed in the resistive walls is of the order of the ratio of the length of a button $l = 1.9$ cm to the absorption length

$$\frac{P}{P_{in}} = (\frac{\omega}{c})\frac{\delta l}{d_{eff}} \tag{36}$$

and is very small.

The Q factor given by these losses is $Q_0 = 534$. The loaded Q_L determined by MAFIA and confirmed in wire measurements on a BPM prototype is much smaller $Q_L \simeq 60$. It is too low to enhance the power loss in a train of bunches.

It is worthwhile to compare the loss factor $k_l = (\omega/2)(R/Q_0)$ of the longitudinal mode $f = 6.8$ GHz with the broad-band loss $k_l = 2.7 \times 10^{-3}$. Taking $Q_0 = Q_L$ and $R_s = 22\,\Omega$ per BPM, we get $k_l = 0.46/Q_L$ per BPM what, for $Q_L = 100$, is larger than the broad-band loss factor. That indicates again that the loaded Q_L should be much less than Q_0 and has to be dominated by the radiation back to the beam pipe.

For heating, the relevant parameter is the wall losses by a propagating wave multiplied by the number of passes of a wave, $Q_L c/\omega l \simeq 36$ for $Q_L = 60$. That gives absorbed power 2.5 W and the heating of the button at the normal conditions should not be a problem.

If a button cable is accidentally disconnected, the situation may be different. First, reflection from the open unmatched end can produce a standing mode within the BPM. Consider a button as a transmission line. The currents and voltages at the both ends of the line are related by the characteristic impedance of the line Z_L and the impedance of a termination Z_t

$$V_{in} = V_t[\cos\psi + i\frac{Z_L}{Z_t}\sin\psi], \quad I_{in} = I_t[\cos\psi + i\frac{Z_t}{Z_L}\sin\psi].$$

At the normal conditions, the characteristic impedance of the line is matched to the impedance of the cable and the voltage and current at both ends of the button are the same, except of a phase $\psi = ql$ where q is the propagating constant and l is the length of the line. For a disconnected cable, the current at the output port of the button is zero. The current at the input port is related to the density of the image current induced by the beam and, therefore, is the same as at the normal operation. Hence, the voltage at the input port increases compared to the normal operation by a factor $\cot\psi$. For a TEM wave with frequency ω, the phase ψ is $\psi = \omega l/c$. From a reciprocity theorem it follows, that the voltage induced at the beam current and, hence, the energy loss by the beam and heating are also increased by the same factor $\cot\psi$, or by a factor 6.25 for $f = 7.5$ GHz and $l = 1.9$ cm. Radiation to the beam pipe is increase also due to the reflected TEM mode. Simulations with MAFIA confirmed appearence of the new resonances in the beam impedance with a disconnected cable.

The same design of a BPM-s with flat buttons will be used in the arcs and straight sections. In the straight sections, a flat button will be flush with the round beam pipe only at the center making small cavities at the edges. The effect was simulated with MAFIA and changes the broad band impedance only by few percent.

To screen BPM-s from halo electrons, buttons will be recessed by 0.5 mm (including tolerance for installation). Other factors such as direct or secondary synchrotron radiation, or electrons emitted from the chamber walls are not affected by small recess under consideration. For the beam pipe gap $b = 2.5$ cm and the betatron wave length $\lambda_\beta \simeq 50$ m the incident angle of a halo electron is $\theta = 4b/\lambda_\beta$ and the recess $\Delta \simeq 2r\theta = 0.75 \times 10^{-3}$ cm would be enough for the button with radius $r = 0.75$

cm. This number is very small, and practically recess is defined by the tolerances of the BPM installation. Excessive recess may, however, produce trapped modes, see Appendix 2.

The lowest TM mode in a rectangular beam pipe with dimensions $a \times b$, $a > b$ is

$$H_x = \frac{A}{b} \sin \frac{\pi x}{a} \cos \frac{\pi y}{b}, \quad H_y = -\frac{A}{a} \cos \frac{\pi x}{a} \sin \frac{\pi y}{b} \tag{37}$$

and has the cut-off frequency $(\omega_c/c)^2 = (\pi/a)^2 + (\pi/b)^2$. For 4 buttons with radius r located at $x = x_b = a/4$, $y = 0$ or $y = b$ and recessed by Δ, the total volume of bulging is $V_b = 4\pi r^2 \Delta$, and the ratio ζ defined in Eq. (A2-3) is

$$\zeta = \frac{4a^2 \sin^2(\pi x_b/a)}{a^2 + b^2} = \frac{2a^2}{a^2 + b^2}. \tag{38}$$

Eq. (A2-4) gives

$$\frac{\Delta\omega}{\omega} = \frac{(2\pi)^4 r^4 \Delta^2}{2b^4(a^2 + b^2)}. \tag{39}$$

Resistive wall gives in this case is

$$(\frac{\Delta\omega}{\omega})_{RW} = \frac{\delta}{ab} \frac{a^3 + b^3}{a^2 + b^2}. \tag{40}$$

Recess is small if it gives the frequency shift small compared to the shift due to resistive wall:

$$\Delta < (\frac{b}{2\pi r})^2 \sqrt{\frac{2\delta}{ab}(a^3 + b^3)}. \tag{41}$$

Take $a = 9.0$ cm, $b = 4.8$ cm, $r = 0.75$ cm, $\delta = 1\mu m$. Then $\Delta < 0.64mm$ has to be taken as the maximum acceptable recess of a button in the arcs. In the round pipe of the straights, the resistive wall frequency shift is

$$(\frac{\Delta\omega}{\omega})_{RW} = \frac{\delta}{2b}. \tag{42}$$

The acceptable button recess for 4-button BPM in the beam pipe with radius b is

$$\Delta < \frac{b^3}{2\nu r^2} \sqrt{\frac{\delta}{b}} \tag{43}$$

and larger than that in the arcs: $\Delta < 1.6$ mm for $b = 4.5$ cm, and $r = 0.75$ cm.

The estimate of the acceptable recess is conservative not taking into account losses to a BPM cable.

Bellows, Quad/dipole offset, RF seals

We compared several designs of a bellows module. The final design uses fingers outside of the beam pipe and does not use large synchrotron radiation masks. Instead, the beam pipes are offset horizontally by few mm and the transitions are tapered (see Figs. 18 a,b), to produce sufficient protection from the synchrotron radiation.

The impedance of the quadrupole/dipole transition with the tapered beam pipe offset of 5 mm was modeled with MAFIA. The loss factor of the transition is $k_l = 4.5\,10^{-4}$ V/pC. No trapped modes were found either by considering propagation of the Rf Gaussian bunch or in the S-matrix calculations.

The impedance of the bellows module is generated by finger slots, slots in the bellows corners, small tapers of the synchrotron radiation masks, and the RF seals. All contributions are small and correspond to an inductive impedance.

Impedances of the tapers of the bellow module were modeled as independent axi-symmetric structures with radii equal to the distances from the beam line to the corresponding taper. The results then were averaged proportional to the azimuthal filling factors. That gives the inductance $L = 0.044$ nH and the loss factor $k_l = 3.3 \times 10^{-3}$ V/pC per bellows. For 300 bellows the total inductive impedance is only $L = 13$ nH and $k_l = 1$ V/pC. The taper with the large 20^o angle gives after averaging small contribution due to the larger distance of the taper from the beam and the small vertical size of the vacuum chamber.

Impedance of the 50 finger slots with the length 1.25 cm, and width 0.76 mm can be estimated using Eqs. (A1-24) and (A1-26). That gives $L = 1.5 \times 10^{-4}$ nH for 50 fingers per bellows. Eight slots in the corners are wider $w = 4$ mm and, although they are farther away from the beam, give $L = 7.6 \times 10^{-4}$ nH per bellow, more than the finger slots. The total inductance of the slots is $L = 0.27$ nH per 300 bellows. The difference in the dimensions of the beam pipe in the arcs and straights is of no significance here.

The RF seals in a bellows module are designed to give a small 1 mm high and 5 mm wide recess in the beam pipe. The height of the recess can not be known exactly but the RF seal should not look like a groove which may generate trapped modes. The impedance of the RF seal is inductive[10]

$$L = \frac{4\Delta^2}{b}. \tag{44}$$

To be conservative, we take $\Delta = 1$ mm, $g = 0.25$ mm, $< 1/b >= 0.33\, cm^{-1}$. Then $L = 1.6 \times 10^{-2}$ nH per RF seal. ABCI gives the same $L = 1.07 \times 10^{-2}$ nH and the loss factor $k_l = 1.1 \times 10^{-4}$. Neglecting again the difference between dimensions of the bellows in the straights and arcs, we get $L = 0.47$ nH or $Z/n = 0.4 \times 10^{-3}\ \Omega$ for the 290 RF bellows seals in the ring. (Note, that this is an overestimate of the actual impedance).

The estimate of the impedance of the Rf bellows seals is valid also for the flange/gap rings. These give an additional $L = 0.47$ nH per ring.

Clearly, the main issue for the bellows is not the beam impedance but the heating and operational reliability of the fingers.

The heating, in particular, may be produced by the radiation through the slots, and by the coupling of the beam to the modes of the cavity between fingers and the bellow convolutions.

Radiation of the slots is the dipole radiation with the dipole moment induced by the field of a bunch or by the field of a TM HOM generated somewhere upstream from the bellow. The first mechanism gives the average radiated power due to the beam

$$P_{beam} = \frac{Z_0 I_{av}^2}{2\pi^{3/2}} \left(\frac{s_B}{\sigma_B}\right) \left(\frac{lw^2}{32 b \sigma_B^2}\right)^2. \tag{45}$$

For $I_{av} = 3$ A, $\sigma_B = 1$ cm, and $b = 3.3$ cm that gives $P = 0.45$ W/bellow from 8 corner slots. 50 finger slots, being narrower, give less by a factor of 123.

Consider now the TM modes generated by the beam somewhere upstream at the components with the total broad-band loss factor k_l. That defines the power

of the incoming HOM modes averaged over frequencies within the bunch spectrum $P_{TM} = I_{av}^2 k_l s_B/c$. Power P_{TM} radiated from a slot due to incoming TM mode may be compared then with the power radiated by the beam P_{beam}:

$$P_{TM} = 2\sqrt{\pi} k_l \sigma_B P_{beam} \tag{46}$$

and, for the total loss factor $k_l \simeq 3$V/pC can be larger than P_{beam} by a factor of 10.6. The radiated power becomes of the order of 5 W per bellows module. This estimate does not take into account local variation of the power in TM HOM-s.

Radiation from the finger slots induced by a TE mode is 1290 times larger than radiation due to regular TM modes mostly due to the factor $(l/w)^4$. Taking into account difference in the number of finger and corner slots, we get the power $P = 312.8$ W per bellow module provided that the power of the incoming TE and TM modes are the same. However, beam does not couple with the TE modes: they can be produced by the transformation of the TM-modes or due to decay of modes in asymmetric structures with hybrid modes. In both cases there is a small factor which makes the power of the TE modes of the order of few percent of the average power of the TM HOM-s reducing the radiation power due to TE HOM-s to few watts per bellows module.

Another mechanism which may be important for heating is the resonance excitation of the eigen modes in the cavity between fingers and bellow convolutions if their frequencies are in resonance with the bunch spacing $\omega s_B/c = 2\pi n$. The enhancement factor of the power deposited by the beam is $D = 4Q_L/(2\pi n)$, see Eq.(A3-6). For a frequency $f \simeq 1$ GHz, the factor $\omega s_B/c = 8\pi$ and D depends on the loaded Q_L, $D_{max} = Q_l/4\pi$. For a TM HOM corresponding $k_l = 3$ V/pC the power $P = 0.02$ W/bellow is still small even for $Q_L = 10^4$, which can be expected with stainless-steel convolutions.

Lumped pumps

Ports of the lumped vacuum pumps are screened with a grid of long and narrow slots. The layout for the straight section of the HER is shown in Fig. 19a, and for

the arcs in Fig. 19b. In the arcs, there are 24 slots altogether in the upper and lower decks with length $l = 15.4$ cm and width $w = 2.54$ mm.

The impedance of each slot of the pumping screen in the arcs, see Eqs. (A1-24), (A1-26) is $L = 1.1 \times 10^{-4}$, and the total contribution of the 24 pumping slots for all of the 200 ports in the arcs is 0.53 nH.

The potential problem here is not the broad-band impedance but the possibility to have trapped modes.

As an example consider a $g = 2$ cm long circular cavity with a depth $\Delta = 3$ mm in the $b = 3$ cm radius beam pipe[11]. The broad-band impedance of such a small cavity is small and mainly inductive, see Eq. (41). However, MAFIA finds a narrow resonance with shunt impedance $R_s = 7$ $k\Omega$ and $Q = 2.7 \times 10^4$. Such a mode can be considered as a modified propagating mode with a frequency close to the cutoff frequency $\omega_m/c = \nu_0/b$ where $\nu_0 = 2.405$ is the first root of the Bessel function $J_0(\nu_0) = 0$. A small bulge of the beam pipe changes the frequency of the mode, shifting it below cutoff and makes a trapped mode. The situation is quite analogous to the frequency shift of a mode in a cavity due to a small perturbation of the boundary. The mechanism is described in the original paper by Stupakov and Kurennoy[12]. The paper gives also a numerical example quite similar to described above. Relevant formulas are given in Appendix 2.

The theory predicts a trapped mode at the grid of the vacuum port in the arcs with the shunt impedance[13] $R_s = 644.\Omega$, Q factor of the order of 3.5×10^4, and localization length $L = 35$ cm. The shunt impedance of a trapped mode at the vacuum ports of the straight sections is smaller, $R_s = 85.\Omega$. MAFIA confirms that slots cut in the circular beam pipe produce a trapped mode with parameters given by the total magnetic polarizability of the slots, Fig. 20a,b.

The frequency shift of the trapped mode is larger than the width given by the resistivity of the wall. Radiation outside of the thick beam pipe from a narrow slot is suppressed at the frequency close to the cut-off. Radiation into the beam pipe is possible only in the TE_{11} mode, which has the cut-off frequency lower than the

cut-off for the TM_{01} mode. However, the width due to this process is very small. For a symmetric placement of the slots, radiation is additionally suppressed.

To eliminate trapping, the beam pipe at the vacuum port may be recessed with the recess volume equal or slightly larger than the polarizability of the slots. Numerical simulations with MAFIA confirmed this statement[13].

A bow-like recess of the slots in the arcs has to have saggita $\Delta > 0.27$ mm and, practically, will be set to be larger than the fabrication tolerances.

A mesh of small holes on the pump side should be used to prevent propagation of TE modes to the pumps.

Tapers

The circular beam pipe of the straight sections ($b = 4.5$ cm) and the rectangular beam pipe of the arcs (2.5×4.5 cm) are connected with tapers (see Fig. 21). The 2D modeling of a 10^o taper connecting 2 circular beam pipes with the radii 2.5 and 4.5 cm gives a conservative estimate of $k_l = 5.1 \times 10^{-3}$ V/pC and $L = 0.3$ nH per taper (see Fig. 22). The wake is inductive. The real part of the impedance is $ReZ < 0.5\Omega$ per taper for frequencies below 5 GHz.

Collimators

A simple model of a collimator as a pair of tapers with a height of 4.5 cm and a taper angle 10^o gives a loss factor $k_l = 2 \times 10^{-2}$ V/pC. The wake is inductive and corresponds to $L = 1.57$ nH per collimator (see Fig. 23).

Feedback kickers

The longitudinal and transverse kickers for PEP-II are modeled after those designed and measured for the ALS[14], see Fig. 24. The longitudinal beam impedance of the ALS transverse kicker was found to be $Z/n = 0.53\ m\Omega$ and the loss parameter was estimated as $k_l = 0.66$ V/pC. For the longitudinal ALS kicker, $Z/n = 25\ m\Omega$ and the shunt impedance is 300 Ω within the passband 1.25 GHz.

Tolerance on the beam pipe misalignment

The misaligned beam pipes can generate additional impedance. For a small mis-

alignment δ of two beam pipes with radius b the impedance is inductive[15]

$$L = \frac{4}{3}\frac{\delta^2}{b}. \tag{43}$$

For $\delta = 2$ mm and $b = 2.5$ cm that gives $L = 0.023$ nH. In the worst case of 300 misalignments of this kind give $L = 7$ nH. That gives the upper bound for the misalignments with rms error 2 mm. We checked this formula with the 2-D code ABCI considering two pipes with radii 4.7 and 4.5 mm. That gives $L = 0.030$ nH, and the loss factor $k_l = 1.4\,10^{-3}$ V/pC. Inductance, after scaling proportional to the azimuthal filling factor 1/2 and ratio of radii is $L = 0.027$ nH in a good agreement with the analytic formula.

Impedance of the Synchrotron Radiation

The maximum value of the impedance caused by the synchrotron radiation

$$max(\frac{Z}{n}) = 300\frac{b}{R}\Omega \tag{44}$$

for $b = 2.5$ cm and the average radius $R = 350$ m is quite large giving $L_{max} = 25$ nH. However, the maximum value corresponds to the harmonic number $n_{th} \simeq (\pi R/b)^{3/2} = 7.5 \times 10^6$. Such frequencies are much larger than frequencies within the bunch spectrum which, for $\sigma = 1$ cm, rolls-off starting from $n = 3.5 \times 10^4$. For frequencies $n < n_{th}$ the impedance of the synchrotron radiation is suppressed exponentially and gives negligible contribution for the PEP-II impedance budget.

Cross-talk

As usual, in this calculations we neglected the cross-talk between spatially close components. Example of the periodic array of irises shows that such an interference tends to reduce the total impedance, but no serious studies of the problem are available, to our knowledge, at the present time. We want to give only few comments.

At high frequencies, diffractional model can be used to estimate the length of the interaction of the wake with a particle. Consider, for example, a scraper with the inner radius a in the beam pipe with radius b. The angle of diffraction θ for

a wave with frequency $\omega = 2\pi f$ is $\theta \simeq c/\omega a$. The elements of the vacuum system can be considered as independent if the distance between is larger than the length of diffraction $L \simeq (b-a)\omega a/c$.

If two recessed elements of the vacuum chamber are close to each other, a mode can be localized between them. However, to have a large Q factor, the mode should not be coupled with propagating modes outside of the elements. This coupling for smooth obstacles with the width w and height of the recess Δ depends exponentially on the parameter

$$\frac{\nu w}{b}\sqrt{\frac{2\Delta}{b}}$$

where b is the beam pipe radius, and $\nu = 2.4$ is a root of the Bessel function. To have large Q, the parameter should be much larger than one.

This problem was considered for the RF seal and recessed vacuum port. Both have very small height (in the model it was 1 mm) and are close to each other. Field pattern found in MAFIA simulations confirmed, as it was expected, that such a system does not confine a mode, see Fig. 26.

Summary

The main contributions to the impedance of PEP-II come from the RF cavities and the resistive wall impedance. Components giving the main contribution to the inductive part of the impedance are summarized in Table 6. The contribution of an element is calculated and multiplied by the number of such elements given in Table 2. These elements are mainly inductive but do have a small resistive part, which give a non-zero loss factor of $k_l = 3.1$ V/pC. We can describe this loss by a constant resistivity R_Ω in Eq. (A1-14) using Eq. (A1-19).

The longitudinal impedance is the sum of the narrow-band impedance and the broad-band impedance as it is discussed in Appendix 1. The narrow-band impedance is given by the modes of the cavities, see Table. 3, and few modes in the BPM-s, and kickers. The broad-band impedance can be parametrized by Eq. (A1-18) with inductance L given by Table 6 and R_W defined by the resistive wall impedance above.

The transverse impedance is dominated by the modes of the RF cavities, Table 4, and resistive wall estimated above. The rest of the ring gives small contribution and, therefore, it may be suffice to have an estimate of such a contribution. It can be obtained in a standard way, see Eq. (A1-8), from results of Table 6.

Table 6. The main contribution to the inductive impedance of PEP-II

		L (nH)	k_l (V/pC)
	Dipole screens	0.10	
	BPM	11.	0.8
	Arc bellow module	13.5	1.41
	Collimators	18.9	0.24
	Pump slots	0.8	
	Flange/gap rings	0.47	0.03
	Tapers oct/round	3.6	0.06
	IR chamber	5.0	0.12
	Feedback kickers	29.8	0.66
	Injection port	0.17	0.004
	Abort dump port	0.23	0.005
Total		83.3	3.4

Figure Caption

Fig. 1. RF cavity shape (without damping ports).

Fig. 2. Longitudinal Wake potential of a RF cavity.

Fig. 3a, and 3b. Real and imaginary part of the monopole broad-band impedance of a RF cavity.

Fig. 4a, and 4b. The same as Fig. 3 but for dipole longitudinal impedance. The beam pipe radius $b = 4.5$ cm.

Fig. 5 a,b. The layout of the DIP screen.

Fig. 6 a,b. The layout of the LER antechamber.

Fig. 7. The electric field pattern for the antechamber.

Fig. 8. The longitudinal wake potential $W(s)$ for different length and depth of the antechamber.

Fig. 9 a,b Layout of the abort system and the model used in MAFIA simulations.

Fig. 10a,b. Layout of the masks of the IR in horizontal and vertical planes.

Fig. 11. Broad-band impedance of the IR.

Fig. 12. Field pattern of trapped modes of the Be pipe of the IR.

Fig. 13 a,b. Injection port and the model used in MAFIA simulations.

Fig. 14. Layout of a 4 button BPM.

Fig. 15 a,b Comparison of MAFIA simulations with wire measurements of a BPM.

Fig. 16. Impedances and wake fields of a 1.5 cm button.

Fig. 17. Dependence of the permeability μ on frequency.

Fig. 18 a,b. Layout of a bellows, x, z and y, z planes.

Fig. 19 a,b. Layout of the slots of a vacuum port for the straight sections

and arcs respectively.

Fig. 20. (a) Dependence of the E_z component of a trapped mode on the distance from the slot center and (b) the electric field pattern.

Fig. 21. Layout of the taper of a transition from a round to a hexagonal pipe.

Fig. 22. Wake potential of the taper.

Fig. 23. Longitudinal wake potential of a model of a typical collimator.

Fig. 24. Layout of a feedback kicker.

Fig. 25. Layout of a valve.

Fig. 26. Field pattern with two 1 mm high restrictions. The beam pipe is closed at the ends. The wide restriction confine the mode but a small one has no effect. In a real system, the mode would propagate to the left.

Appendix 1. Definitions and general properties of impedances and wake fields

The impedance $Z(\omega)$ of an accelerator characterizes (in a linear approximation) the electromagnetic (EM) fields excited in the vacuum chamber by a circulating current. It is one of the main factors defining coherent stability of the beam.

The (δ-functional) wake field $W_l^\delta(s)$ defines the energy loss $\Delta E(s)$ of a particle with a charge e due to the EM field excited by a point-like particle with the charge $N_B e$ moving at the distance $s \geq 0$ ahead of the test particle:

$$\Delta E(s) = -N_B e^2 W_l^{\delta,r}(s). \qquad (A1-1)$$

For axi-symmetric structurs, the wake can be expanded over the transverse offsets of the leading, r_l, and trailing, r_t, particles

$$W_l^\delta(s,r) = W^{(0)}(s) + r_l r_t W^{(1)}(s) + .., \qquad (A1-2)$$

where the first term corresponds to axi-symmetric or monopole modes($m = 0$), and the second term to dipole modes ($m = \pm 1$) of the wake field. For the longitudinal dynamics it is usually sufficient to consider only the first term.

Complementary to the wake $W_l(s)$, the impedance $Z(\omega)$ describes the interaction of the beam with its environment in the frequency domain. They are related by the Fourier transform. In particular, the longitudinal impedance is

$$Z_l(\omega) = \int d(s/c) W_l^\delta(s) e^{i\omega s/c}. \qquad (A1-3)$$

The wake potential $W(s)$ is defined by averaging the wake function $W_l^\delta(s)$ with the bunch distribution function $\rho(s)$, $\int \rho(s)ds = 1$:

$$W(s) = \int_s^\infty ds_1 \rho(s_1) W_l^\delta(s_1 - s). \qquad (A1-4)$$

Sometimes more useful the wake potential $< W(s) >$ averaged also over the distri-

bution of the trailing bunch

$$< W(s) >= \int ds_1 ds_2 \rho(s_1)\rho(s_2) W_l^{\delta}(s_1 - s_2 + s),$$

$$< W(s) >= \int \frac{d\omega}{2\pi} \mathrm{Re} Z_l(\omega) |\rho(\omega)|^2 e^{-i\omega s/c}.$$

For a Gaussian bunch, $|\rho(\omega)|^2 = e^{-(\omega\sigma_B/c)^2}$.

The loss factor κ_l defines the average energy loss per particle. It is given by the wake potential: $\kappa_l =< W(0) >$. In a train of equidistant bunches the loss can be enhanced, see discussion below and in the section describing the interaction region (IR).

Similarly, the transverse components of the field excited by the leading particle give a transverse kick to the trailing particle. The transverse kick for azimuthally symmetric structures is zero for a zero offset of the leading particle $r_l = 0$. Therefore, the transverse wake is defined usually factoring out the offset:

$$c\Delta p_{\perp} = Ne^2 r_l W_{\perp}^{\delta}(s). \qquad (A1-5)$$

The transverse impedance is the Fourier transform of the transverse wake

$$Z_{\perp}(\omega) = -i \int d(s/c) W_{\perp}^{\delta}(s) e^{i\omega s/c}. \qquad (A1-6)$$

The frequency dependence of the broad-band transverse impedance follows from the Panofsky-Wenzel theorem, which relates $Z_{\perp}$ with the dipole longitudinal impedance $Z_l^{(1)}$:

$$\frac{\partial W_{\perp}^{\delta}}{\partial s} = W_l^{(1)}, \qquad Z_{\perp}(\omega) = \frac{Z_l^{(1)}}{(\omega/c)}. \qquad (A1-7)$$

Usually, when azimuthal asymmetry is not too large, $Z^{(1)}(\omega) \simeq Z^{(0)}/b^2$ and $Z_{\perp}(\omega) \simeq Z^{(0)}(\omega)/kb^2$ where $k = \omega/c$. For example, for a RF cavity, see Fig. 1 and Fig. 2, $Z^{(0)} = 0.143$ kΩ. Hence, $Z^{(0)}/b^2 = 70.6\, k\Omega/m^2$ at $b = 4.5$ cm what is very close to $Z^{(1)} = 68\, k\Omega/m^2$ given by ABCI.

In particular, the resistive wall impedances in a beam pipe with radius b are related by

$$Z_\perp(\omega) = \frac{2Z_l(\omega)}{kb^2} = \frac{2R}{b^2}\frac{Z_l}{n} \qquad (A1-8)$$

This relationship is often used as an estimate of the transverse impedance in other cases as well.

The transverse wake potential is defined similarly to Eq.(A1-4):

$$W_\perp(s) = \int ds_1 ds_2 W_\perp^\delta(s_1 - s_2 + s)\rho(s_1)\rho(s_2). \qquad (A1-9)$$

It defines the kick of the bunch centroid $\kappa_\perp = W_\perp(0)$.

Note, that with these definitions the dimensions of the wake fields are V/pC for W_l, and V/pC/m for $W_\perp$. They have the following analytic properties:

$$Z_l(-\omega^*) = Z_l^*(\omega), \quad Z_\perp(-\omega^*) = -Z_\perp^*(\omega). \qquad (A1-10)$$

It is worth noting also that 1 V/pC $= 1.11cm^{-1}$. The dimension of the longitudinal impedance is Ohms and the transverse impedance is measured in $M\Omega/m$.

As a function of frequency, the impedance usually has narrow spikes at certain frequencies and, in addition, a broad and smooth background. The narrow spikes correspond to localized trapped modes of the EM field of the beam and are referred to as narrow-band impedances. The smooth background is referred to as a broad-band impedance.

The trapped modes are usually associated with the fields localized within large structures, such as RF cavities. However, even a small enlargement of the beam pipe radius can result in mode trapping, see Appendix 2 and discussion of the impedance of the lumped vacuum pumps.

The narrow-band impedance may be represented as a sum of resonance terms for each trapped mode, characterized by a loss factor ξ_m, a mode frequency $\omega_m = 2\pi f_m$,

and a resonance width γ_m:

$$Z_l(\omega) = \sum_m i\xi_m[\frac{1}{\omega - \omega_m + i\gamma_m} + \frac{1}{\omega + \omega_m + i\gamma_m}], \qquad (A1-11)$$

$$Z_\perp(\omega) = \sum i\xi_\perp[\frac{1}{\omega - \omega_m + i\gamma_m} - \frac{1}{\omega + \omega_m + i\gamma_m}]. \qquad (A1-12)$$

Usually, the narrow-band impedance is described by the shunt impedance R_m, quality factor Q_m^0, and loaded quality factor Q_m^L: $\xi_m = \omega_m R_m/(2Q_m^0)$, $\gamma_m = \omega_m/(2Q_m^L)$. Similar relations are valid for the transverse case.

The longitudinal wake corresponding to the narrow-band impedance is the sum of the wakes of individual modes. For $s > 0$

$$W_l^\delta(s) = \sum_m 2\xi_m^l \cos(\omega_m s/c)e^{-\omega_m s/2Q_m}. \qquad (A1-13)$$

$$W_\perp^\delta(s) = \sum_m 2\xi_m^\perp \sin(\omega_m s/c)e^{-\omega_m s/2Q_m}. \qquad (A1-14)$$

For $s < 0$, the wake is zero, $W^\delta(s) = 0$.

The loss factor

$$\kappa_l =< W(0) >= \sum_m \xi_m|\rho(\omega_m)|^2. \qquad (A1-15)$$

The kick of the bunch centroid

$$\kappa_\perp =< W_\perp(0) >\simeq \frac{2}{\sqrt{\pi}}\sum_m \xi_m^\perp \frac{\sigma_B\omega_m}{c}|\rho(\omega)|^2. \qquad (A1-16)$$

The variation of the transverse wake field along the bunch defines the relative kick of particles within a bunch

$$< \frac{\partial W_\perp}{\partial s} >= \sum_m \frac{\omega_m}{c}\xi_m^\perp|\rho(\omega)|^2 \qquad (A1-17)$$

The broad-band longitudinal impedance can be parametrized[16][17] by expansion

over $\sqrt{\omega}$. For $\omega > 0$ it takes the form:

$$Z_l(\omega) = -iZ_0\frac{L\omega}{4\pi c} + (1-i)R_W\sqrt{\omega} + R_\Omega + (1+i)R_c\sqrt{\frac{\omega_c}{\omega}}\theta(\omega-\omega_c) + ... \quad (A1-18)$$

where $Z_0 = 4\pi/c = 120\pi\ \Omega$, and $\omega_c/2\pi$ is a cutoff frequency. Usually, it can be set to the cutoff frequency of the beam pipe at the RF cavities. Dependence of the total impedance on the choice of ω_c is weak if the number of modes below cutoff taken into account in the narrow-band impedance and the coefficient R_c are chosen consistently.

The relation between real and imaginary parts of the impedance follow from the analytic property of the impedance, Eq. (A1-10).

The first term here describes inductive impedance generated by all elements in the ring with eigen-frequencies much higher than the frequencies within the bunch spectrum. The inductance L (L in nH, 1 cm=1 nH) defines the low-frequency parameter Z_l/n where $n = \omega/\omega_0$ is the harmonic number, and $\omega_0 = 2\pi f = c/R$ is the revolution frequency:

$$\frac{Z_l}{n} = \frac{Z_0 L}{4\pi R} \quad (A1-19)$$

A purely inductive impedance corresponds to the wake function $W^\delta(s) = L\partial\delta(s)/\partial s$ that is proportional to the derivative of $\delta(s)$. The wake of a bunch with a bunch profile $\rho(s)$ in this case is proportional to $d\rho(s)/ds$. For a Gaussian bunch

$$W(s) = -\frac{L}{\sigma^3\sqrt{2\pi}}se^{-\frac{1}{2}(\frac{s}{\sigma})^2} \qquad W_{max} = L/(\sigma^2\sqrt{2\pi e}). \quad (A1-20)$$

The maximum value can be used to find L in numerical simulations.

The second term in Eq. (A1-18) describes the resistive wall impedance and gives the loss factor

$$k_l = \frac{R_W}{\pi}(\frac{c}{\sigma_B})^{3/2}\frac{\Gamma(3/4)}{2}. \quad (A1-21)$$

The third term describes a constant resistivity and gives the loss factor

$$k_l = \frac{R_\Omega}{Z_0}\frac{2\sqrt{\pi}}{\sigma}. \quad (A1-22)$$

The wake of a bunch in this case

$$W(s) = 4\pi \frac{R_\Omega}{Z_0} \rho(s)$$

is proportional to $\rho(s)$.

The last term is a good parametrization of the high-frequency tail of the RF cavities. For $\omega_c \sigma_B / c << 1$ it gives the loss factor

$$k_l = \frac{2R_c}{Z_0} \sqrt{\frac{\omega_c}{c\sigma_B}} [\Gamma(1/4) - 4\sqrt{\frac{\omega_c \sigma_b}{c}}], \quad \Gamma(1/4) = 3.6256. \qquad (A1-23)$$

The transverse $Z_\perp$ can be expanded in $1/\sqrt{\omega}$ similarly to Eq. (A1-18). The expansion starts with a constant term that gives an inductive wake of a bunch proportional to the bunch profile $\rho(s)$.

In the accelerators of the last generation, the vacuum chambers are designed to be very smooth minimizing impedance. As a result, small discontinuities of the vacuum chamber such as holes and slots in the beam pipe become important giving substantial contribution to the total impedance. The problem has been carefully studied recently[8][18].

The impedances of small holes and slots are inductive[8]

$$Z_l(\omega) = -iZ_0 \frac{\omega}{c} \frac{\alpha_c + \alpha_m}{(2\pi b)^2}, \qquad L = \frac{\alpha_e + \alpha_m}{\pi b^2} \qquad (A1-24)$$

where $\alpha_{e,m}$ are polarizabilities which depend on the geometry of the opening. For a circular hole with radius r:

$$\alpha_m = \frac{4r^3}{3}, \qquad \alpha_e = -\frac{2r^3}{3}. \qquad (A1-25)$$

For a slot parallel to the beam with length l and width w, $w << l$, in a thin wall

$$\alpha_m = -\alpha_e = \frac{\pi}{16} w^2 l, \qquad \alpha_e + \alpha_m = (\pi/24) w^3. \qquad (A1-26)$$

The formulas remains valid for a slot tilted by a small angle θ with respect to the

beam axis, provided that

$$\theta^2 << (w/l)^3 \qquad (A1-27)$$

For a transverse slot perpendicular to the beam direction $\alpha_m >> \alpha_e$,

$$\alpha_m = \frac{\pi l^3}{24[\ln(4l/w) - 1]}. \qquad (A1-28)$$

The transverse impedance of a hole with inductance L is

$$Z_\perp = Z_l \frac{4}{kb^2} = -i\frac{Z_0 L}{\pi b^2}. \qquad (A1-29)$$

The transverse impedance of a narrow slot, $w << l < b$ depends on its orientation and is given by

$$Z_\perp = -Z_0 \frac{w^3}{24\pi b^4} \quad (\textit{slot along the beam})$$

$$Z_\perp = -Z_0 \frac{l^3}{24\pi b^4 (\ln \frac{4l}{w} - 1)} \quad (\textit{slot perpendicular to the beam}). \qquad (A1-30)$$

These formulas are given for the openings in a thin wall. For a thick wall the impedances are smaller. For example, polarizabilities of a slot parallel to the beam are

$$\alpha_m = -\alpha_e = \frac{1}{2\pi} w^2 l.$$

For an infinitely thick wall, the longitudinal impedance of a hole is reduced[18] by a factor of 0.56.

The real part of the impedance and the loss factor are second order effects and much smaller[19][8]

$$ReZ_l(\omega) = 2Z_0 \frac{\alpha_e^2 + \alpha_m^2}{3\pi(2\pi b)^2} (\frac{\omega}{c})^4, \qquad k_l = \frac{\alpha_e^2 + \alpha_m^2}{(2\pi b)^2 \sqrt{\pi}\sigma_b^5}. \qquad (A1-31)$$

(Kurennoy's result is corrected here, according to G. Stupakov, by a factor four to retain definitions of Eq. (A1-25). These definitions are smaller than the Bethe's result by the factor 2 but are consistent with Eq. (A1-24)).

For a hole

$$k_l = 0.03\frac{1}{\sigma_b}(\frac{r}{\sigma_B})^4(\frac{r}{b})^2. \qquad (A1-32)$$

For a slot along the beam,

$$ReZ_l = \frac{Z_0}{768\pi}(\frac{\omega w}{c})^4(\frac{l}{b})^2,$$

and the loss factor

$$k_l = \frac{1}{512\sqrt{\pi}\sigma_B}(\frac{w}{\sigma_B})^4(\frac{l}{b})^2. \qquad (A1-33)$$

The energy loss due to dipole radiation from an opening (in CI units) by a magnetic moment $M_\omega = \alpha_m H_\omega$ and an electric dipole moment $P_\omega = \alpha_e \epsilon_0 E_\omega$ is

$$\Delta U = \frac{Z_0 \epsilon_0^2}{6\pi c^2}\int \frac{d\omega}{2\pi}\omega^4[(\alpha_e)^2|E_\omega|^2 + (Z_0\alpha_m)^2|H_\omega|^2] \qquad (A1-34)$$

where E_ω and H_ω are the frequency components of the field exciting dipoles. For a bunch with a charge $N_b e$, the fields are $E_\omega = Z_0 H_\omega = 2N_B e/(cb)\rho(\omega)$, $\rho(\omega = 0) = 1$, giving result Eq. (A1-33).

For a TM_{01} mode the ratio of the radiated power to the power of the incoming wave

$$P_{in} = \frac{1}{2}\int dS E_\omega \times H_\omega^* \qquad (A1-35)$$

is

$$\frac{P}{P_{in}} = \frac{2q}{3\pi^2 b^2}(\frac{\omega}{c})^3[\alpha_e^2 + \alpha_m^2(\frac{\omega}{qc})^2] \qquad (A1-36)$$

where q is the propagation constant of the wave in the beam pipe with radius b, and α_m of a slot is given by Eq. (A1-26).

For a TE_{11} mode losses are given by the magnetic polarizability Eq. (A1-28)

$$\frac{P}{P_{in}} = \frac{4}{3\pi^2}(\frac{\omega}{c})^3\alpha_m^2\frac{q_c^4}{q(q_c^2b^2 - 1)} \qquad (A1-37)$$

where q is the propagation constant, $q_c = \omega_c/c$, and ω_c is the cut-off frequency. For a rectangular beam pipe, the factor $4/(\pi b^2)$ is replaced by $2/(ab)$.

Appendix 2. Trapped modes in a beam pipe

The mechanism of the mode trapping by a small bulging of a beam pipe was described in the paper by Stupakov and Kurennoy[12]. Consider a propagating mode with the frequency ω in a straight beam pipe, which is close to the cut-off frequency ω_c. If the beam pipe has a bulging with the additional volume V_b, the frequency may change and, if the frequency shift $\Delta\omega < 0$ and large, the mode may be shifted below the cut-off and be trapped. The transverse spatial structure of such a mode is close to the structure of the propagating mode but with the z-dependence of the form $e^{-q|z|}$. The mode is localized within the distance $\pm L$ from the bulge location where $L = 1/q$, and q is related to $\Delta\omega$:

$$\frac{\Delta\omega}{\omega} = \frac{q^2}{2k_c^2} \qquad k_c = \omega_c/c. \tag{A2-1}$$

Theory[12] gives

$$\frac{\Delta\omega}{\omega} = \frac{\nu^2}{2}\left(\frac{A}{b^2}\right)^2 \tag{A2-2}$$

for an axi-symmetric bulging with the surface area A in the (r, z) plane in a round beam pipe with radius b. Here ν is the root of the Bessel function $J_0(\nu) = 0$, and $\omega_c/c = \nu/b$.

In a general 3-D case (axial symmetry is not required)

$$q = \zeta\frac{k_c^2 V_b}{2S} \tag{A2-3}$$

where V is the additional volume of the bulging, S is the beam pipe cross-section, and ζ is the ratio of the field $|H^2|$ of the mode at the bulge opening to the averaged value $< |H^2| >$ over the beam pipe cross-section. For a round beam pipe, $\zeta = 1$.

The effective bulging of the opening in the beam pipe can be considered as a result of the magnetic field leaking out of the beam pipe. A hole with radius a in a thick beam pipe corresponds from this point of view to a volume $V_b = \pi a^2\delta/2$ where factor 2 takes into account that field pattern in the hole is triangular in (r, z) plane, and

$\delta \simeq a$ is the maximum depth to which the field penetrate into the hole. This gives $V_b/(2\pi b) = a^3/(4b)$. Exact solution[12] gives for this quantity $(8/3\pi)(a^3/4b)$. For a long slot parallel to the beam the same arguments give $V_b = lw^2/2$, what corresponds to the magnetic polarizability $\alpha = \pi lw^2/16$ of a slot.

Exact result for an opening replaces the volume V_b by the magnetic polarizability of the opening. If there are several openings within the localization length, the sum of the polarizabilities of all openings should be taken instead of V_b.

The frequency shift $(1/(2Q) = \delta\omega/\omega$ should be compared with the sum of the damping due to the finite skin depth δ of a resistive wall

$$(\Delta\omega/\omega)_{RW} = \frac{\delta}{2b} \qquad (A2-4)$$

and the damping due to radiation outside of the beam pipe. The Q_{ext} due to radiation, $Q_{ext} = \frac{\omega U}{(P/2)}$, is given[12] by the ratio of the energy U stored in the trapped mode, $U = \int |H|^2 dV/4\pi$, to the half of the power $P/2$ radiated by a magnetic dipole $M = \alpha H$, $P = (2c/3)(\omega/c)^4 M^2$, where α is polarizability of the opening. For a round beam pipe with the cross-section S

$$\frac{1}{Q_{ext}} = \frac{2\pi}{3}(\frac{\omega}{c})^3 \frac{q\alpha^2}{S}. \qquad (A2-5)$$

For a round beam pipe with radius b, the shunt impedance of a trapped TM_{0n} mode is[12]

$$R_s = \frac{Z_0}{2\pi} \frac{\nu}{J_1^2(\nu)} \frac{b}{\delta} (\frac{\alpha_m}{\pi b^3})^3 \qquad (A2-6)$$

where ν is the n-th root of the Bessel function $J_0(\nu) = 0$.

The shunt impedance of a lowest TM_{01} mode in a rectangular chamber with the full dimensions $a \times b$, $a > b$, and with a slot located at x_s, $0 < x_s < a$ in the upper or lower decks is

$$R_s = Z_0 \frac{a}{b} (\frac{1}{k_c a})^5 (\frac{b_{eff}}{\delta}) [\frac{4\pi^2 \alpha_m}{b^3} \sin^2(\frac{\pi x_s}{a})]^3. \qquad (A2-7)$$

Here $k_c = \omega_c/c$ is given by the cut-off frequency, and $b_{eff} = ab(a^2+b^2)/(a^3+b^3)$.

Appendix 3. Energy loss by a train of bunches

The energy loss of a single bunch due to excitation of a narrow-band mode with the loss factor k_l is

$$\Delta U = (N_B e)^2 \kappa_l. \qquad (A3-1)$$

One might expect that a train of bunches separated by the bunch spacing s_B has the power loss

$$P_0 = \frac{\Delta U}{(s_B/c)} = I_{av}^2 \kappa_l \frac{s_B}{c}. \qquad (A3-2)$$

In the train of bunches, however, a bunch interacts not only with its own wake field but with wakes excited by all previous bunches[20]:

$$\Delta U = 2N_b^2 e^2 \kappa_l \sum_{m=0}^{\infty} \zeta_m \cos(\omega_l s_m/c) e^{-\omega_l s_m/(2cQ_l^L)}. \qquad (A3-3)$$

For a train of equidistant bunches $s_m = m s_B$. Here Q_l^L is the loaded Q factor of the mode, and $\zeta_m = 1/2$ for $m = 0$ and $\zeta = 1$ otherwise. Wake fields of different bunches tend to cancel each other. Exception is a resonance where the mode frequency ω_l is close to the multiples of the inverse bunch spacing

$$|\frac{\omega_l s_B}{c} - 2\pi n| << \frac{1}{Q_L}, \quad n = ineteger. \qquad (A3-4)$$

In this case, all contributions build up giving:

$$\Delta U = (N_b e)^2 \kappa_l \frac{1}{2\pi n} \frac{1/Q_l^L}{(\Delta\omega/\omega_l)^2 + (1/2Q_l^L)^2}. \qquad (A3-5)$$

The energy loss of each bunch in the resonance is enhanced compared to Eq. (A3-1) by a factor

$$D = \frac{4Q_l^L c}{\omega_l s_B}. \qquad (A3-6)$$

The width of the resonance is $\Delta\omega/\omega = (2Q_L)^{-1}$. Such resonances are separated in frequency by $\Delta f = c/s_B$.

The same result can be obtained in frequency domain. That allows also the estimate of the heating due to coherent coupled-bunch motion. These resonances of the coherent motion are separated only by the revolution frequency and much denser than resonances with the bunch spacing considered above.

The power loss is defined by averaging the product $V(t) \times I(t)$ over a large period of time T. The frequency components of the voltage and current are related by the impedance. Hence, in the frequency domain we get for the power loss

$$P = \frac{1}{T} \int \frac{d\omega}{2\pi} Z(\omega) |I(\omega)|^2, \qquad (A3-7)$$

where $I(\omega) \int dt e^{i\omega t} I_N(t)$ is the Fourier transform of a bunch current

$$I_N(t) = I^{av}_{bunch} T_r \sum_n [1 - \frac{d\tau_N}{dt}] \rho_N(t - nT_r - N\tau_B - \tau_N(t)). \qquad (A3-8)$$

Here N is bunch number, $1 < N < n_b$, $\rho(t)$ is normalized to one bunch profile, $c\tau_B = s_B$, $T_r = 2\pi/\omega_r$ is the revolution time, and the sum is over the number of turns. The coherent motion of a bunch $\tau_N(t)$ can be described as a sum of coupled-bunch modes with frequencies Ω_k and amplitudes Δ_k. For a ring filled with bunches uniformly,

$$\tau_N(t) = \sum_{k=0}^{n_B - 1} \Delta_k \cos(2\pi k N / n_B) \cos(\Omega_k t + \psi_k). \qquad (A3-9)$$

Fourier transform of the bunch density and summation over n

$$\sum_n e^{-i\omega T_r n} = \omega_r \sum_l \delta(\omega - \omega_r l) \qquad (A3-10)$$

gives in the first order in $\tau_N(t)$

$$I_N(t) = \sum_l I^{av}_{bunch} \rho_N(\omega_r l) e^{i\omega_r l (t - N\tau_B)} [1 - \frac{d\tau_N}{dt} - i\omega_r l \tau_N(t)]. \qquad (A3-11)$$

For a point-like bunch, $\rho(\omega) = 1$.

This defines the Fourier spectrum of a bunch current $I_N(\omega)$

$$I_N(\omega) = 2\pi \sum_l I^{av}_{bunch}\rho_N(\omega_r l)e^{-i\omega_r l N\tau_B}[\delta(\omega_r l-\omega)$$

$$+\frac{i}{2}\sum_k \Delta_k \cos(\frac{2\pi k}{n_B}N)[e^{-i\psi_k}(\Omega_k-\omega)\delta(\omega_r l-\omega-\Omega_k)-e^{i\psi_l}(\Omega_k+\omega)\delta(\omega_r l-\omega+\Omega_k)]. \quad (A3-12)$$

The spectrum of the beam current is given by the sum over bunches in the ring. For identical point-like bunches, ($\rho_N = \rho$), the result is

$$I(\omega) = 2\pi I^{av}_{beam}\sum_p \delta(\omega - n_b\omega_r p)\rho(\omega)$$

$$-i\pi\omega I^{av}_{beam}\sum_{p,k}\Delta_k\rho(\omega)[e^{-i\psi_{(k+n_bp)}}\delta(\omega_r n_B p+\omega_r k-\Omega_k-\omega)+e^{i\psi_{(k+n_bp)}}\delta(\omega_r n_B p+\omega_r k+\Omega_k-\omega)]. \quad (A3-13)$$

Note, that $\delta(\omega=0) = T/(2\pi)$. Neglecting coherent modes, we get

$$|I(\omega)|^2 = 2\pi T\sum_p (I^{av}_{beam})^2\delta(\omega-n_b\omega_r p)|\rho(\omega)|^2. \quad (A3-14)$$

The power loss Eq. (A3-7) is

$$P = \sum_{p=-\infty}^{\infty}(I^{av}_{beam})^2 Z(n_b\omega_r p)|\rho(n_b\omega_r p)|^2. \quad (A3-15)$$

If the resonance frequency is equal to a frequency ω_l of a mode of a narrow-band impedance with the shunt impedance R_l, and loaded Q_L, the loss is

$$P_{max} = 2(I^{av}_{beam})^2 Q_L(\frac{R}{Q_0})_l. \quad (A3-16)$$

This is larger than uncorrelated loss P_0 Eq. (A3-1) by the factor Eq. (A3-6).

Loss due to coherent modes does not interfere with the loss of rigid bunches. Eqs.(A3-7) and (A3-13) give the loss due to a coherent modes

$$P = \sum_{p,k} [\frac{\Delta_k \omega_{pk}}{2} I^{av}_{beam}]^2 [Z(\omega_r(n_B p + k) - \Omega_k) + Z(\omega_r(n_B p + k) + \Omega_k)] \quad (A3-17)$$

where $\omega_{pk} = \omega_r(n_b p + k)$. To estimate the amplitude the rms Δ_k let us assume that rms coherent motion of a bunch is of the order of the rms bunch length

$$< \tau_N^2(t) >= \sum_k \frac{\Delta_k^2}{4} \simeq \frac{n_B < \Delta_k^2 >}{4} = (\sigma_B/c)^2. \quad (A3-18)$$

If the frequency of a coherent mode $\omega = \omega_r(n_b p + k) \pm \Omega_k$ is equal to the frequency ω_m of a narrow-band mode and the width of the mode is small compared to ω_r, the loss Eq. (A3-17) is smaller than the loss Eq. (A3-16) by the factor $1/n_b$. If the narrow-band resonance is wide,

$$\Delta\omega = \frac{\omega_m}{(2Q_L)} >> \omega_r$$

then the coherent modes give the power loss

$$P \simeq P_0 (\frac{\omega \sigma_B}{c})^2, \quad (A3-19)$$

of the order of P_0 Eq. (A3-2).

REFERENCES

1. PEP-II An Asymmetric B factory, CDR, LBL PUB-5379, SLAC-418, June 1993
2. R. L. Gluckstern, J. van Zeijts, B. Zotter, Coupling Impedance of Beam Pipes of General Cross Section, CERN SL/AP 92-25, June 1992
3. J. Byrd, G. Lambertson Resistive wall impedance of the B-factory, PEP-II AP Note 9-93, March 1993
4. J.D. Jackson, SSC Central Design Group Report, SSC-N-110 (1986), E. D. Courant, M. Month BNL Report BNL-50875, 1978
5. E. Henestroza, Numerical Calculations of the Longitudinal Wakefield and Impedance of the B-factory Antechamber, PEP-II Note 1994
6. A. Kulikov, J. Seeman, M. Zolotarev, PEP-II Abort System Specifications, PEP-II Note 61, 10/1994
7. A. Piwinsky, IEEE nucl. sci., V 24, No. 3, 1364, 1977
8. S. Kurennoy Beam Coupling Impedance of Holes in Vacuum- Chamber Walls, IHEP 92-84, UNK, 1992
9. N. Kurita, D. Martin, C.-K Ng, S. Smith and T. Weiland, Simulation of PEP-II Beam Position Monitor, PEP-II Note 87, March 1995
10. K. Bane, The Calculated Longitudinal Impedance of the SLC Damping Ring, SLAC-PUB-4618, 1988
11. Cho K. Ng and T. Weiland, Cho Ng Impedance analysis of the PEP-II Vacuum Chamber, SLAC report, unpublished, 1994
12. G. V. Stupakov, S. S. Kurennoy, Trapped EM Modes in a Waveguide with a small discontinuity, SSCL-Preprint-459, June 1993
13. S. Heifets, G. Stupakov Study of the Trapped Modes at the Vacuum Ports, PEP-II Note No. 80, January 1995
14. J. Corlett, J. Johnson, G. Lambertson, F. Voelker, Longitudinal and Transverse Feedback Kickers for the ALS, LBL-34955, UC-410, 1994

15. J.F. Crawford The electro-Magnetic Properties of Vacuum Chambers, TM-12-90-04, Paul Scherrer Institute, November 1991

16. S. Heifets Broad band Impedance of the B-factory, SLAC/AP-93, February 1992

17. S. Bartalucci, M. Serio, B. Sparato, M. Zobov, L. Palumbo Broad-band model impedance for DAPHNE Main Rings, Nucl Inst. and Methods, A337, 1994

18. R. L. Gluckstern Preprint CERN SL/92-05 (AP) Geneva, 1992

19. M. Sands, Preprint PEP-253, SLAC 1977

20. K. Bane, P.B. Wilson and T. Weiland Wakefields and Wakefield Acceleration, SLAC-PUB-3528, 1984

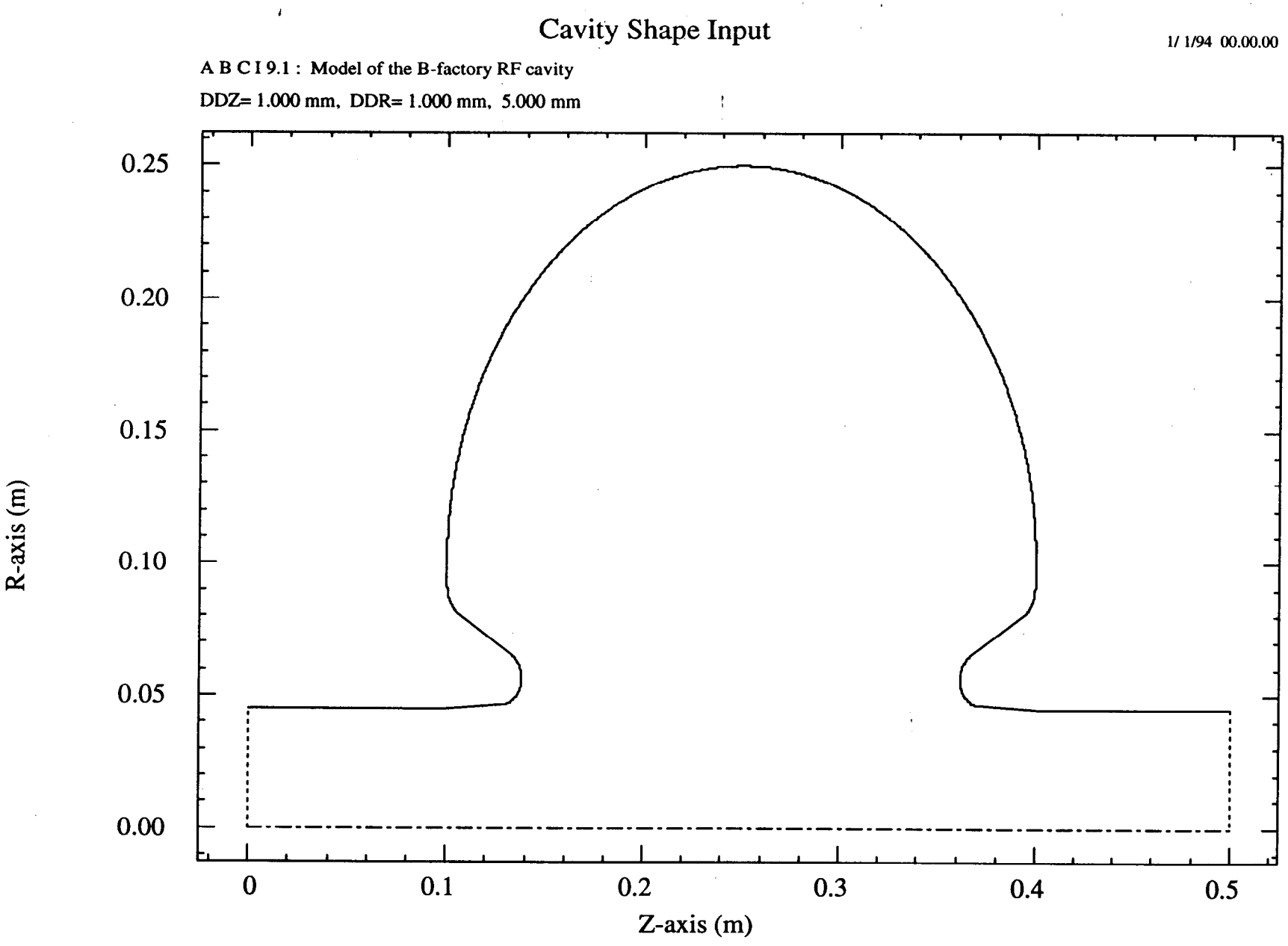
Cavity Shape Input
1/ 1/94 00.00.00
A B C I 9.1 : Model of the B-factory RF cavity
DDZ= 1.000 mm, DDR= 1.000 mm, 5.000 mm
R-axis (m)
0.25
0.20
0.15
0.10
0.05
0.00
0
0.1
0.2
0.3
0.4
0.5
Z-axis (m)

Fig. 1

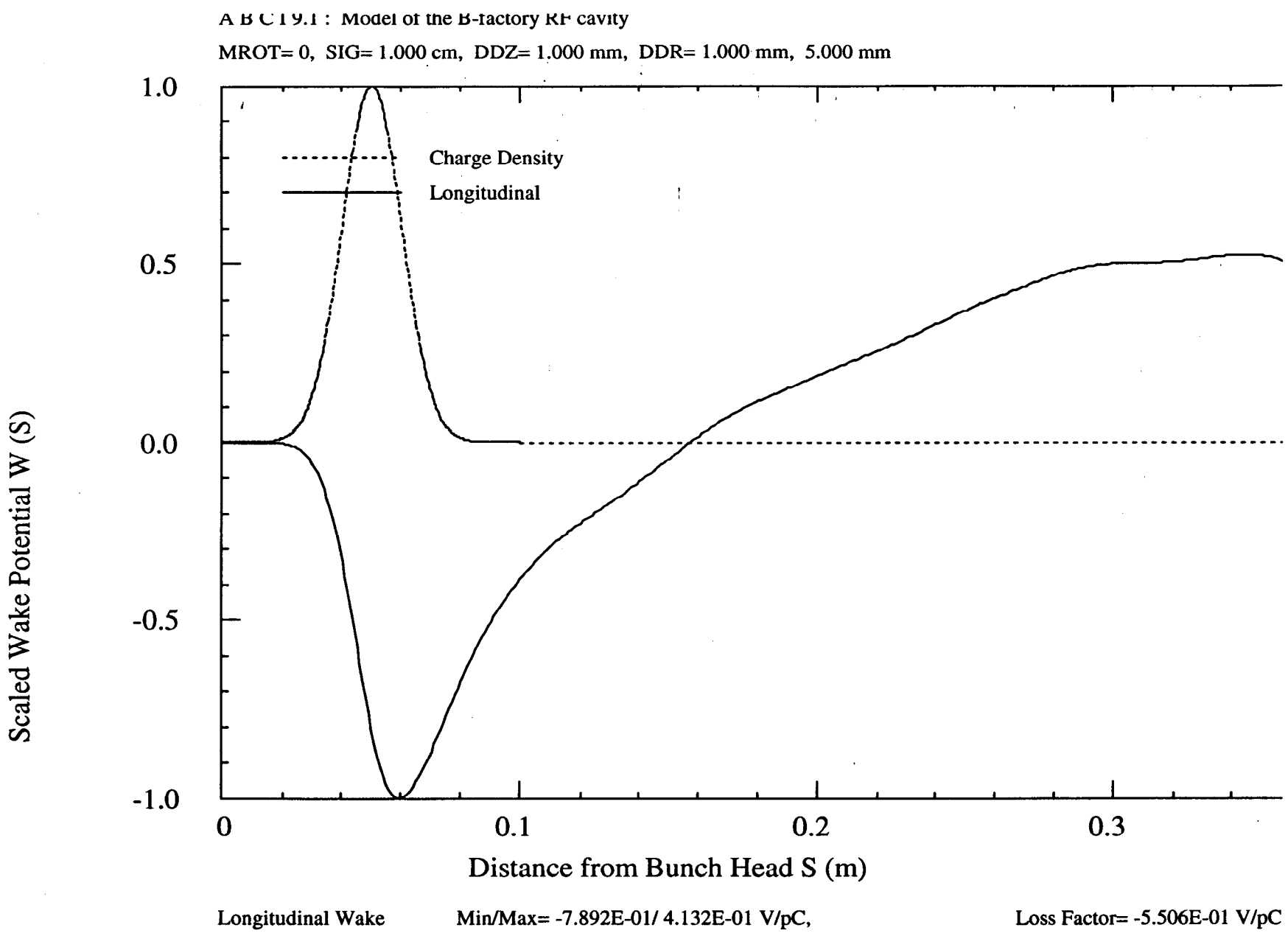
A B C 19.1 : Model of the B-factory RF cavity
MROT= 0, SIG= 1.000 cm, DDZ= 1.000 mm, DDR= 1.000 mm, 5.000 mm
Charge Density
Longitudinal
Scaled Wake Potential W (S)
1.0
0.5
0.0
-0.5
-1.0
0
0.1
0.2
0.3
Distance from Bunch Head S (m)
Longitudinal Wake
Min/Max= -7.892E-01/ 4.132E-01 V/pC,
Loss Factor= -5.506E-01 V/pC

Fig. 2

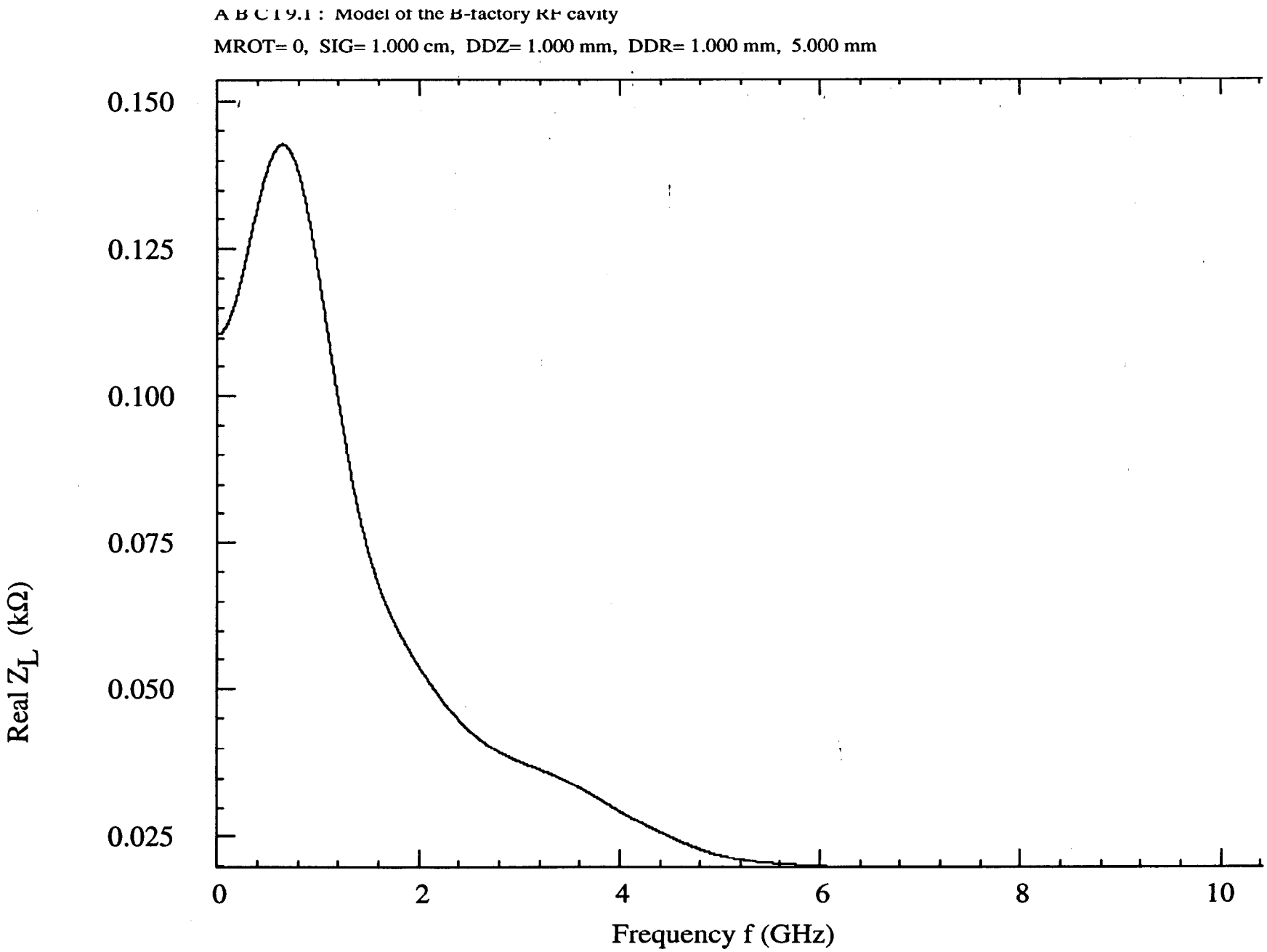
A B C 19.1 : Model of the B-factory RF cavity
MROT= 0, SIG= 1.000 cm, DDZ= 1.000 mm, DDR= 1.000 mm, 5.000 mm
0.150
0.125
0.100
0.075
0.050
0.025
Real Z_L (kΩ)
0
2
4
6
8
10
Frequency f (GHz)

Fig. 3a

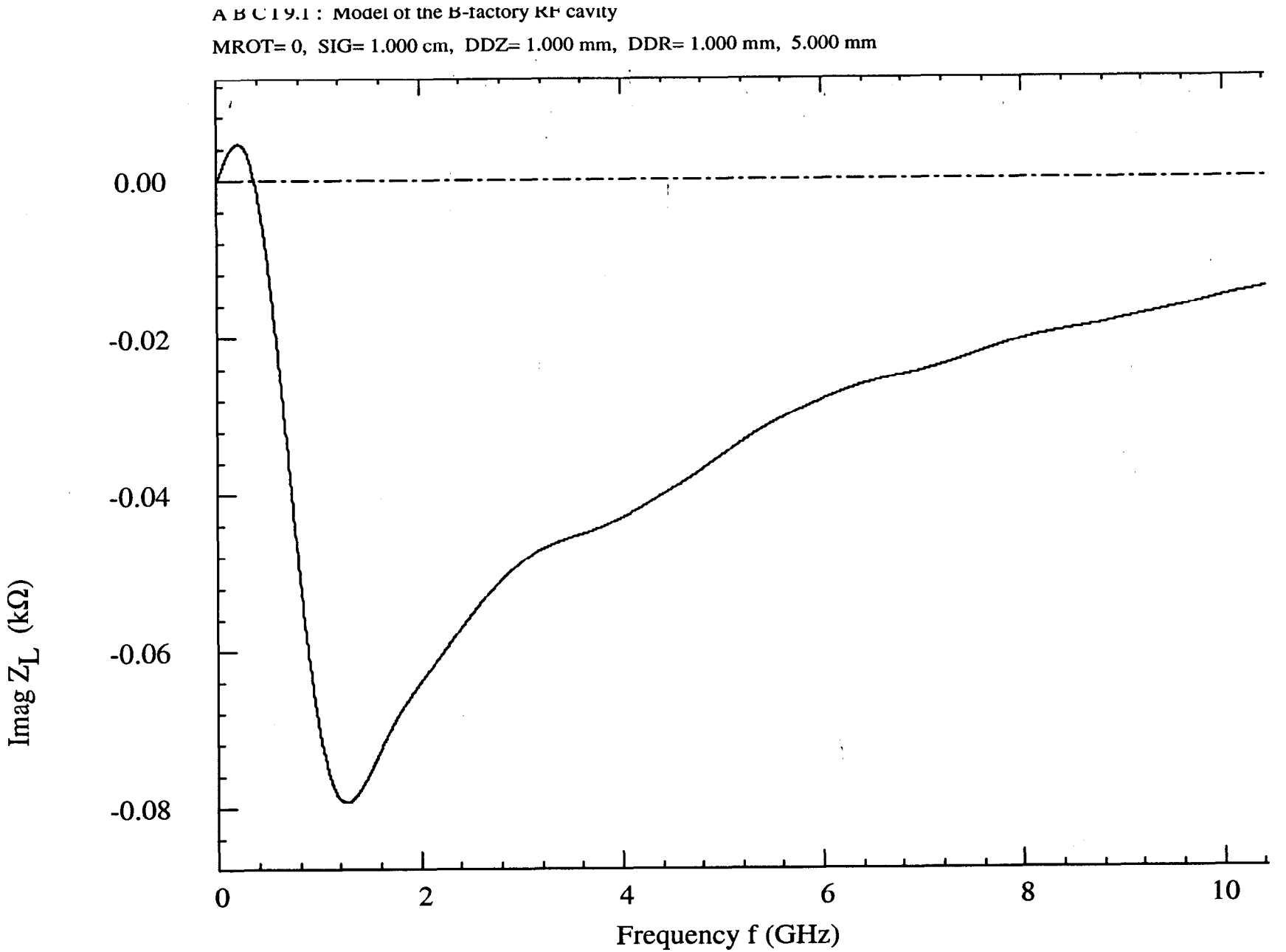
A B C 19.1 : Model of the B-factory RF cavity
MROT= 0, SIG= 1.000 cm, DDZ= 1.000 mm, DDR= 1.000 mm, 5.000 mm
0.00
-0.02
-0.04
-0.06
-0.08
Imag Z_L (kΩ)
0
2
4
6
8
10
Frequency f (GHz)

Fig. 3b

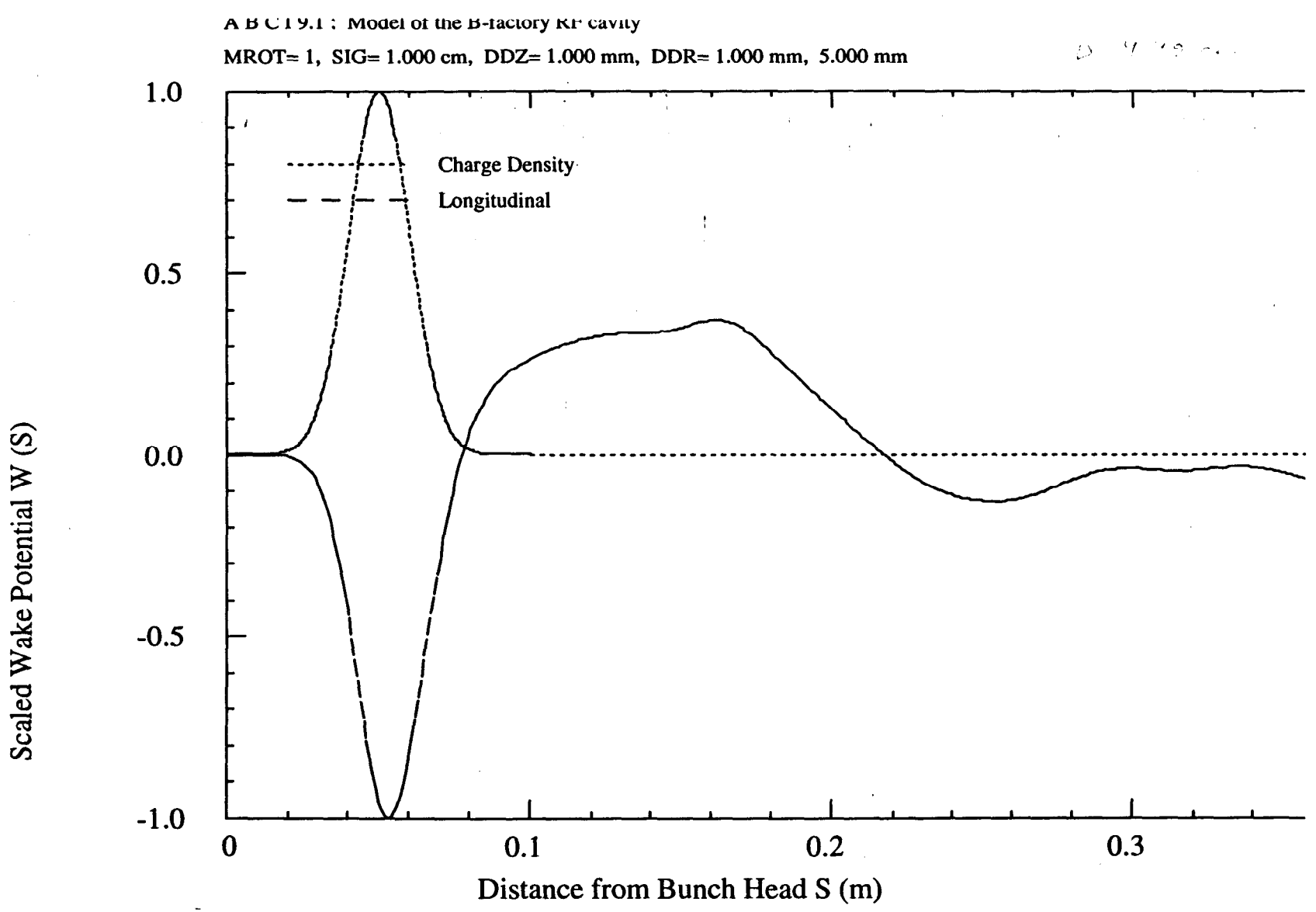
A B C 19.1 : Model of the B-factory RF cavity
MROT= 1, SIG= 1.000 cm, DDZ= 1.000 mm, DDR= 1.000 mm, 5.000 mm
1.0
0.5
0.0
-0.5
-1.0
Charge Density
Longitudinal
Scaled Wake Potential W (S)
0
0.1
0.2
0.3
Distance from Bunch Head S (m)
Azimuthal Wake Min/Max= -1.263E+01/ 4.633E+00 V/pC/m, Loss Factor= -5.278E+00 V/pC
Transverse Wake Min/Max= -4.633E+00/ 1.263E+01 V/pC/m, Loss Factor= 5.266E+00 V/pC
Longitudinal Wake Min/Max= -4.868E+02/ 1.804E+02 V/pC/m², Loss Factor= -3.451E+02 V/pC

Fig. 4a

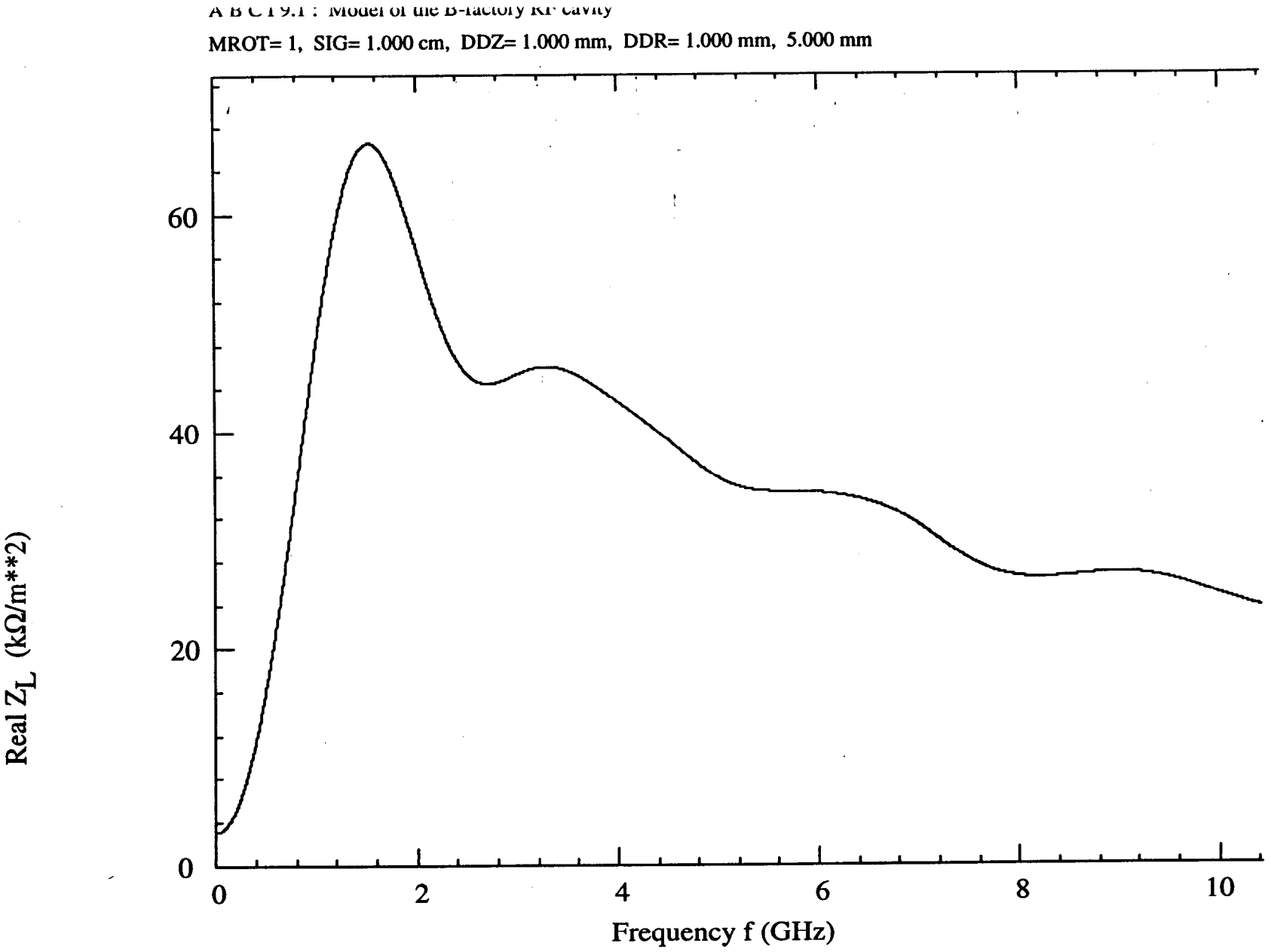
A B C T9.1 : Model of the B-factory RF cavity
MROT= 1, SIG= 1.000 cm, DDZ= 1.000 mm, DDR= 1.000 mm, 5.000 mm
Real Z_L (kΩ/m**2)
0
20
40
60
0
2
4
6
8
10
Frequency f (GHz)

Fig. 4b

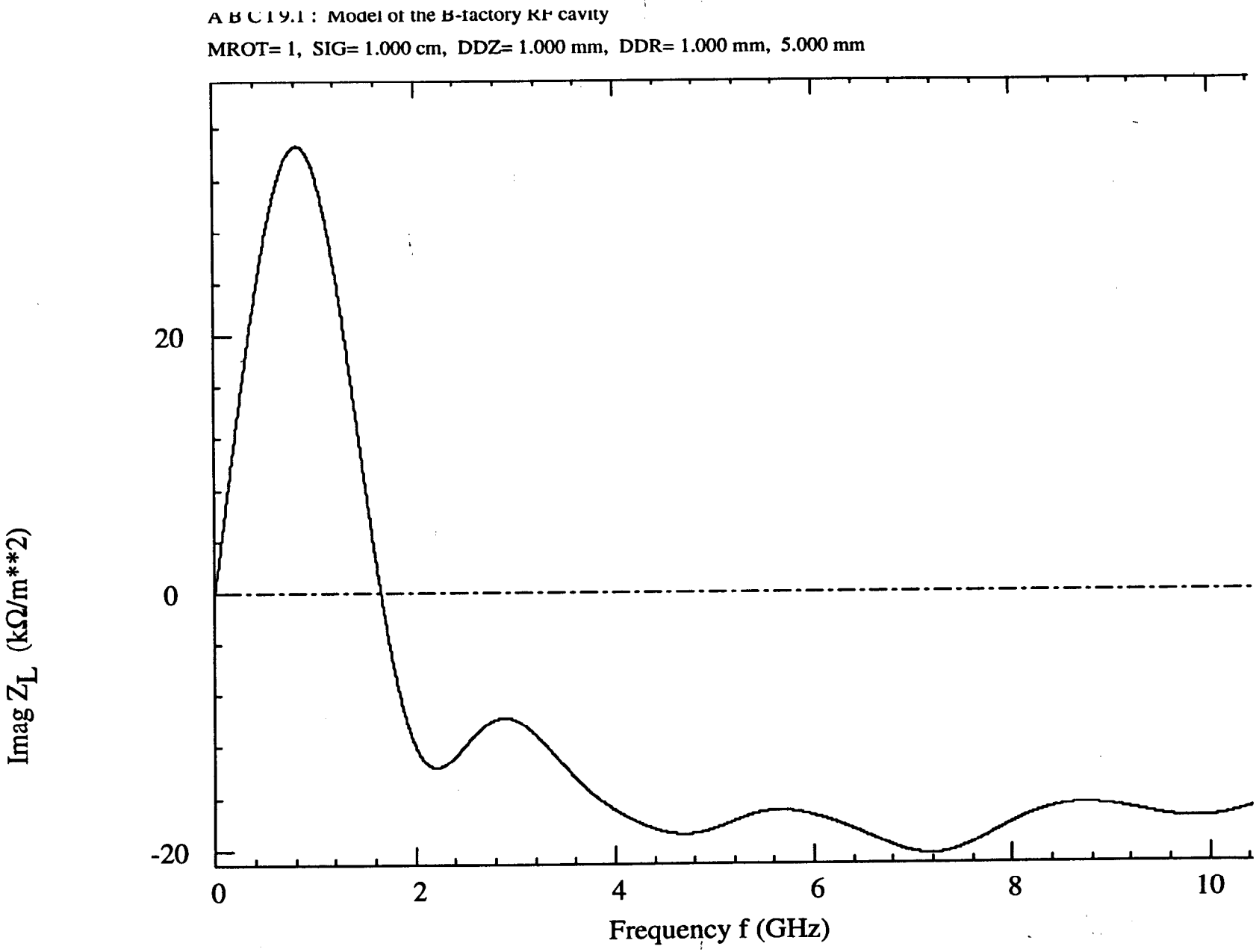
A B C 19.1 : Model of the B-factory RF cavity
MROT= 1, SIG= 1.000 cm, DDZ= 1.000 mm, DDR= 1.000 mm, 5.000 mm
Imag Z_L (kΩ/m**2)
20
0
-20
0
2
4
6
8
10
Frequency f (GHz)

Fig. 4c

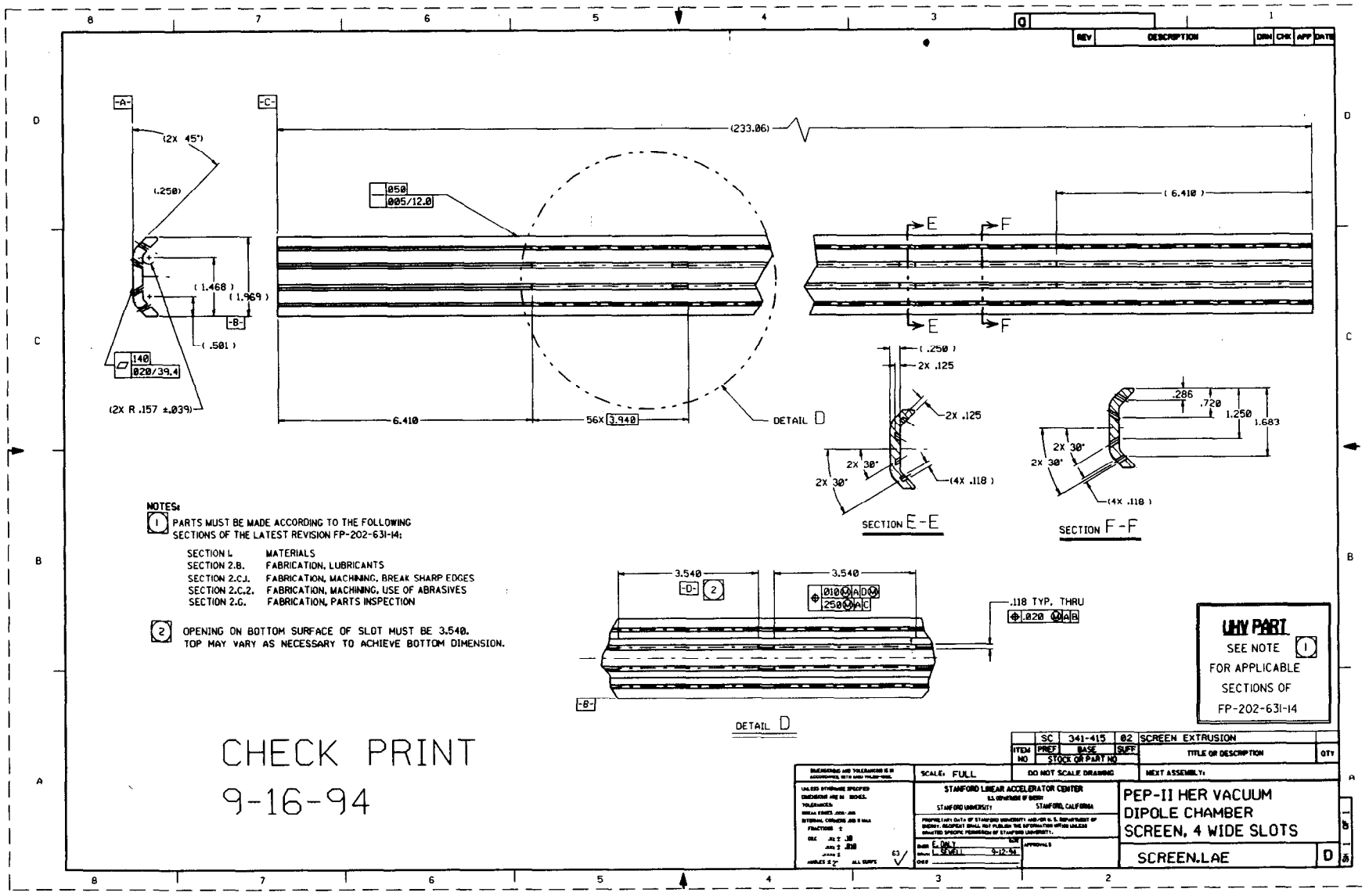
REV DESCRIPTION DRN CHK APP DATE
(233.86)
(6.410)
(2X 45°)
(.250)
(1.468)
(1.969)
(.501)
.140
.020/39.4
(2X R .157 ±.039)
.050
.005/12.0
6.410
56X 3.940
DETAIL D
E F
(.250)
2X .125
2X .125
2X 30°
2X 30°
(4X .118)
SECTION E-E
.286
.720
1.250
1.683
2X 30°
2X 30°
(4X .118)
SECTION F-F
NOTES:
1 PARTS MUST BE MADE ACCORDING TO THE FOLLOWING SECTIONS OF THE LATEST REVISION FP-202-631-14:
SECTION 1. MATERIALS
SECTION 2.B. FABRICATION, LUBRICANTS
SECTION 2.C.1. FABRICATION, MACHINING, BREAK SHARP EDGES
SECTION 2.C.2. FABRICATION, MACHINING, USE OF ABRASIVES
SECTION 2.G. FABRICATION, PARTS INSPECTION
2 OPENING ON BOTTOM SURFACE OF SLOT MUST BE 3.540. TOP MAY VARY AS NECESSARY TO ACHIEVE BOTTOM DIMENSION.
3.540
-D- 2
3.540
.010 M A D M
.250 M A C
.118 TYP. THRU
.020 M A B
-B-
DETAIL D
UHV PART
SEE NOTE 1
FOR APPLICABLE
SECTIONS OF
FP-202-631-14
CHECK PRINT
9-16-94
SC 341-415 02 SCREEN EXTRUSION
ITEM NO PREF BASE SUFF STOCK OR PART NO TITLE OR DESCRIPTION QTY
SCALE: FULL
DO NOT SCALE DRAWING
NEXT ASSEMBLY:
STANFORD LINEAR ACCELERATOR CENTER
STANFORD UNIVERSITY STANFORD, CALIFORNIA
E. ONLY
L. SEWELL 9-12-94
PEP-II HER VACUUM
DIPOLE CHAMBER
SCREEN, 4 WIDE SLOTS
SCREEN.LAE
D

Fig. 5a

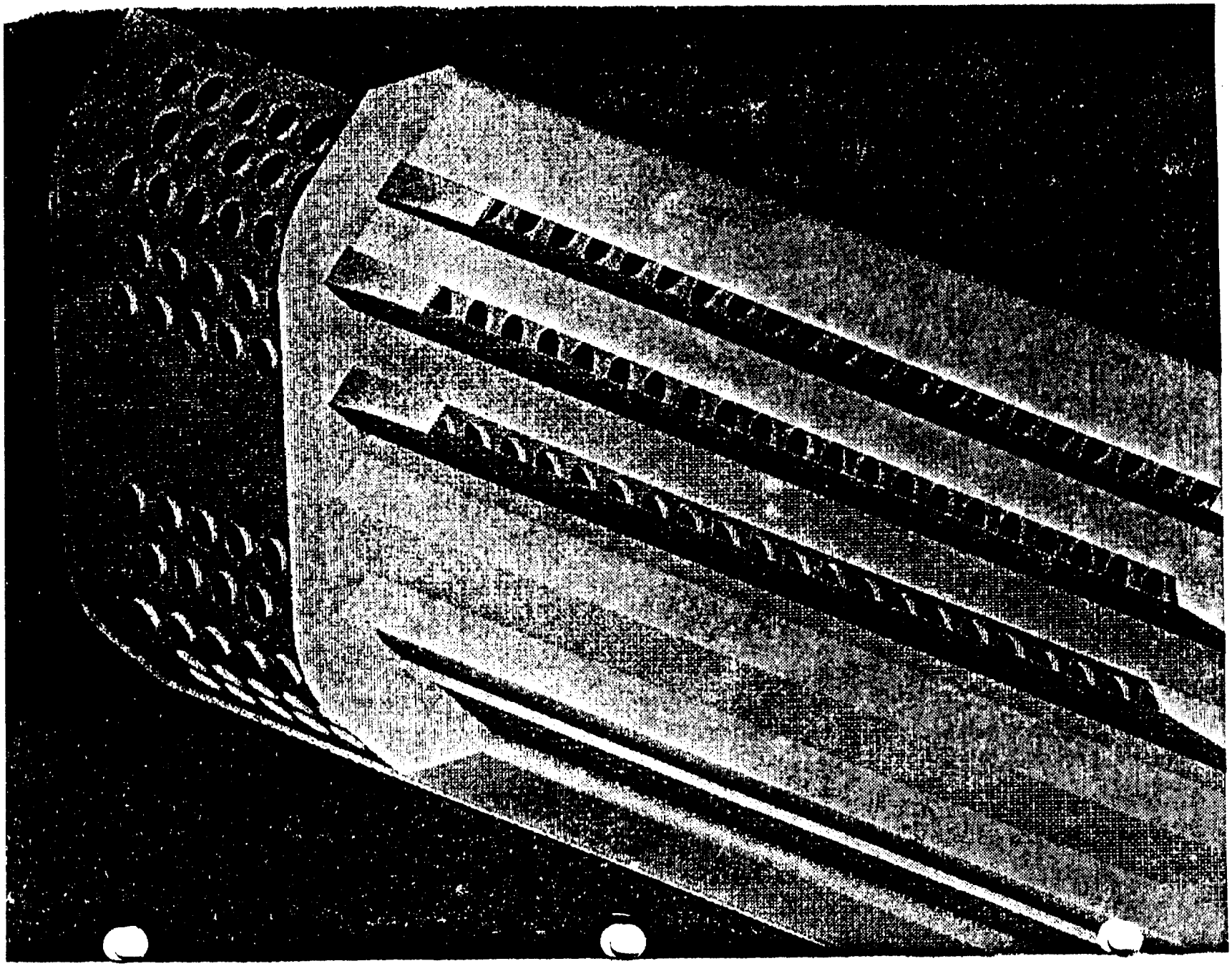

Fig. 5b

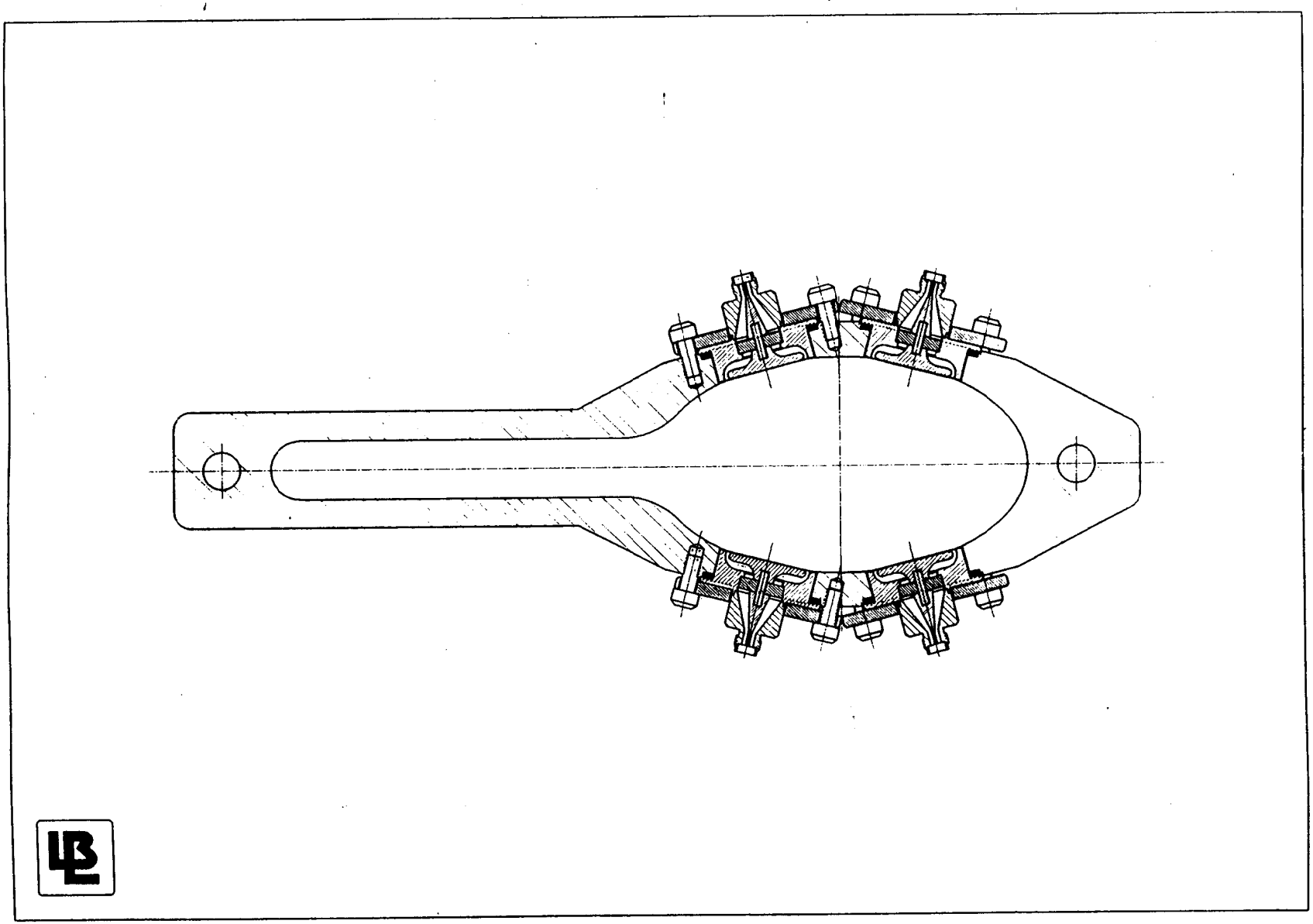

Fig. 6a

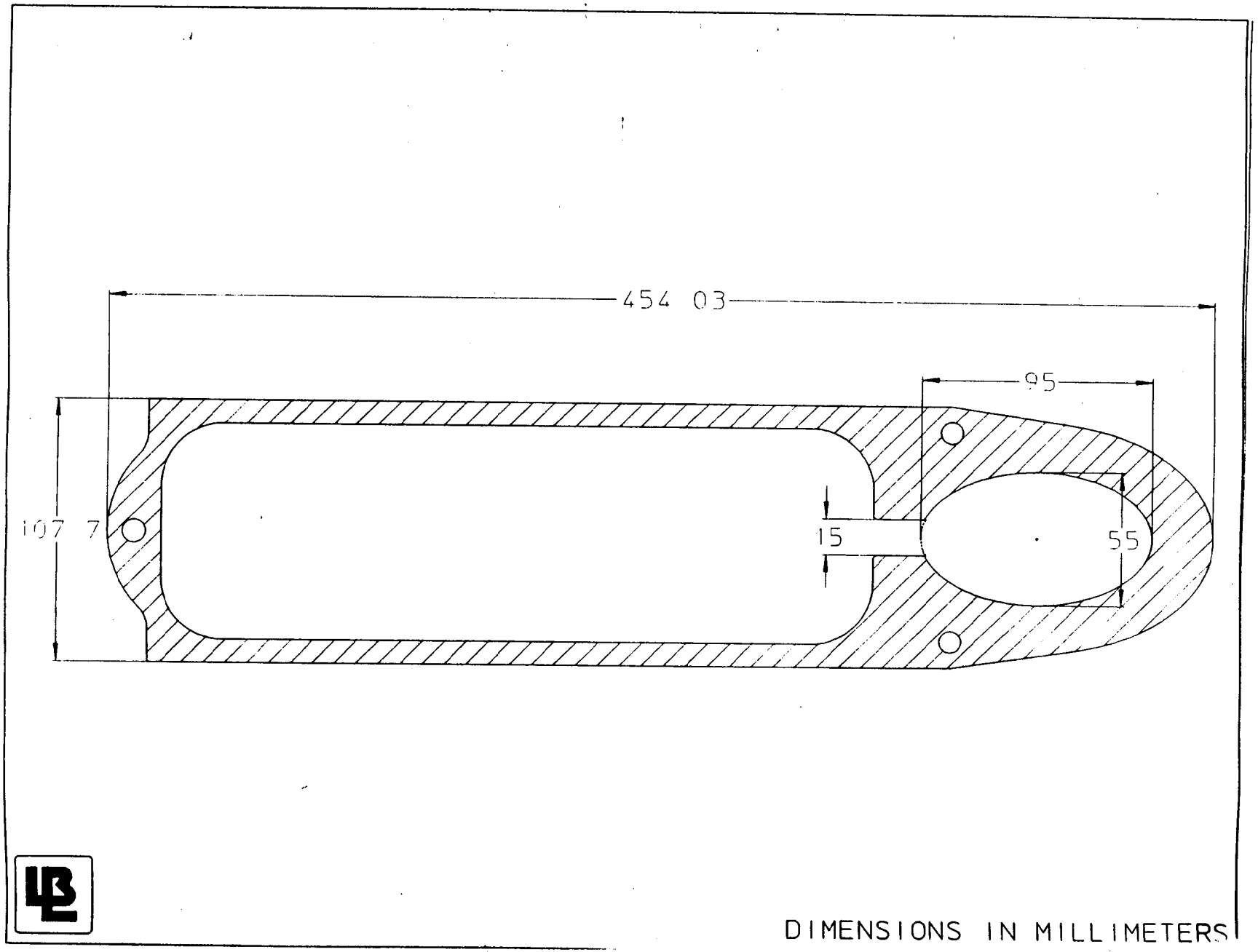

Fig. 6b

E. Henestroza

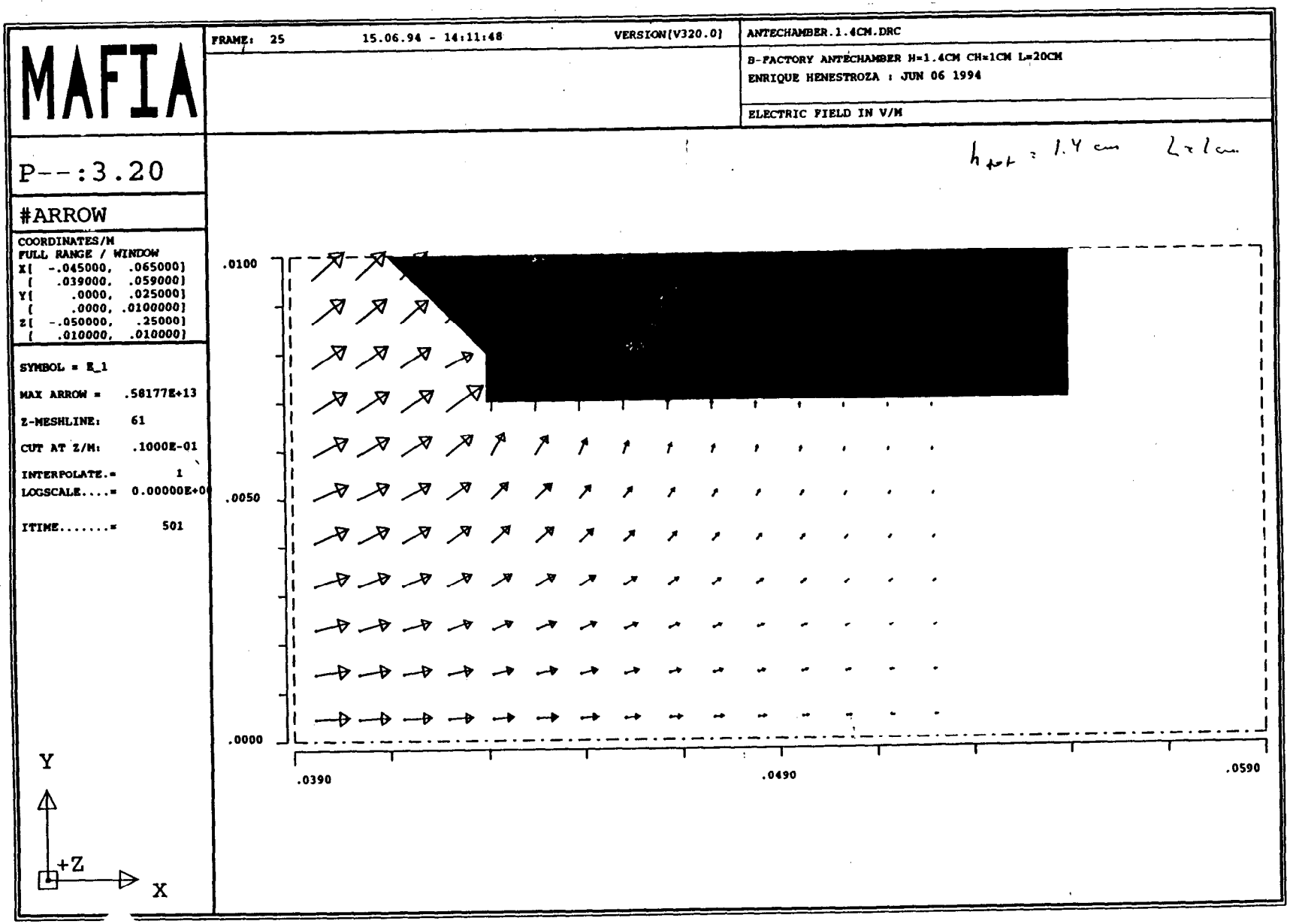

h_{tot} : 1.4 cm L = 1 cm

Fig. 7

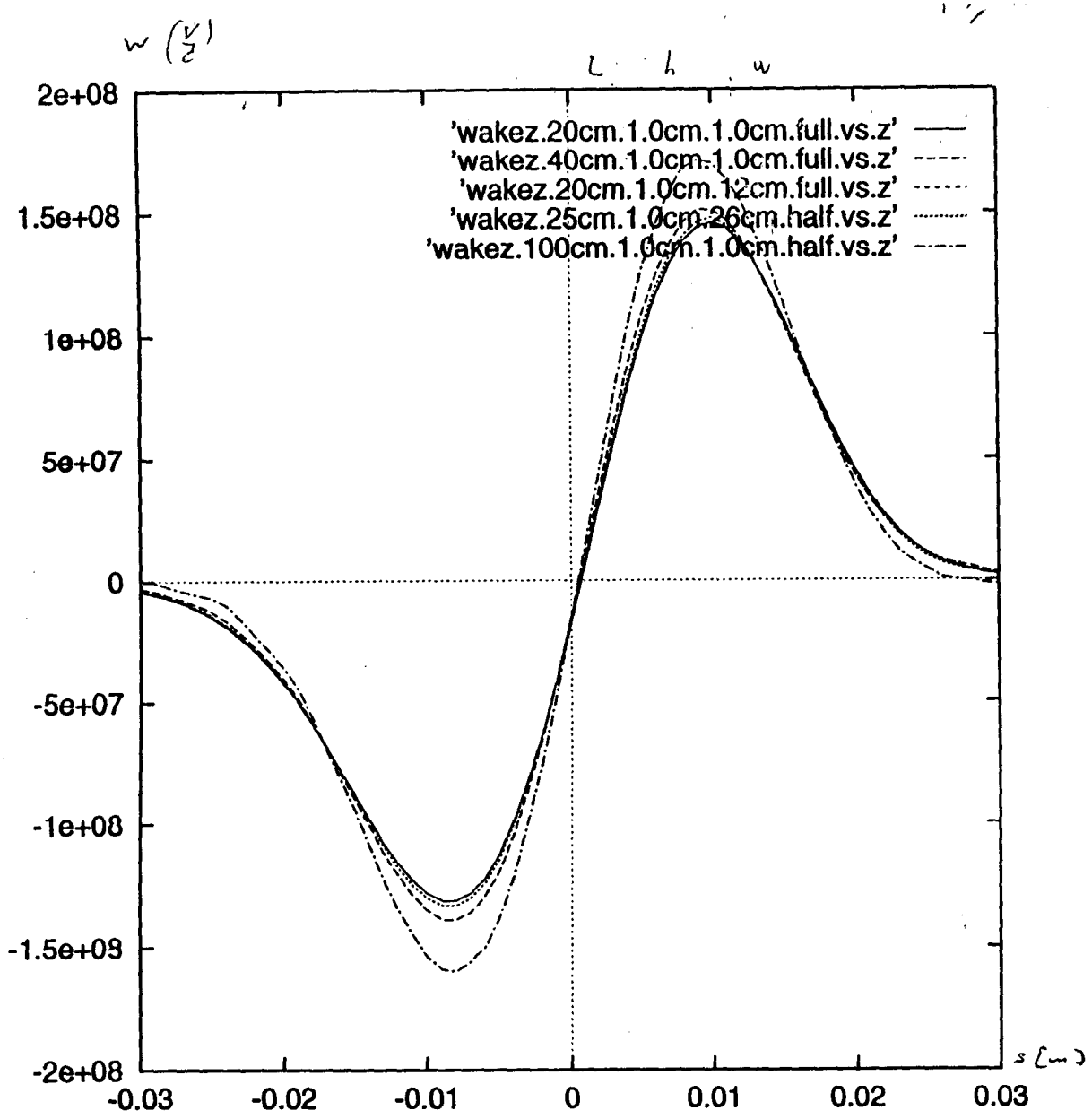

$$L = 0.7\ pH$$

$$W_{-} = \frac{1/5^2}{\sqrt{2\pi e}}$$

$$\bar{z} = -i\frac{z_0}{4\pi^2}\frac{\omega L^3}{c\,b^2}$$

$$L = \frac{4\pi}{6\pi^2}\frac{h^3}{b^2} = \frac{2}{3\pi}\frac{h^3}{b^2}$$

$h = 0.5\,cm$; $b = 2.5\,cm$

$$\frac{2}{10}\cdot\frac{1}{8\cdot 6.25} = \frac{1}{250}$$

$$= 4\cdot 10^{-3}\,nH$$

Fig. 8

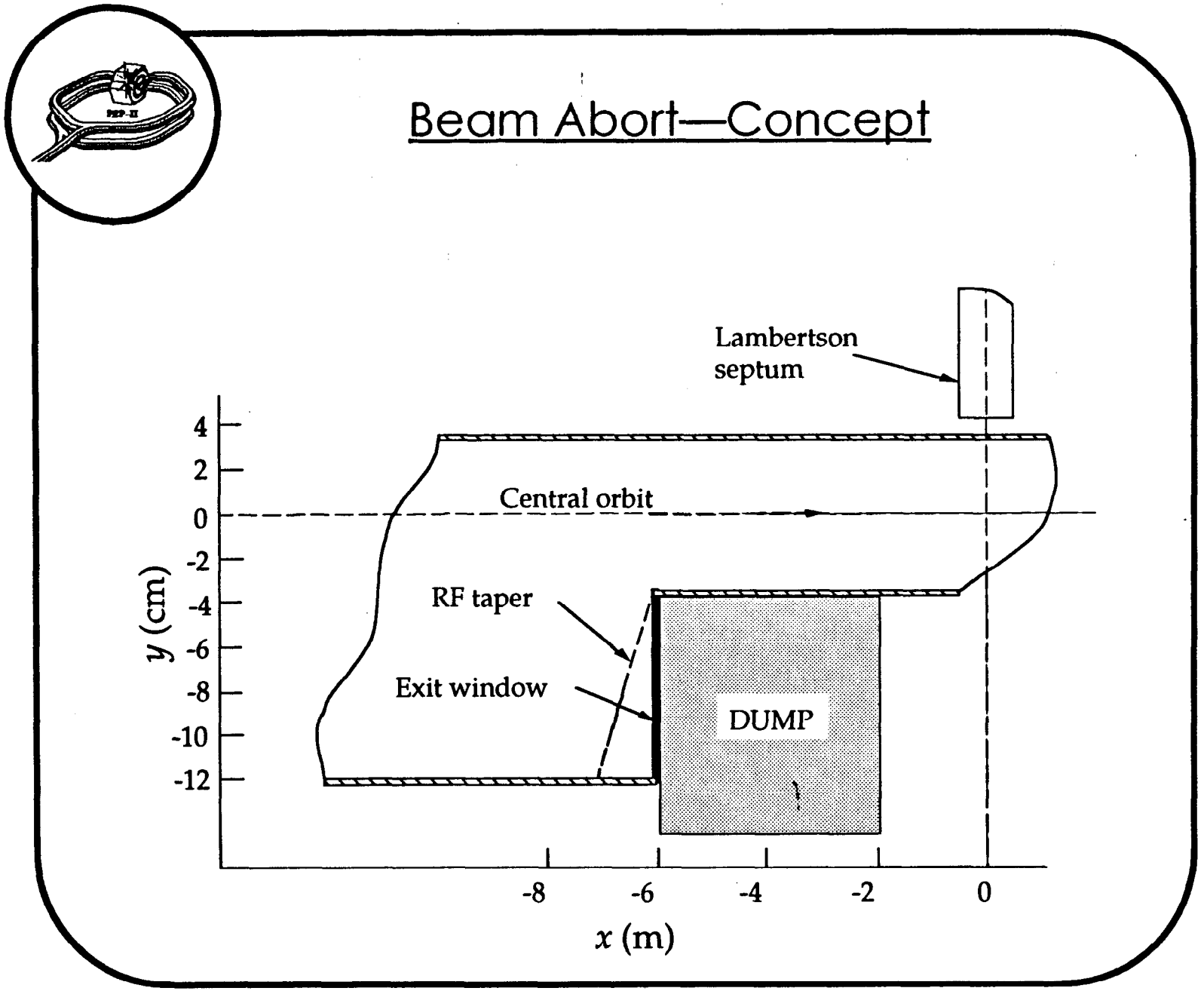
Beam Abort—Concept
Lambertson
septum
Central orbit
RF taper
Exit window
DUMP
4
2
0
-2
-4
-6
-8
-10
-12
y (cm)
-8
-6
-4
-2
0
x (m)
12/2/94 12:35
Beam Abort concept.cnv

Fig. 9a

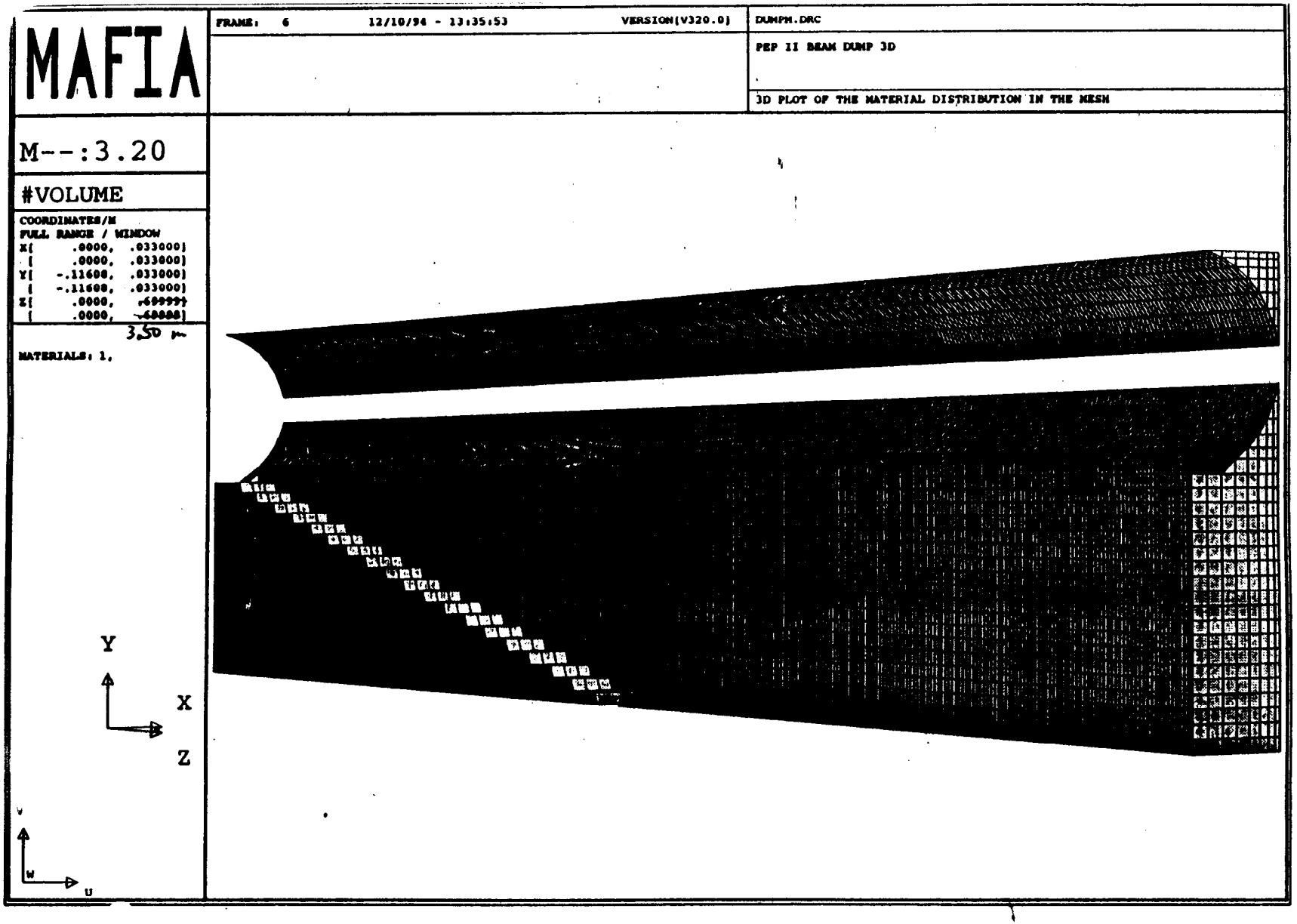
MAFIA
FRAME: 6 12/10/94 - 13:35:53 VERSION(V320.0)
DUMPH.DRC
PEP II BEAM DUMP 3D
3D PLOT OF THE MATERIAL DISTRIBUTION IN THE MESH
M--:3.20
#VOLUME
COORDINATES/M
FULL RANGE / WINDOW
X[.0000, .033000]
[.0000, .033000]
Y[-.11600, .033000]
[-.11600, .033000]
Z[.0000, .609997]
[.0000, .609998]
3.5D
MATERIALS: 1,
Y
X
Z
V
W
U

Fig. 9b

M. Sullivan

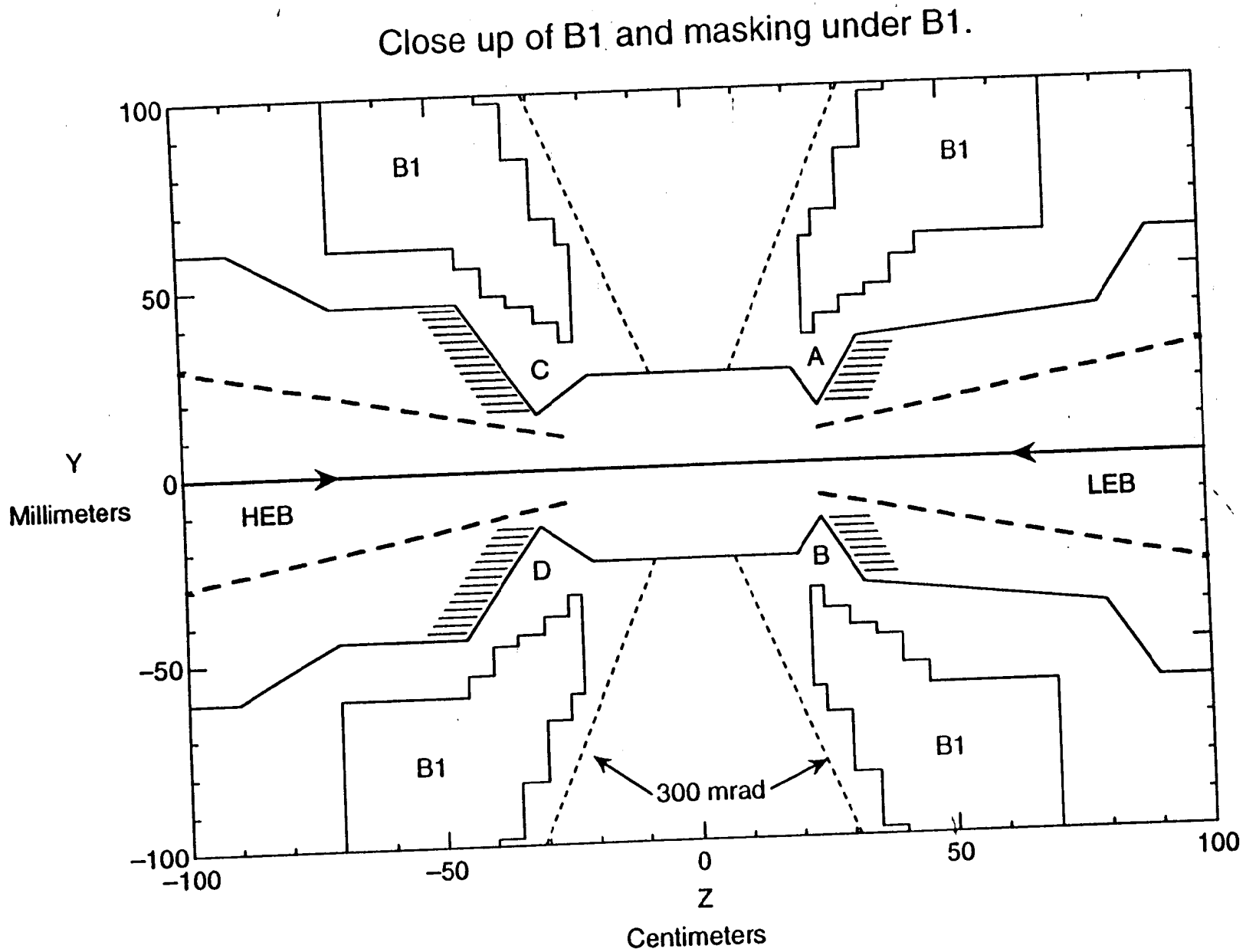

Fig. 10a

M. Sullivan

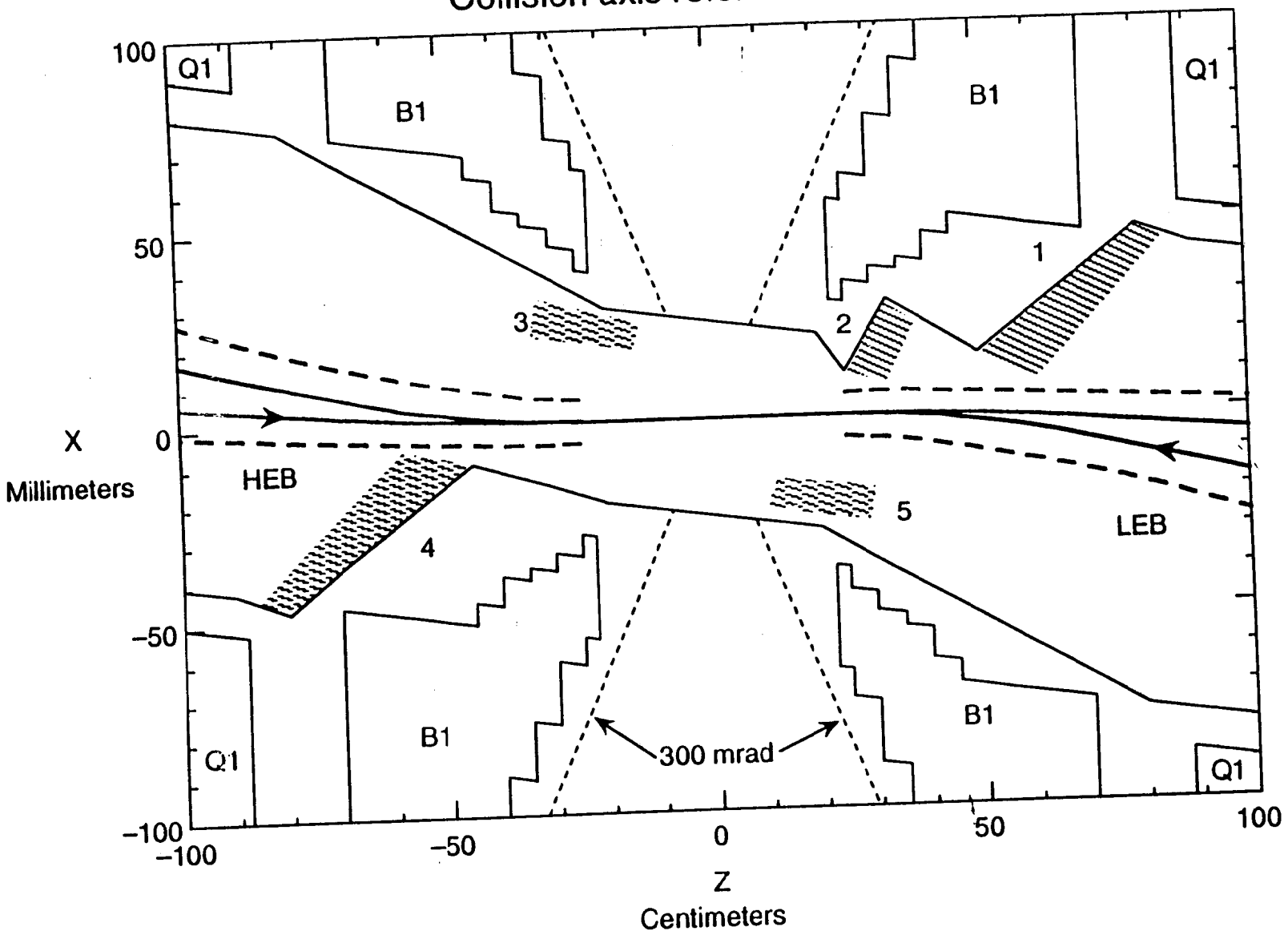

Fig. 10b

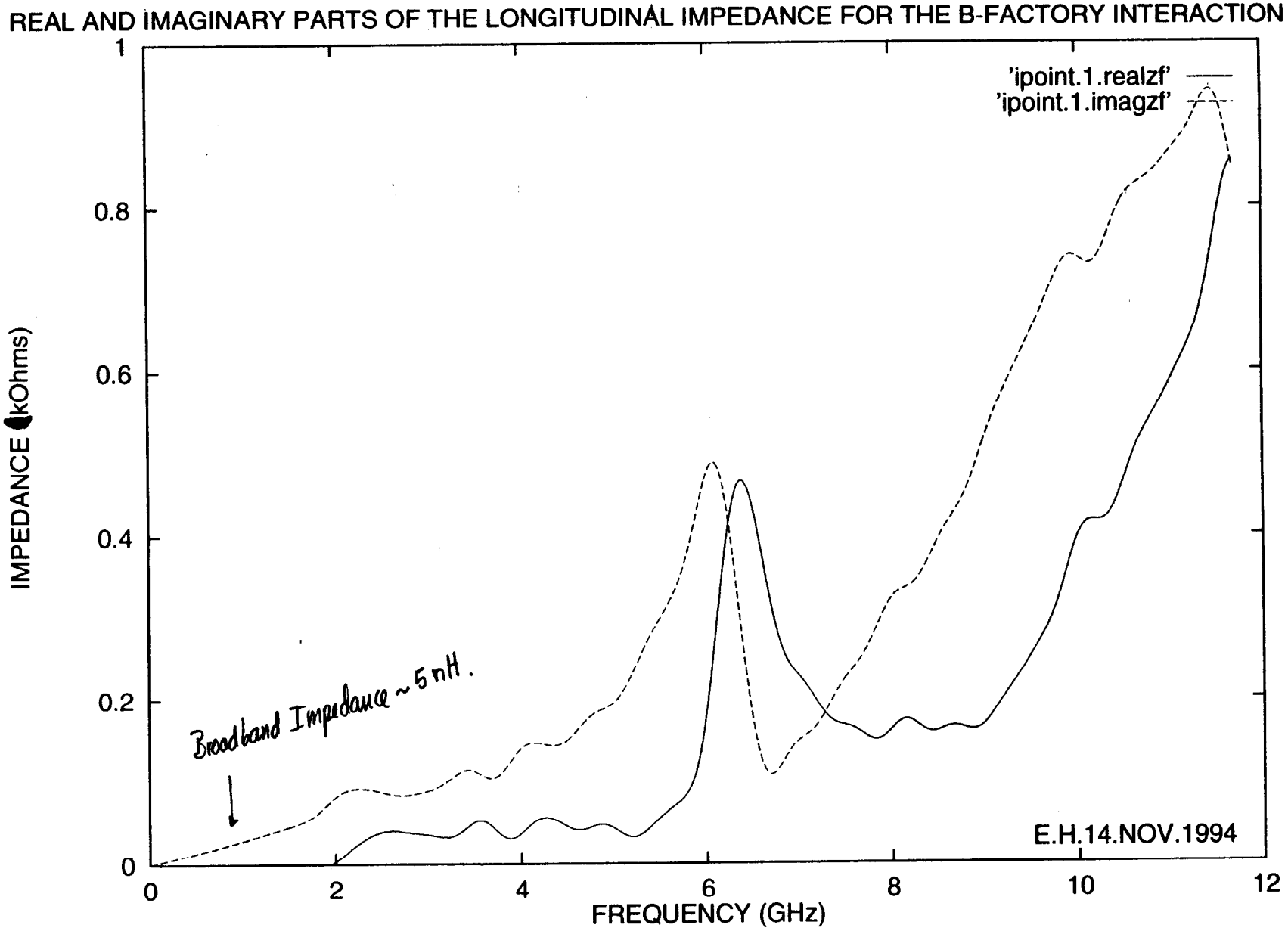
REAL AND IMAGINARY PARTS OF THE LONGITUDINAL IMPEDANCE FOR THE B-FACTORY INTERACTION R
'ipoint.1.realzf'
'ipoint.1.imagzf'
IMPEDANCE (kOhms)
FREQUENCY (GHz)
0
0.2
0.4
0.6
0.8
1
0
2
4
6
8
10
12
Broadband Impedance ~ 5 nH.
E.H.14.NOV.1994

Fig. 11

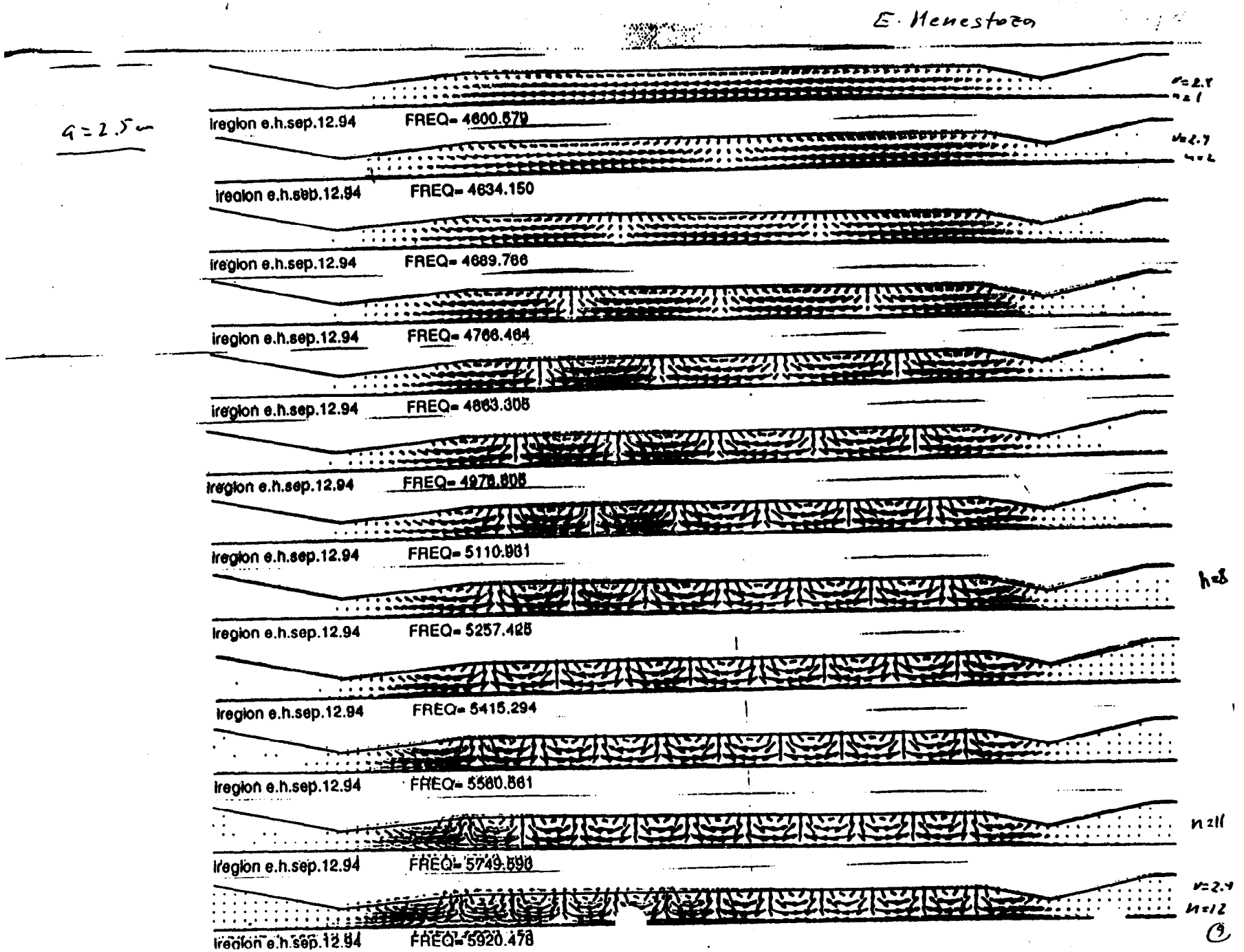
E. Menestrina
q = 2.5 m
lregion e.h.sep.12.94 FREQ= 4600.679
lregion e.h.sep.12.94 FREQ= 4634.150
lregion e.h.sep.12.94 FREQ= 4669.766
lregion e.h.sep.12.94 FREQ= 4766.464
lregion e.h.sep.12.94 FREQ= 4863.305
lregion e.h.sep.12.94 FREQ= 4978.808
lregion e.h.sep.12.94 FREQ= 5110.961
lregion e.h.sep.12.94 FREQ= 5257.425
lregion e.h.sep.12.94 FREQ= 5415.294
lregion e.h.sep.12.94 FREQ= 5580.861
lregion e.h.sep.12.94 FREQ= 5749.898
lregion e.h.sep.12.94 FREQ= 5920.478

Fig. 12

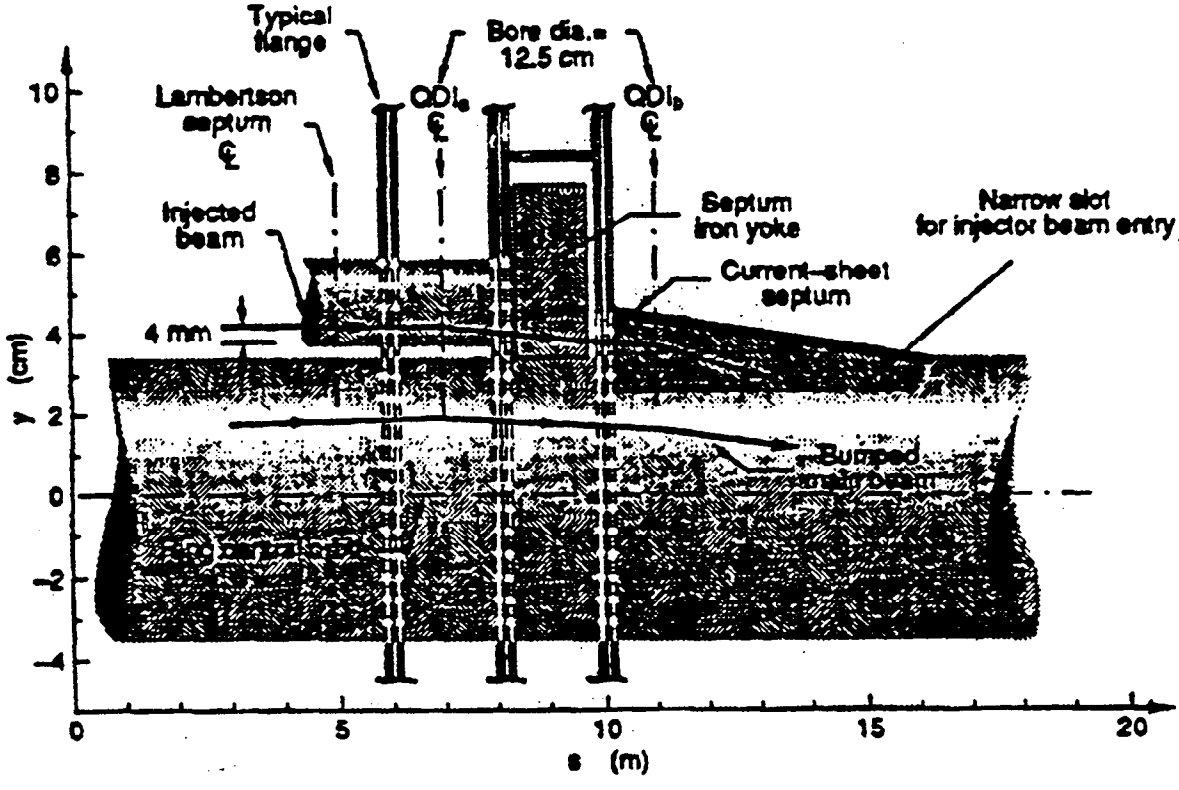
Typical flange
Bore dia.= 12.5 cm
Lambertson septum
QDI$_a$
QDI$_b$
Injected beam
Septum iron yoke
Narrow slot for injector beam entry
Current-sheet septum
4 mm
Bumped beam
y (cm)
s (m)
10
8
6
4
2
0
−2
−4
0
5
10
15
20

Fig. 13a

E. Lyn

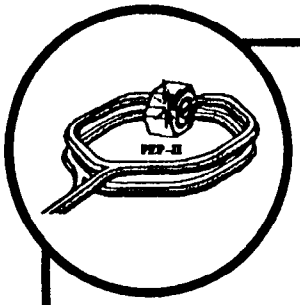

Injection Slot Geometry

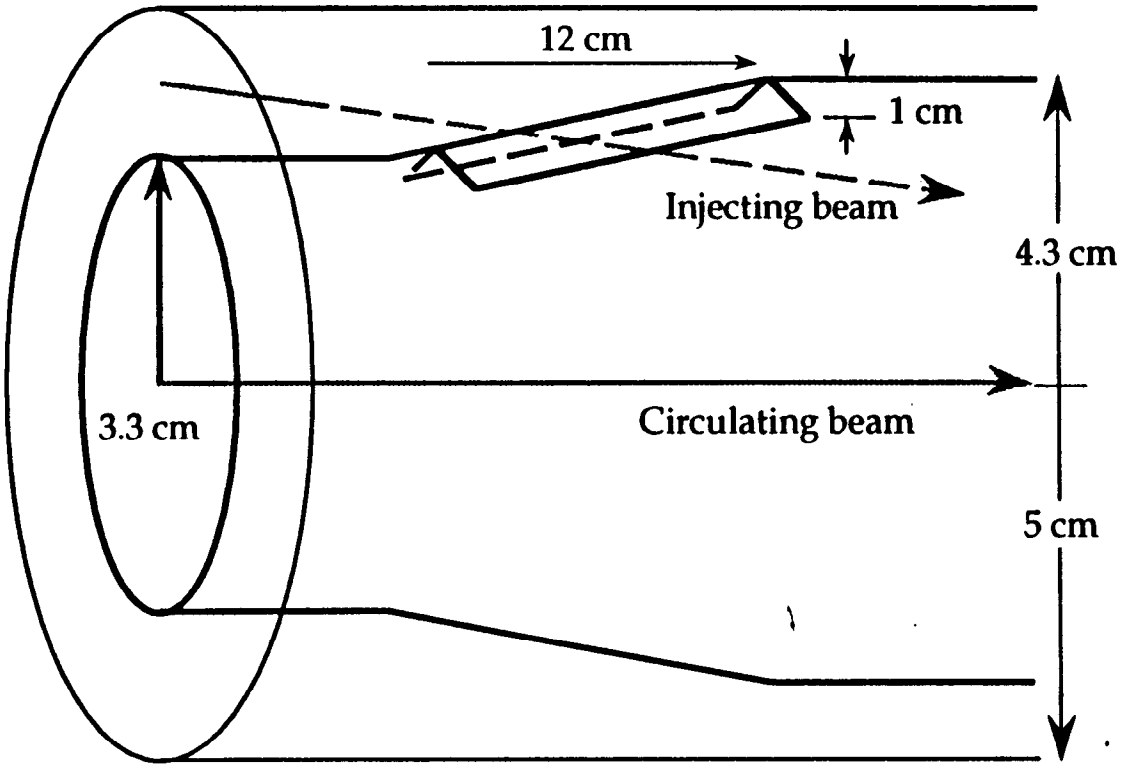

11-94

12/2/94 11:16 injection slot.cnv

Fig. 13b

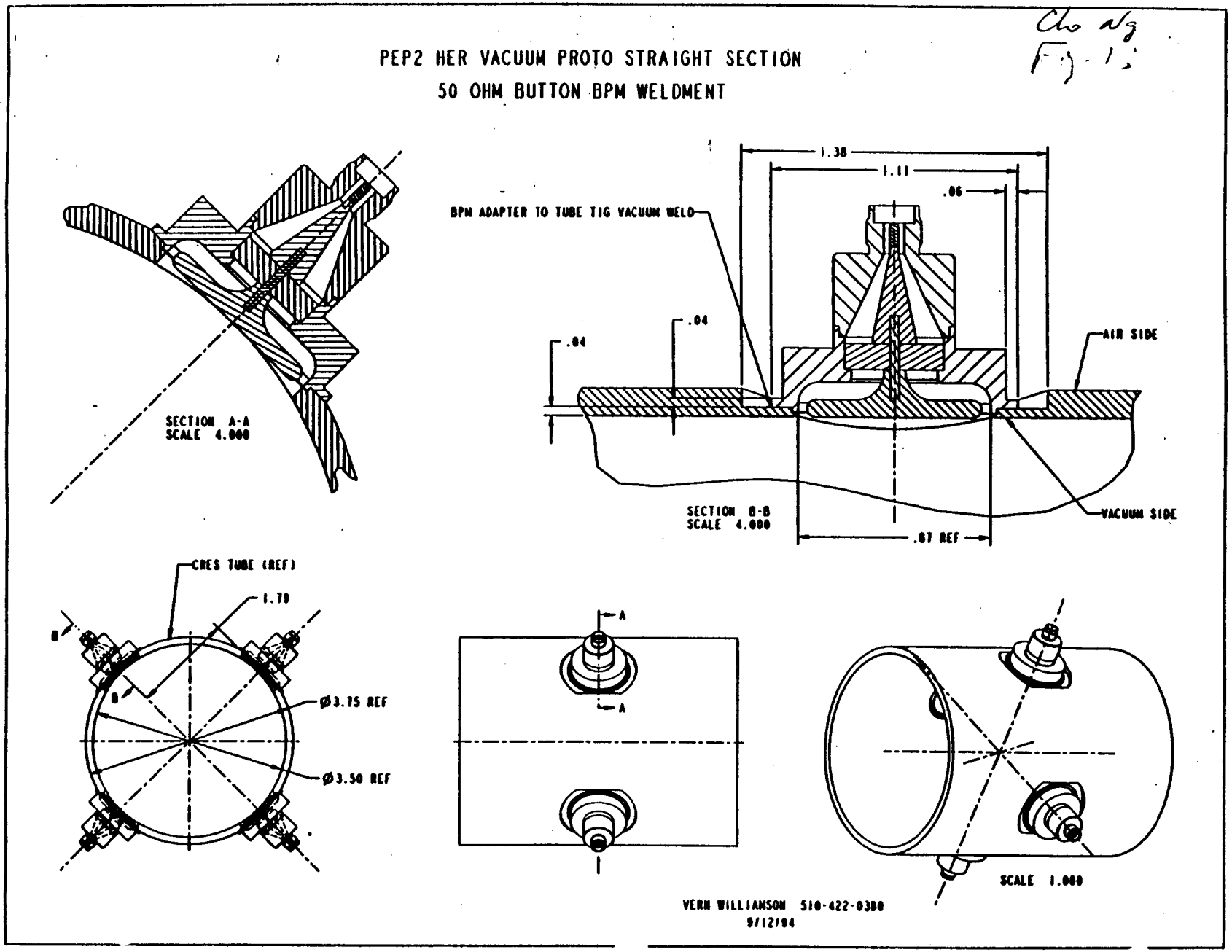
PEP2 HER VACUUM PROTO STRAIGHT SECTION
50 OHM BUTTON BPM WELDMENT
SECTION A-A
SCALE 4.000
1.38
1.11
.06
BPM ADAPTER TO TUBE TIG VACUUM WELD
.04
.04
AIR SIDE
SECTION B-B
SCALE 4.000
VACUUM SIDE
.87 REF
CRES TUBE (REF)
1.79
B
B
Ø3.75 REF
Ø3.50 REF
A
A
SCALE 1.000
VERN WILLIAMSON 510-422-0388
9/12/94

Fig. 14

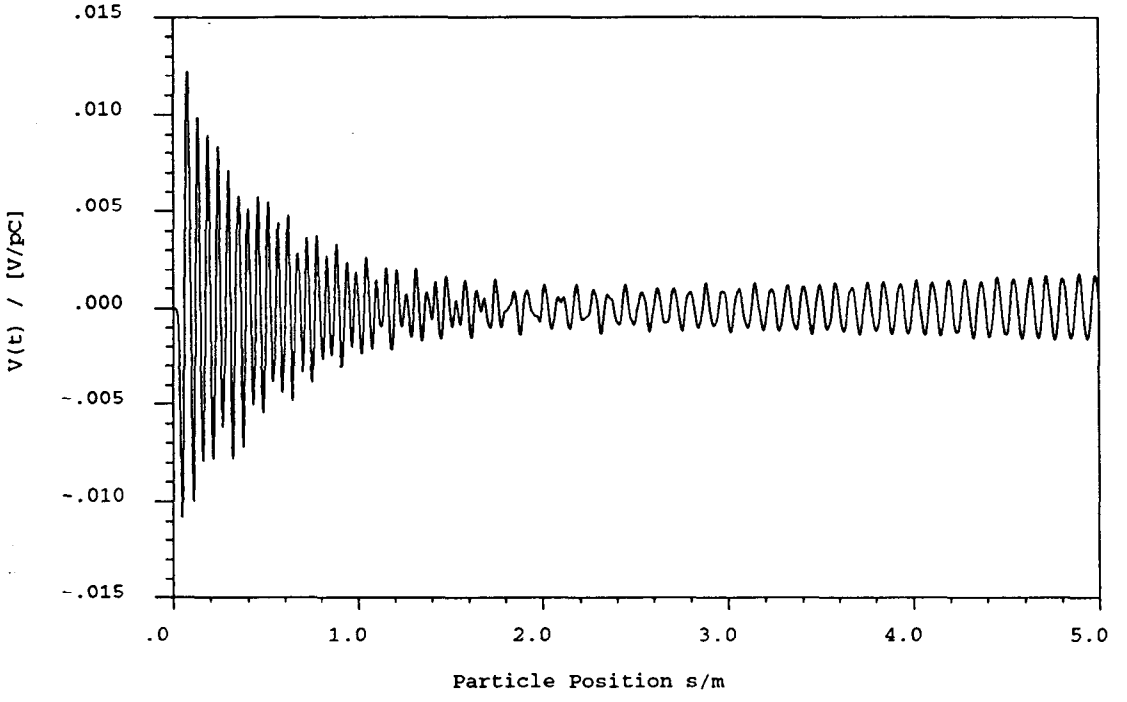

Figure 3: Longitudinal wakefield of the 2-cm BPM as a function of the particle position for a Gaussian bunch with $\sigma_z = 1$ cm.

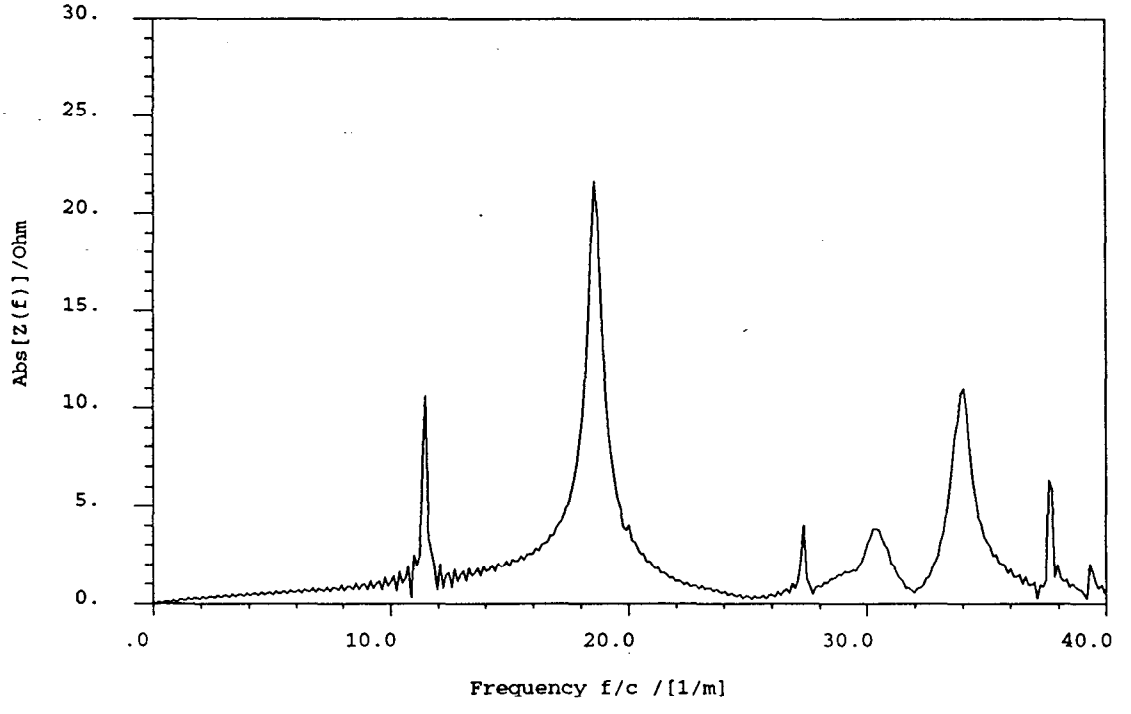

Figure 4: Longitudinal impedance spectrum of the 2-cm BPM as a function of the inverse wavelength for a Gaussian bunch with $\sigma_z = 1$ cm.

CIRCULAR BEAM PIPE (2 cm) J. Gratt Fig. 15b

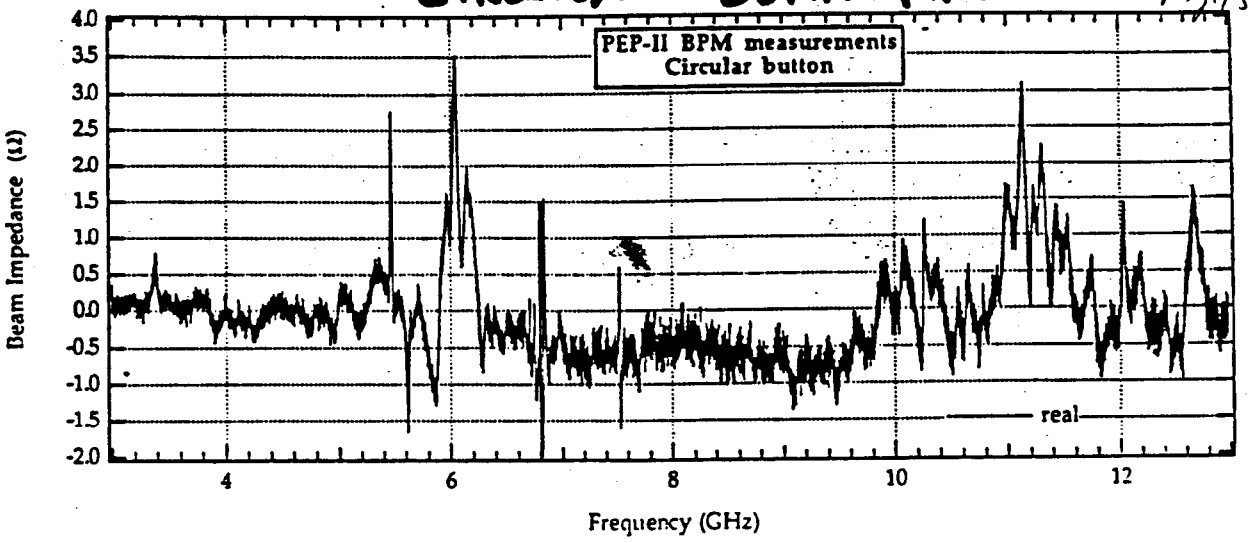

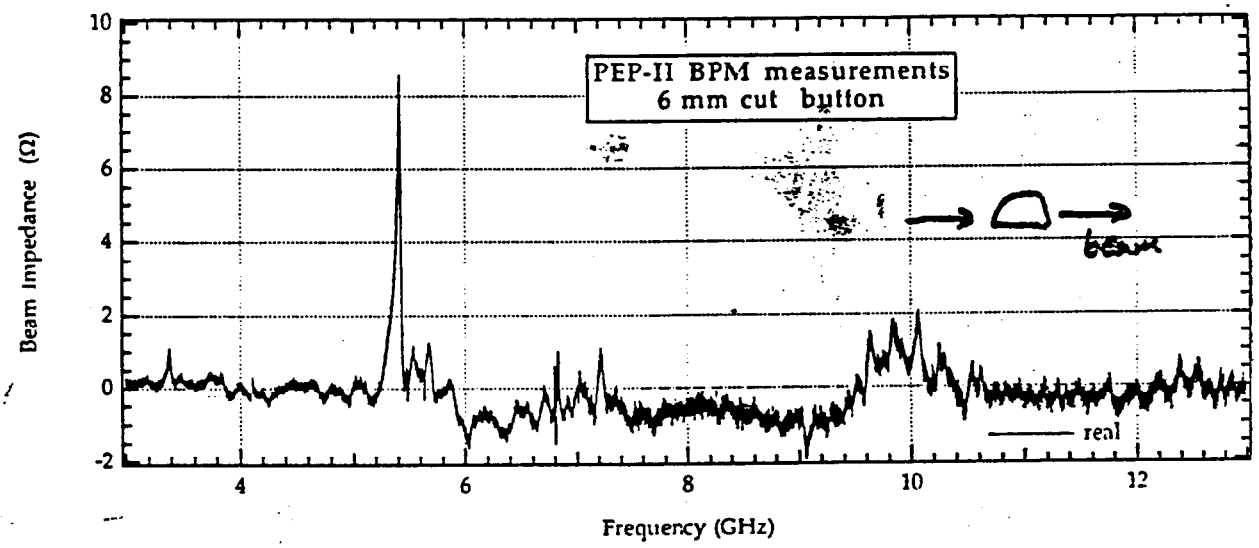

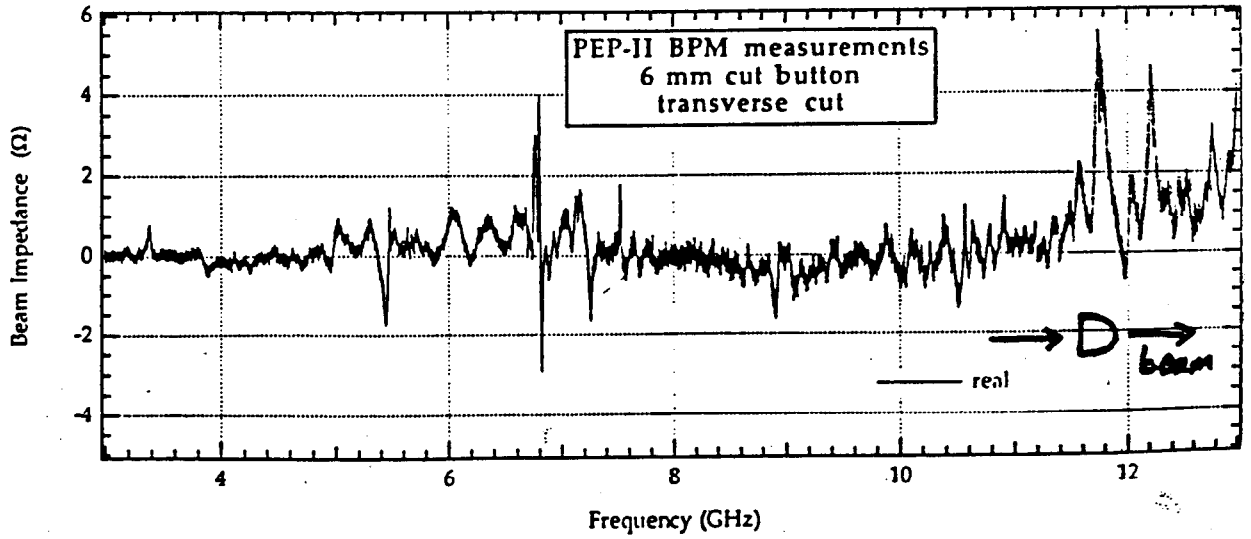

Fig. 15b

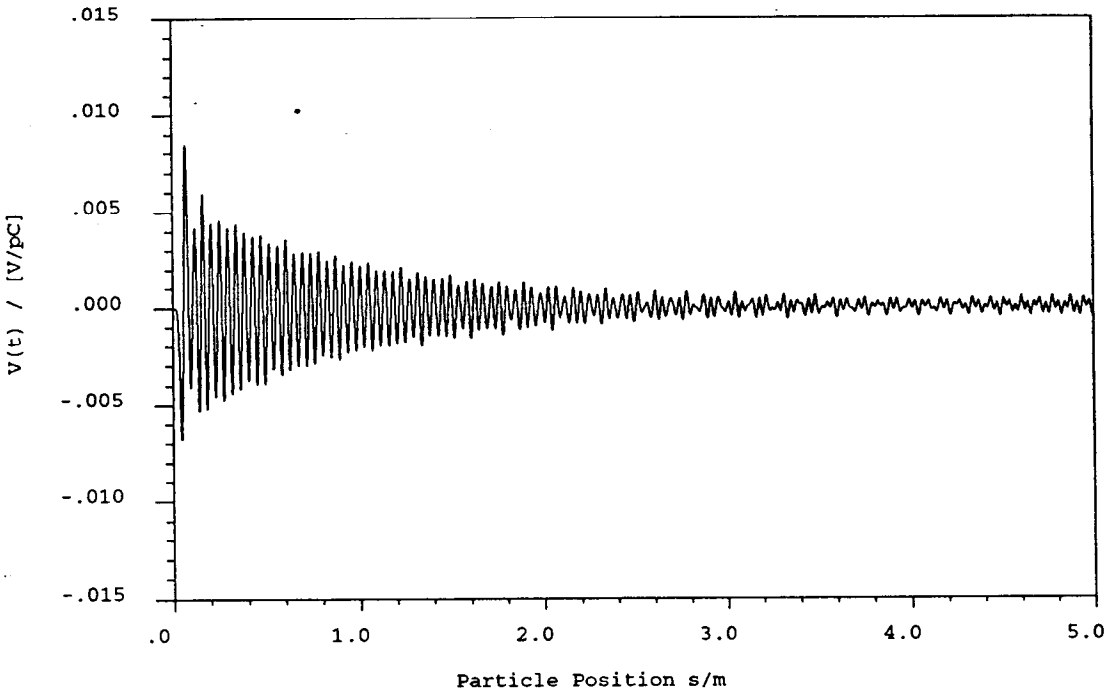

Figure 12: Longitudinal wakefield of the 1.5-cm BPM as a function of the particle position for a Gaussian bunch with $\sigma_z = 1$ cm.

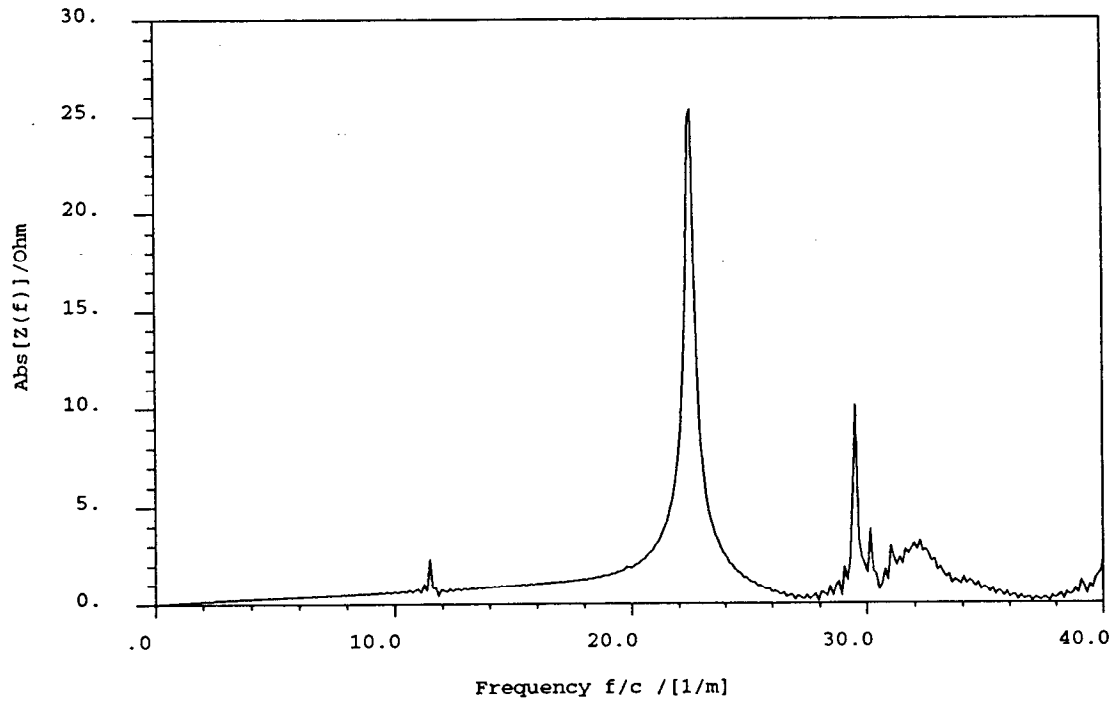

Figure 13: Longitudinal impedance spectrum of the 1.5-cm BPM as a function of the inverse wavelength for a Gaussian bunch with $\sigma_z = 1$ cm.

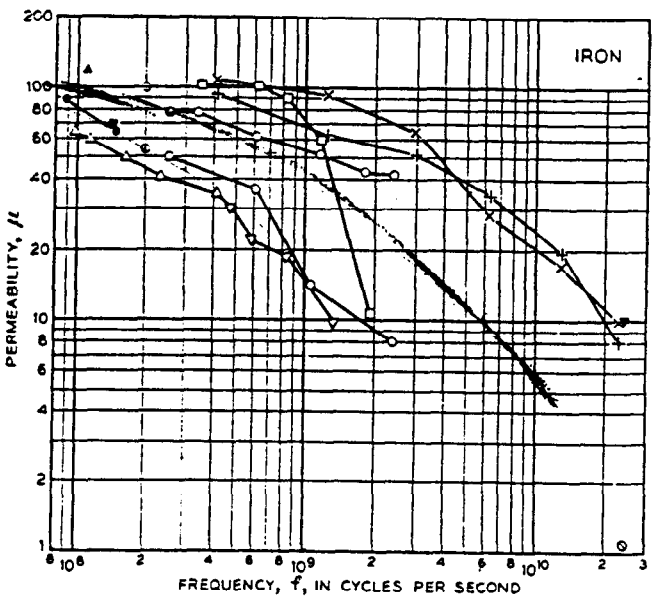

FIG. 17-23. Collection of data on the permeability of iron at high frequencies. Sources: ○, Sänger [34S7]; + and ×, Arkadiew [19A1]; △, Hoag and Gottlieb [39H3]; ▽, Hoag and Jones [32H4]; □, Lindman; ●, Möhring [39M3]; ▲, Schwarz [32S8]; ⊘, Maxwell [46M1]; ■, Procopiu and d'Albon [37P2]; ⊖, Johnson, Rado and Maloof [47J1]; ⊙, Glathart [39G5].

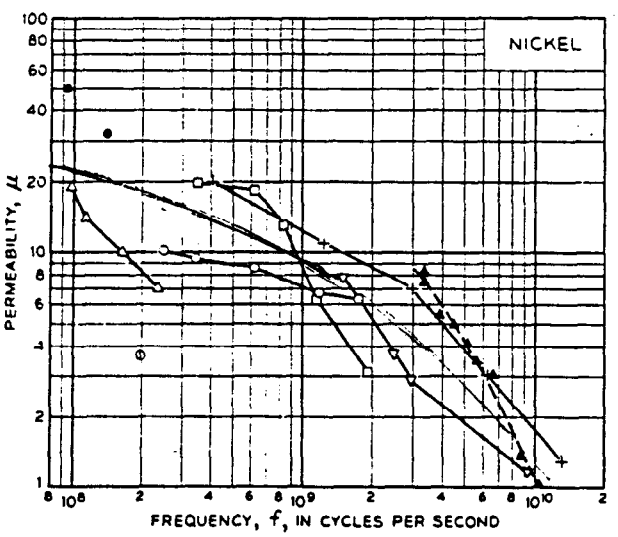

FIG. 17-24. Collection of data on the permeability of nickel at high frequencies. Sources: +, Arkadiew [19A1]; △, Hoag and Gottlieb [39H3]; □, Lindman [38L2]; ▽, Simon [46S1]; ●, Möhring [39M3]; ⊙, Glathart [39G5]; ○, Potapenko and Sänger ([33P1] and private communication to C. Kittel); ▲, Hodsman *et al.* [49H2].

Fig. 17

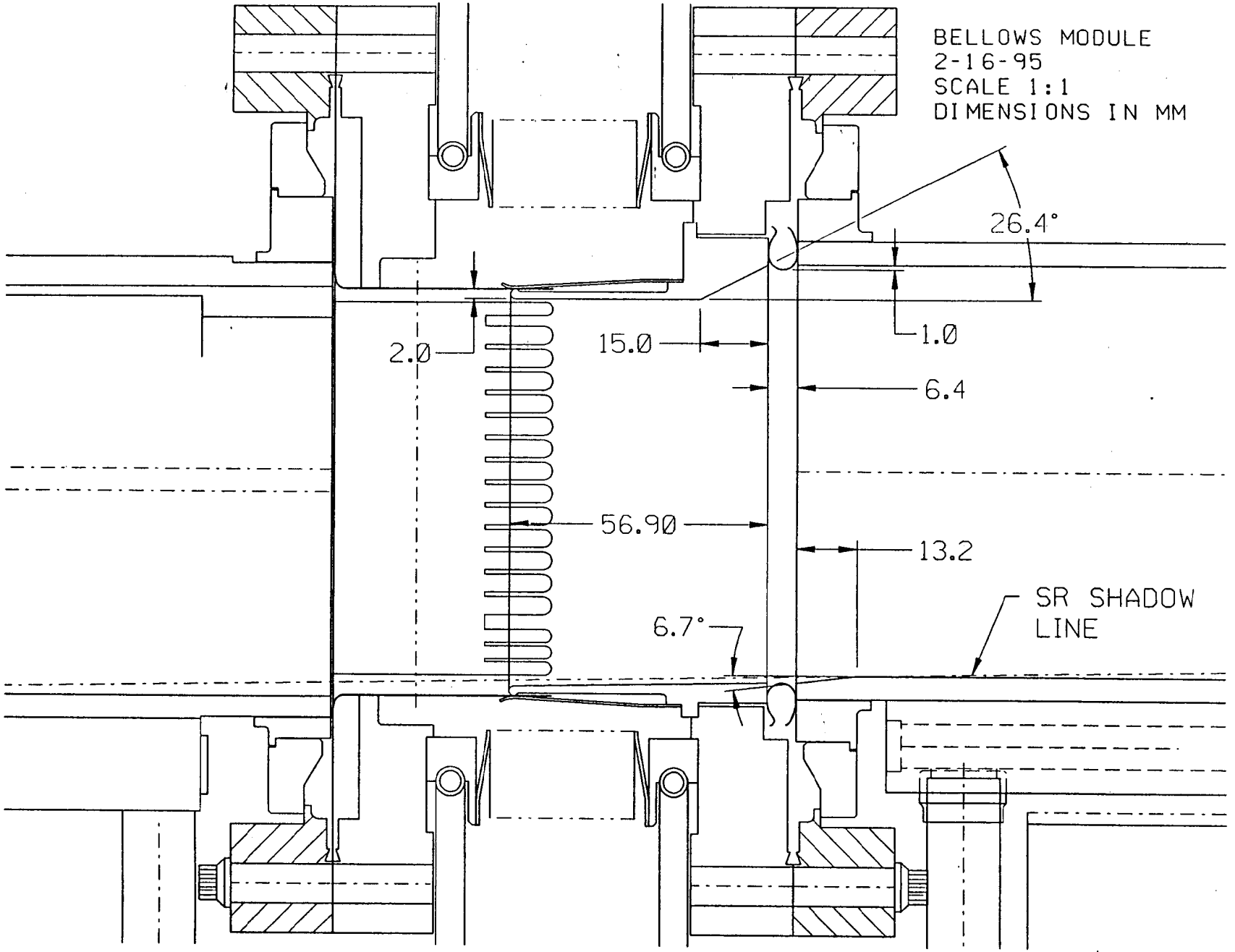
BELLOWS MODULE
2-16-95
SCALE 1:1
DIMENSIONS IN MM
26.4°
2.0
15.0
1.0
6.4
56.90
13.2
SR SHADOW
LINE
6.7°

Fig. 18a

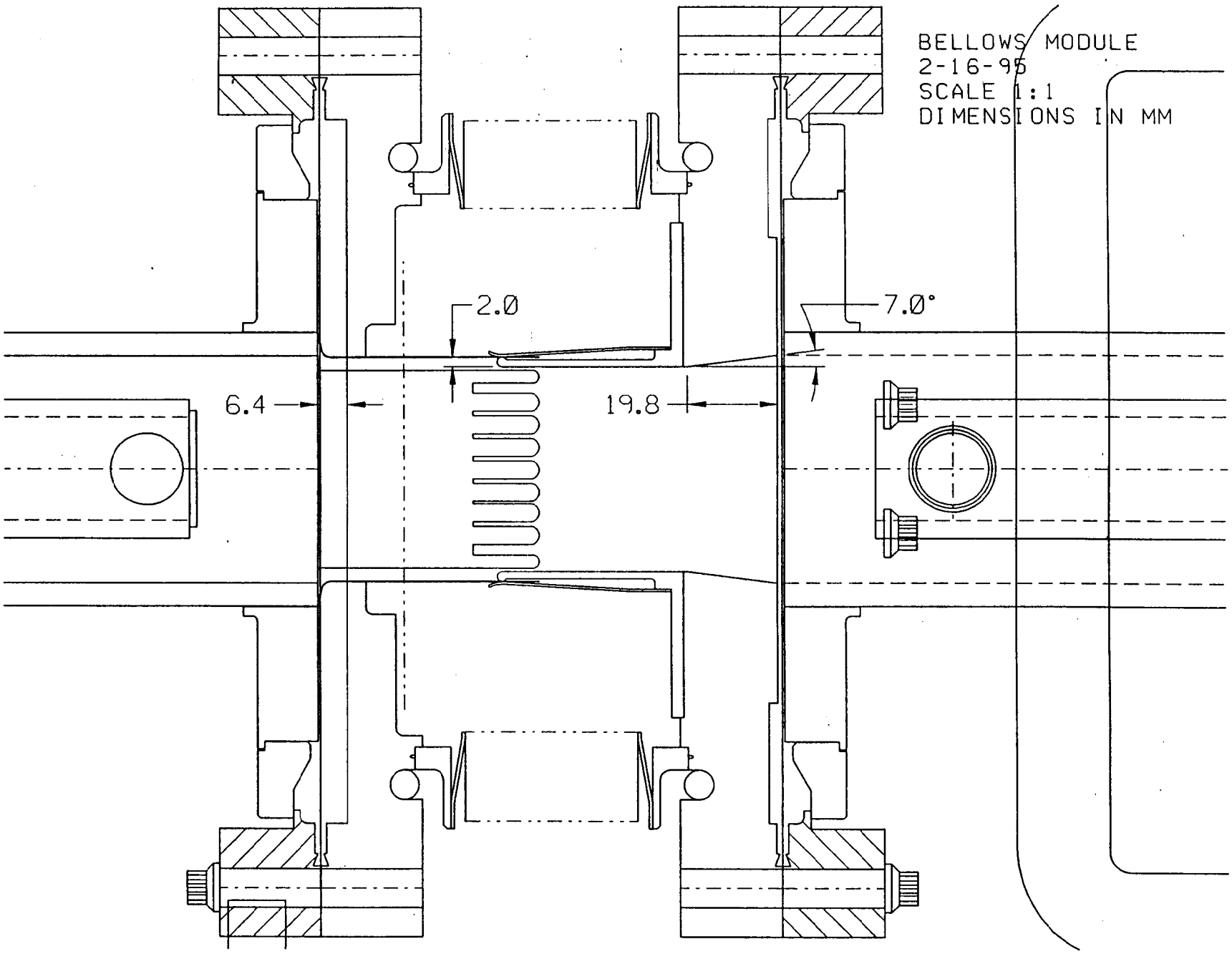

Fig. 18b

PEP-II HER STRAIGHT PUMP-TEE MODULAR PLENUM CONCEPT

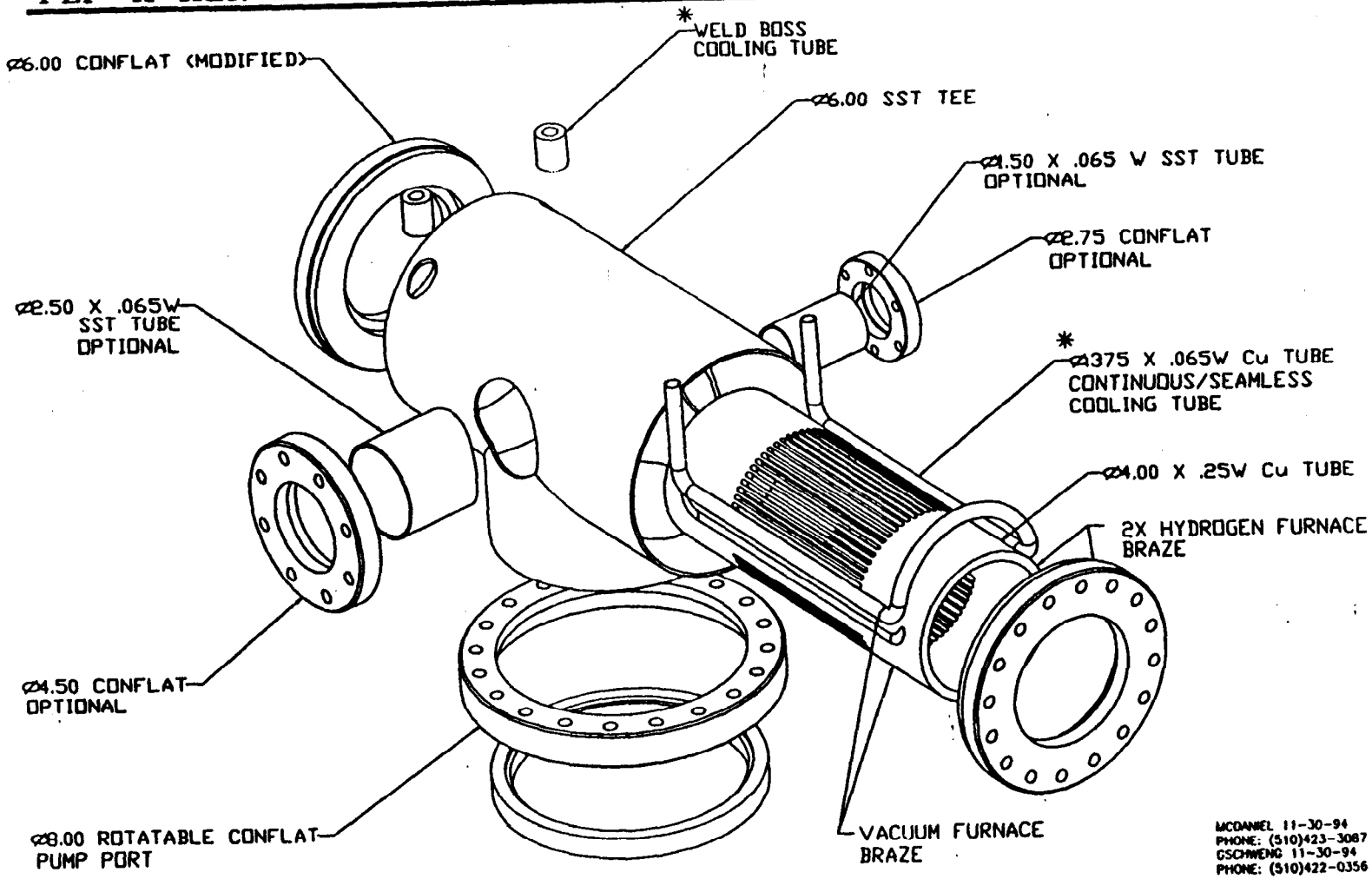

MCDANIEL 11-30-94
PHONE: (510)423-3087
GSCHWEND 11-30-94
PHONE: (510)422-0356

SHEET 3

NOTES:
ALL STAINLESS COMPONENTS ARE WELDED VACUUM TIGHT
VACUUM FURNACE BRAZE (VACUUM TIGHT)

Fig. 19a

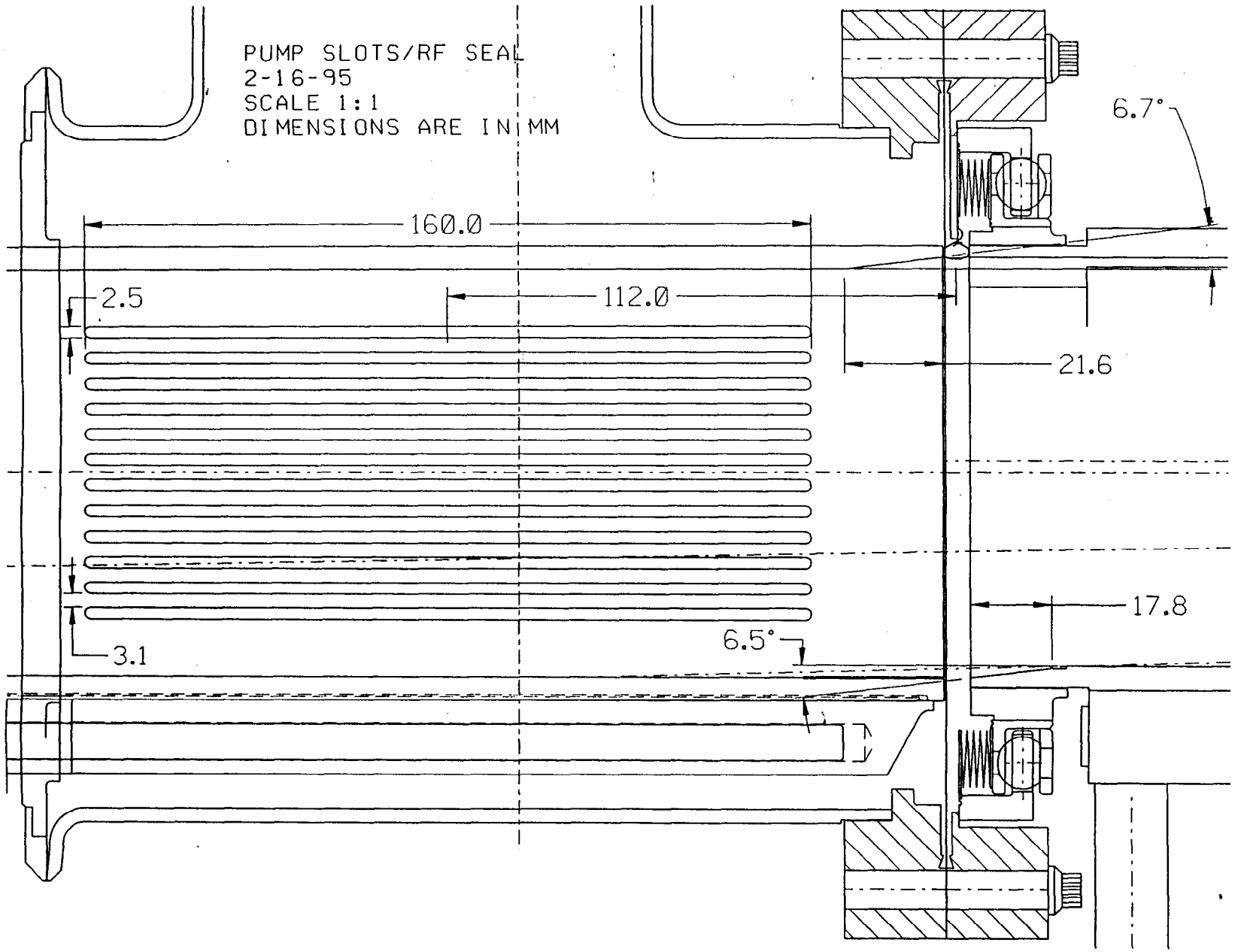
PUMP SLOTS/RF SEAL
2-16-95
SCALE 1:1
DIMENSIONS ARE IN MM
160.0
2.5
112.0
21.6
6.7°
17.8
3.1
6.5°

Fig. 19b

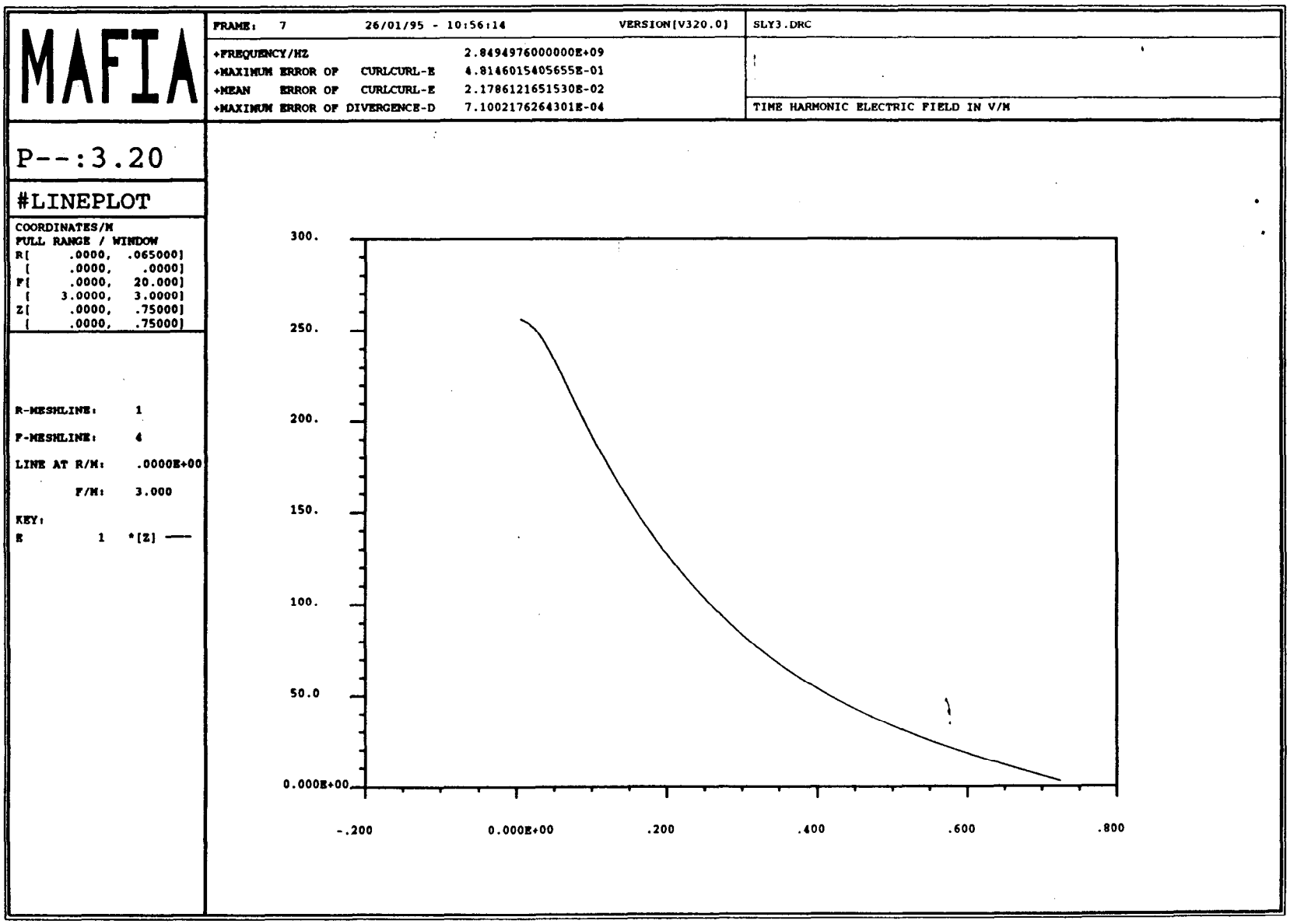
MAFIA
FRAME: 7 26/01/95 - 10:56:14 VERSION[V320.0]
SLY3.DRC
+FREQUENCY/HZ 2.8494976000000E+09
+MAXIMUM ERROR OF CURLCURL-E 4.81460154056555E-01
+MEAN ERROR OF CURLCURL-E 2.17861216515308E-02
+MAXIMUM ERROR OF DIVERGENCE-D 7.10021762643018E-04
TIME HARMONIC ELECTRIC FIELD IN V/M
P--:3.20
#LINEPLOT
COORDINATES/M
FULL RANGE / WINDOW
R[.0000, .065000]
[.0000, .0000]
F[.0000, 20.000]
[3.0000, 3.0000]
Z[.0000, .75000]
[.0000, .75000]
R-MESHLINE: 1
F-MESHLINE: 4
LINE AT R/M: .0000E+00
F/M: 3.000
KEY:
E 1 *[Z]
300.
250.
200.
150.
100.
50.0
0.000E+00
-.200
0.000E+00
.200
.400
.600
.800

Fig. 20a

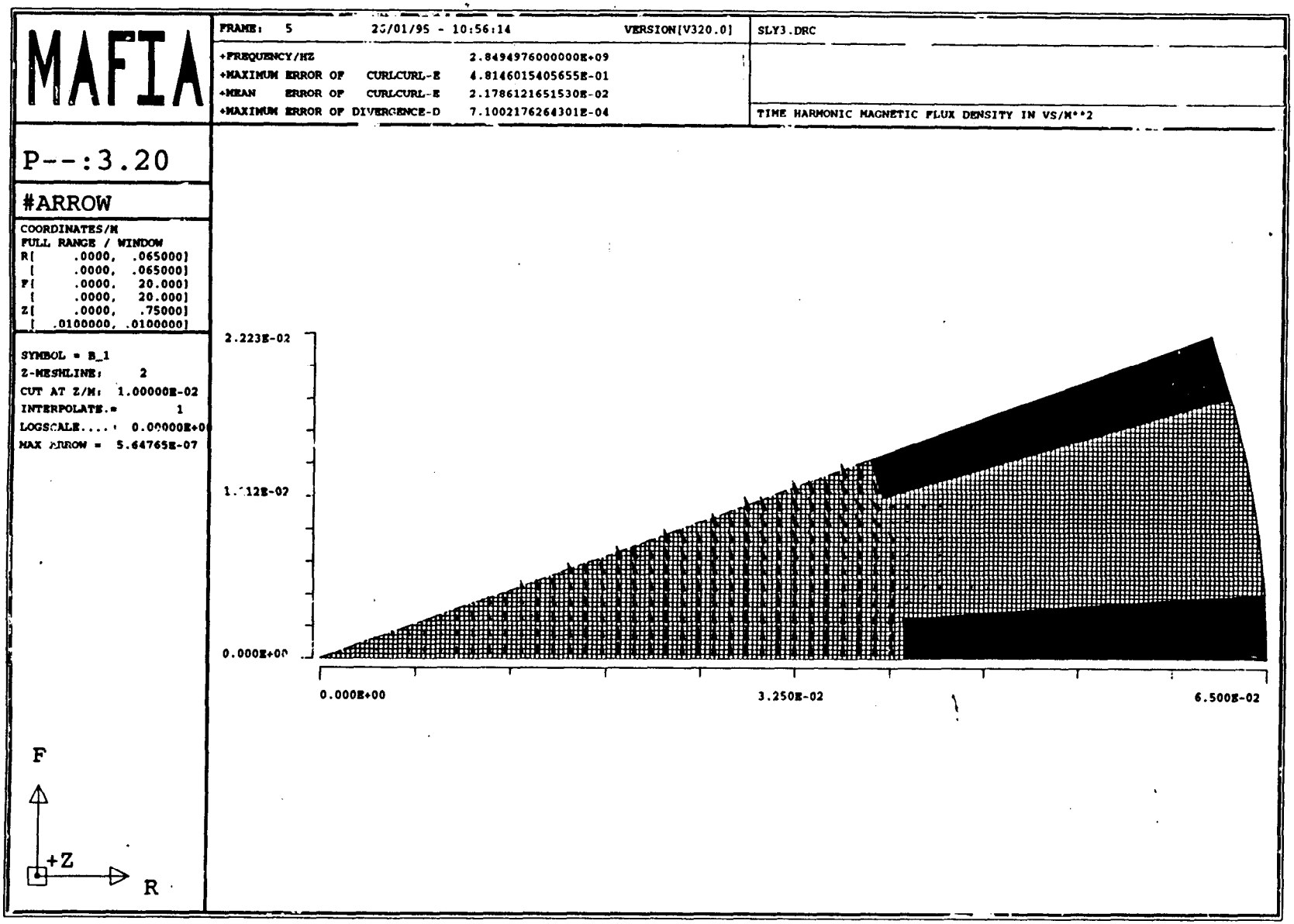
MAFIA
FRAME: 5 20/01/95 - 10:56:14 VERSION[V320.0]
SLY3.DRC
+FREQUENCY/HZ 2.8494976000000E+09
+MAXIMUM ERROR OF CURLCURL-E 4.8146015405655E-01
+MEAN ERROR OF CURLCURL-E 2.1786121651530E-02
+MAXIMUM ERROR OF DIVERGENCE-D 7.1002176264301E-04
TIME HARMONIC MAGNETIC FLUX DENSITY IN VS/M**2
P--:3.20
#ARROW
COORDINATES/M
FULL RANGE / WINDOW
R[.0000, .065000]
[.0000, .065000]
F[.0000, 20.000]
[.0000, 20.000]
Z[.0000, .75000]
[.0100000, .0100000]
SYMBOL = B_1
Z-MESHLINE: 2
CUT AT Z/M: 1.00000E-02
INTERPOLATE.= 1
LOGSCALE.... 0.00000E+0
MAX ARROW = 5.64765E-07
2.223E-02
1.112E-02
0.000E+00
0.000E+00
3.250E-02
6.500E-02
F
+Z
R

Fig. 20b

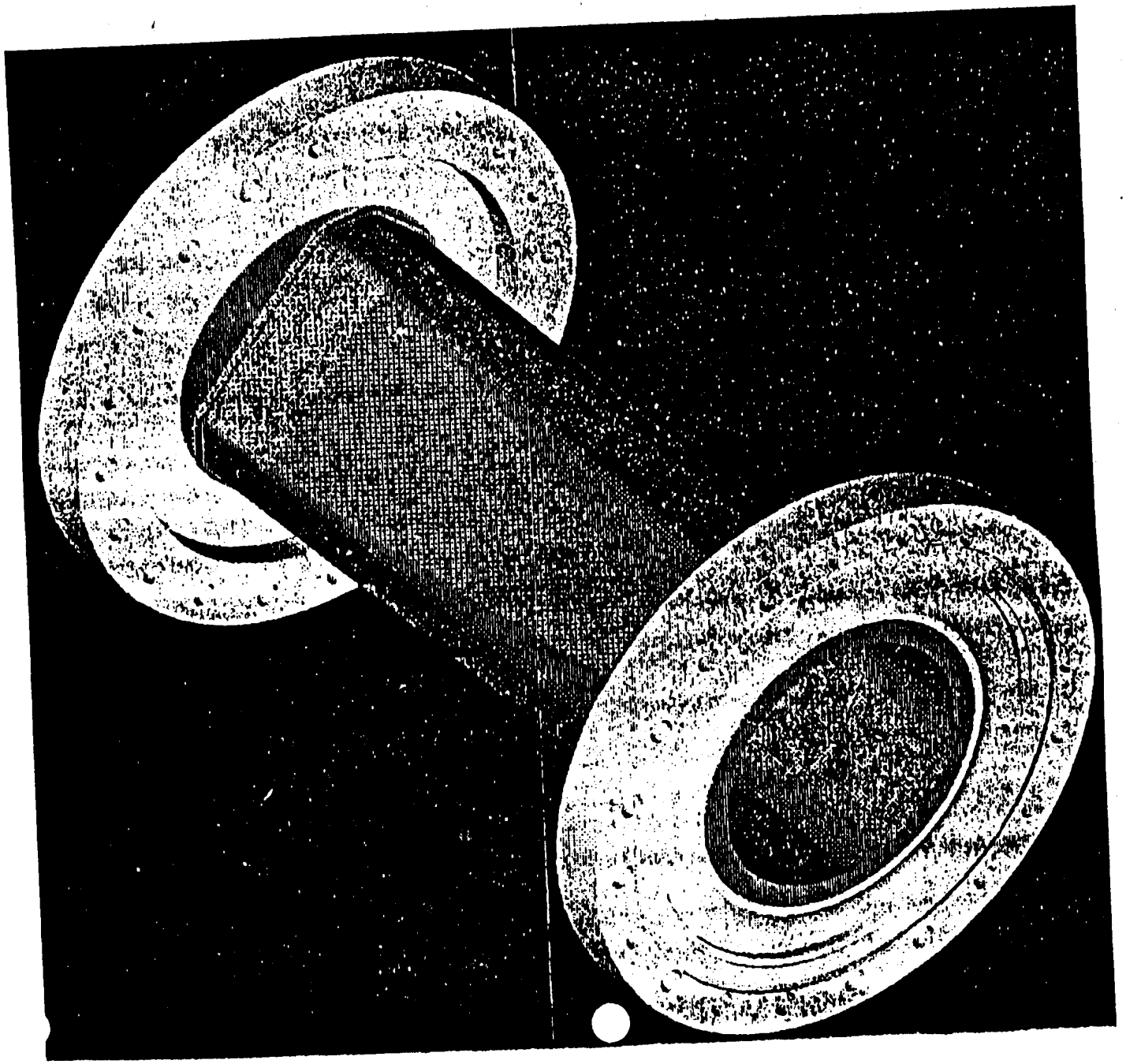

C. Daly

Fig. 21

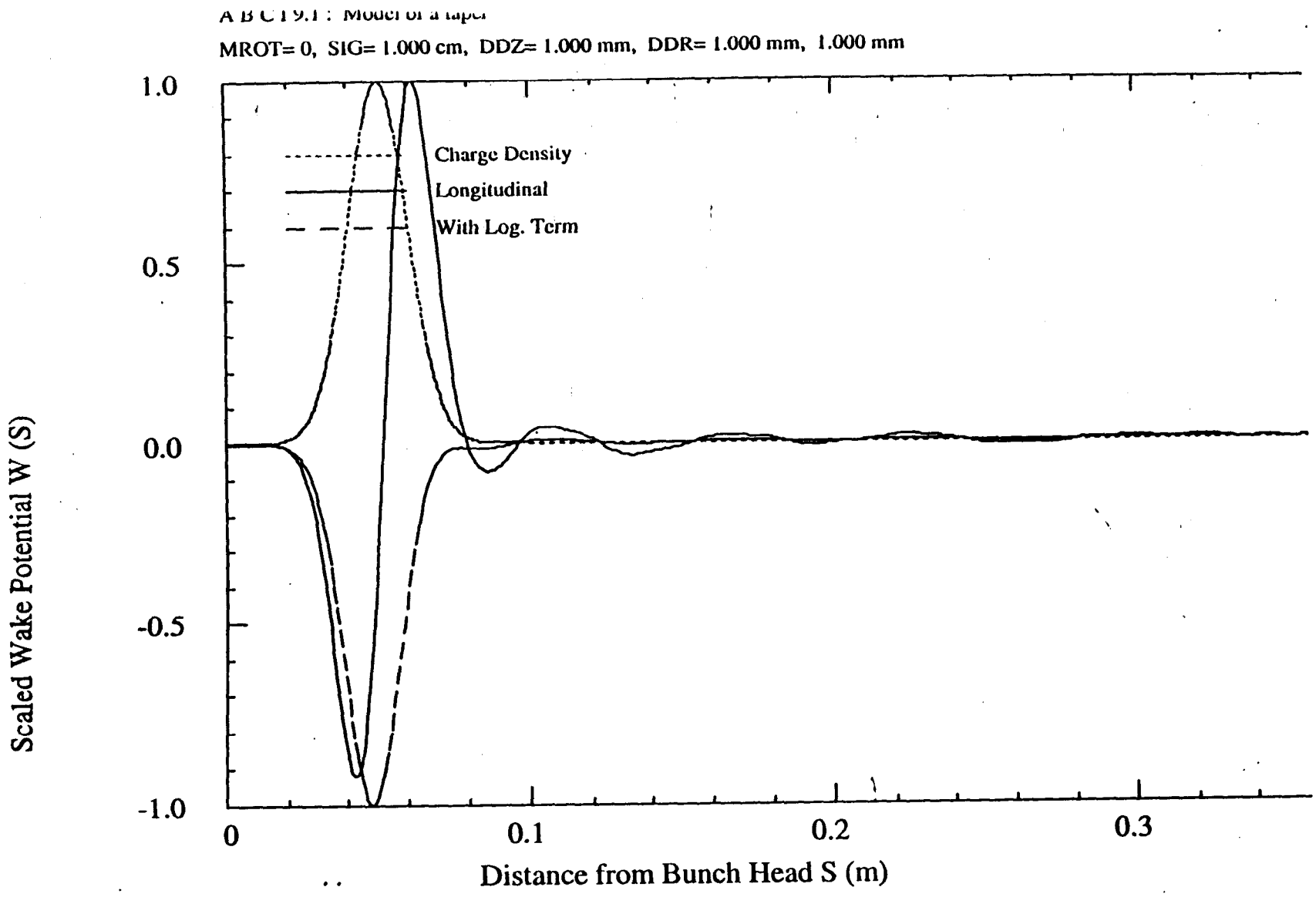
A B C 19.1 : Model of a taper
MROT= 0, SIG= 1.000 cm, DDZ= 1.000 mm, DDR= 1.000 mm, 1.000 mm
1.0
0.5
0.0
-0.5
-1.0
Charge Density
Longitudinal
With Log. Term
Scaled Wake Potential W (S)
0
0.1
0.2
0.3
Distance from Bunch Head S (m)
Longitudinal Wake
Min/Max= -7.056E-02/ 7.634E-02 V/pC,
Loss Factor= -5.097E-03 V/pC
With Log. Term
Min/Max= -4.546E-01/ 3.287E-03 V/pC,
Loss Factor= -3.031E-01 V/pC

Fig. 22

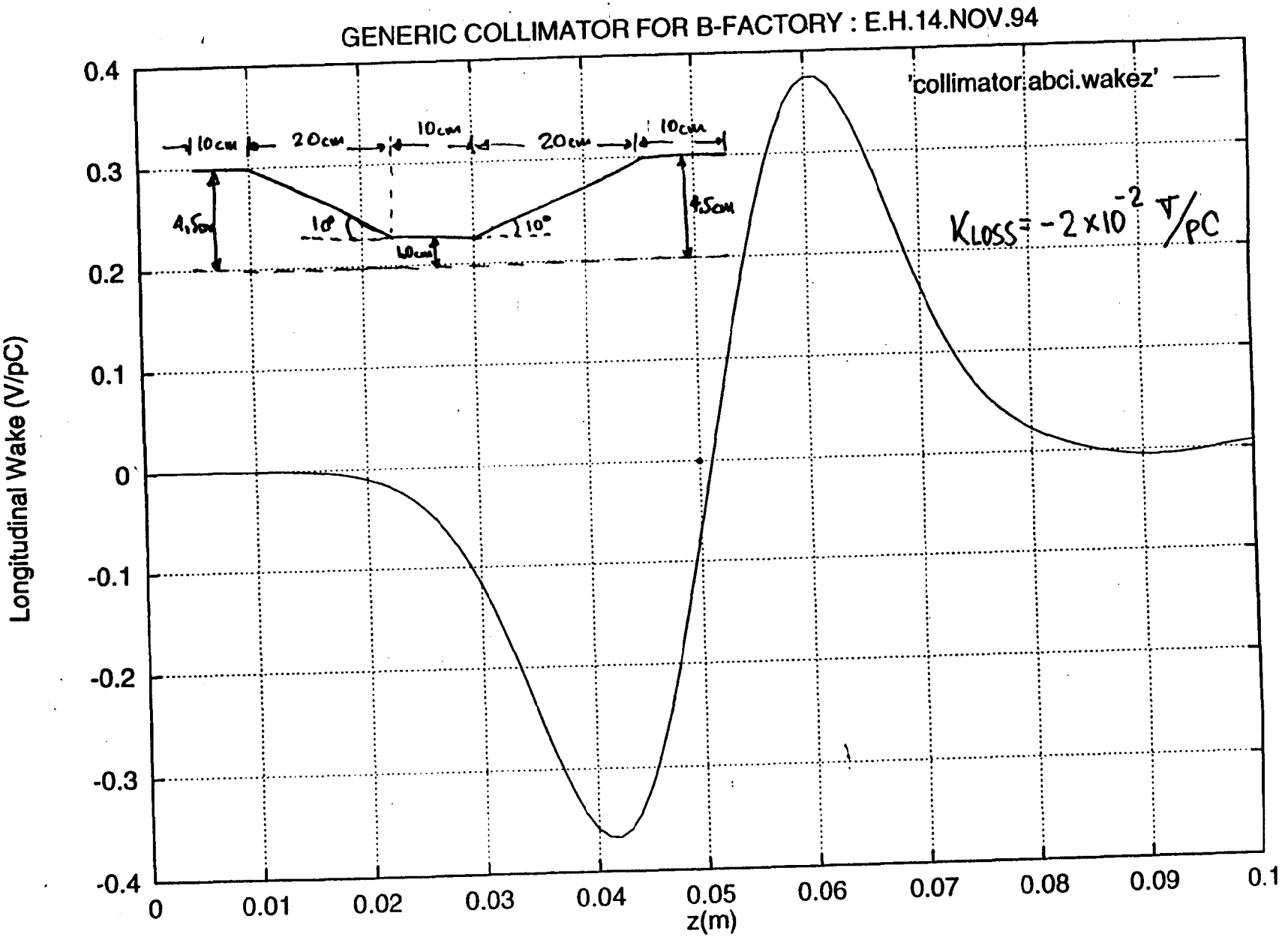
GENERIC COLLIMATOR FOR B-FACTORY : E.H.14.NOV.94
'collimator.abci.wakez'
10cm
20cm
10cm
20cm
10cm
4.5cm
10°
10°
4.5cm
4.5cm
$K_{LOSS} = -2 \times 10^{-2}$ V/pC
Longitudinal Wake (V/pC)
0.4
0.3
0.2
0.1
0
-0.1
-0.2
-0.3
-0.4
0
0.01
0.02
0.03
0.04
0.05
0.06
0.07
0.08
0.09
0.1
z(m)

Fig. 23

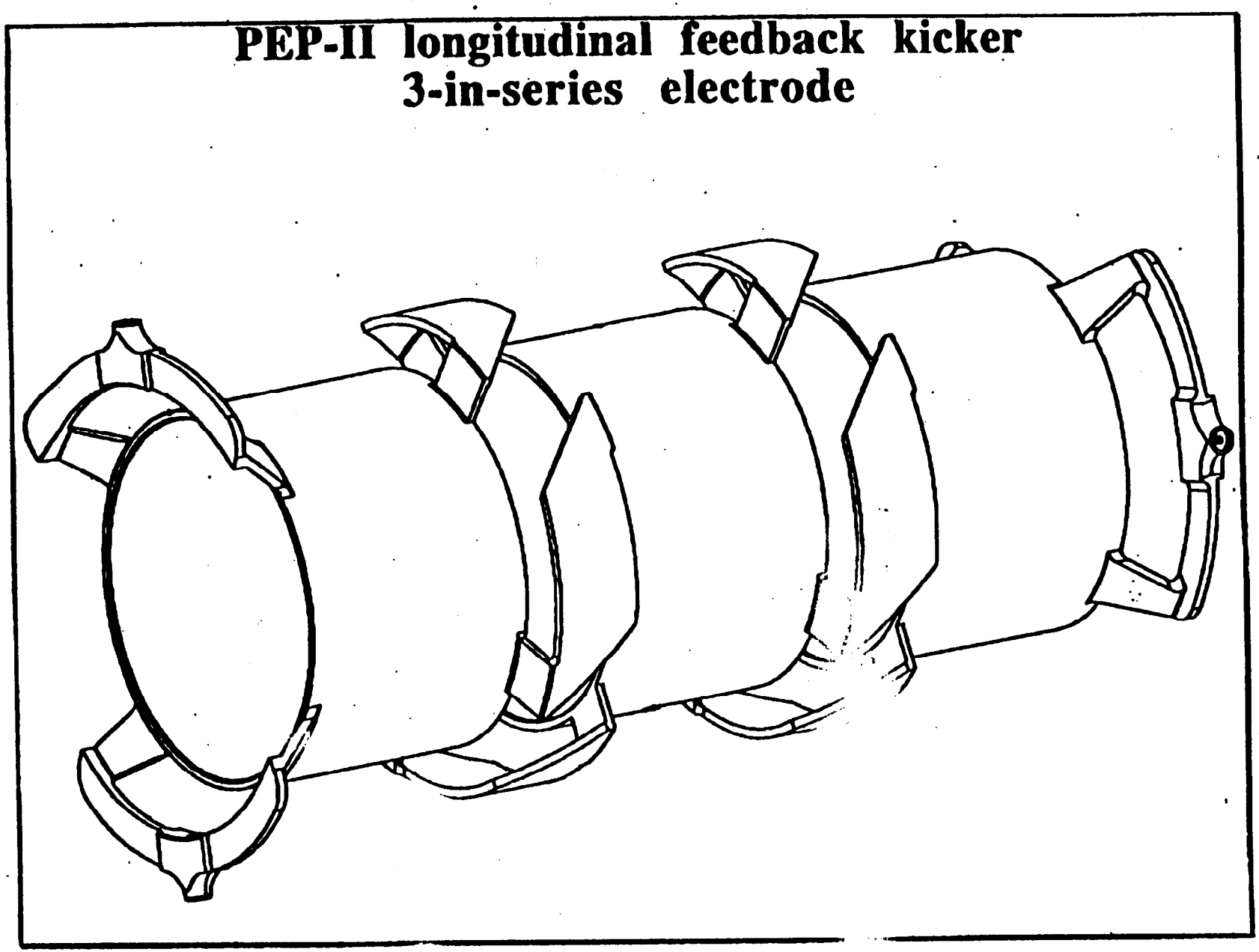

Fig. 24

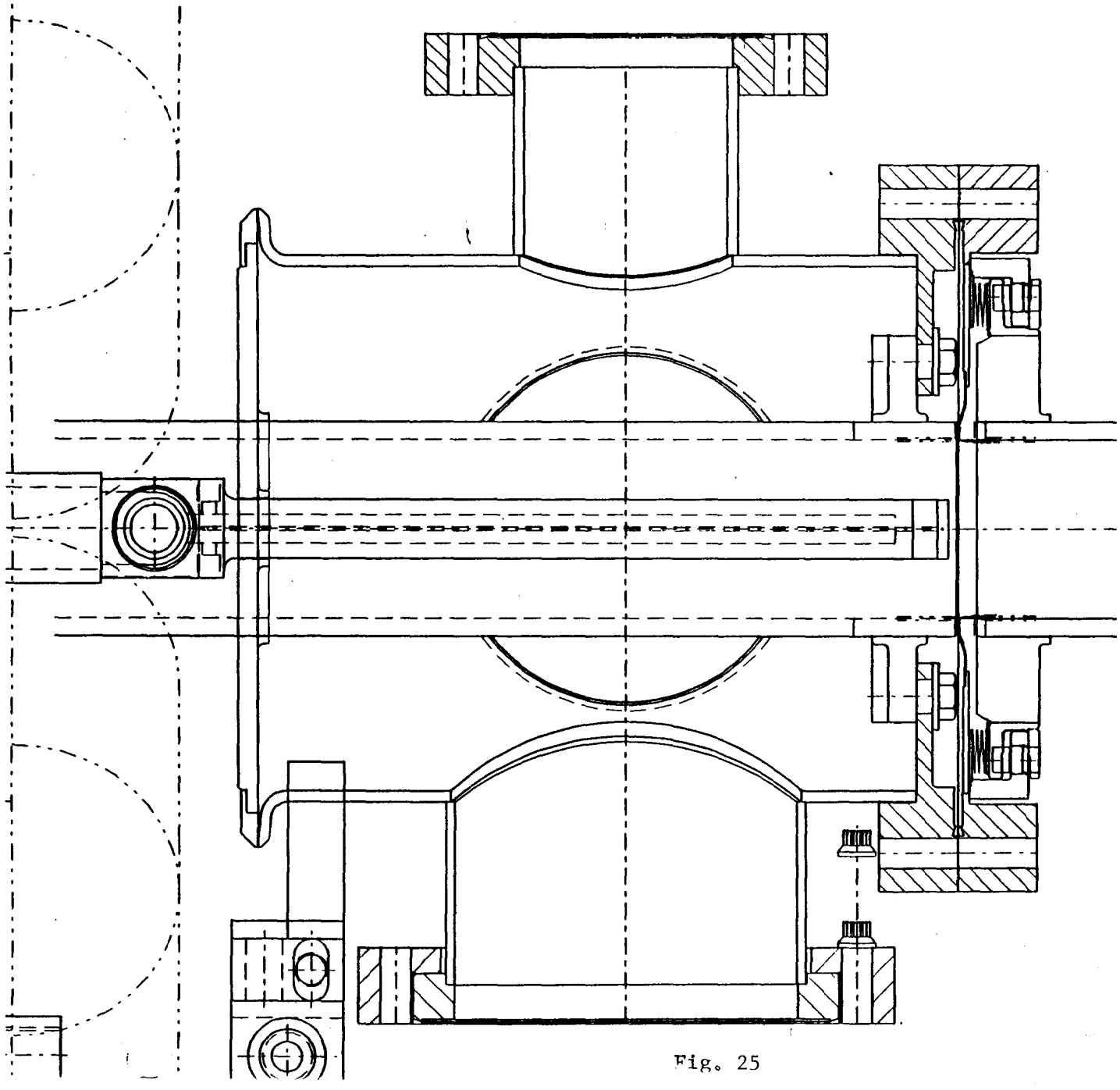

Fig. 25

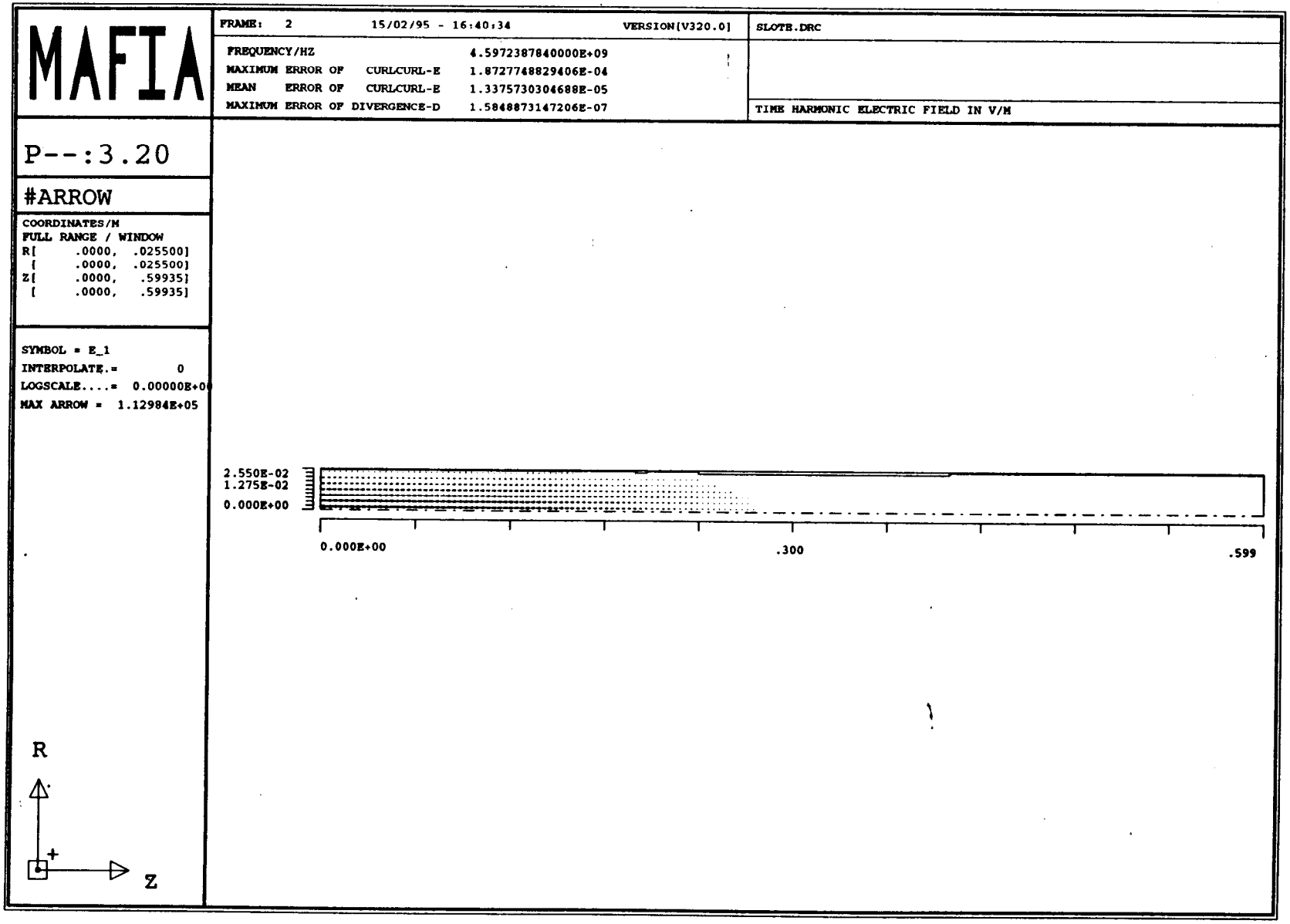
MAFIA
FRAME: 2 15/02/95 - 16:40:34 VERSION[V320.0]
SLOTE.DRC
FREQUENCY/HZ 4.5972387840000E+09
MAXIMUM ERROR OF CURLCURL-E 1.8727748829406E-04
MEAN ERROR OF CURLCURL-E 1.3375730304688E-05
MAXIMUM ERROR OF DIVERGENCE-D 1.5848873147206E-07
TIME HARMONIC ELECTRIC FIELD IN V/M
P--:3.20
#ARROW
COORDINATES/M
FULL RANGE / WINDOW
R[.0000, .025500]
[.0000, .025500]
Z[.0000, .59935]
[.0000, .59935]
SYMBOL = E_1
INTERPOLATE.= 0
LOGSCALE....= 0.00000E+00
MAX ARROW = 1.12984E+05
2.550E-02
1.275E-02
0.000E+00
0.000E+00
.300
.599
R
Z

Fig. 26